

4th INTERNATIONAL SYMPOSIUM OF IGCP PROJECT 283



GEOLOGY AND TECTONICS OF GORNY ALTAI

Guide-book

NOVOSIBIRSK 1993

RUSSIAN ACADEMY OF SCIENCES
SIBERIAN BRANCH
UNITED INSTITUTE OF GEOLOGY, GEOPHYSICS
AND MINERALOGY

GEOLOGY AND TECTONICS OF GORNY ALTAI

**Guide-book for post-symposium excursion
The 4th International Symposium
of the IGCP Project 283**

"Geodynamic Evolution of the Paleoasian Ocean"

NOVOSIBIRSK 1993

Compiled by

M.M.Buslov, N.A.Bersin, N.L.Dobretsov, V.A.Simonov

Edited by

N.L.Dobretsov

Translated into English by

I.Yu.Saphonova



M.M.Buslov, N.A.Bersin, .
N.L.Dobretsov, V.A.Simonov, 1993

INTRODUCTION

This guide-book includes new information on geological structure and geodynamic interpretation for the Gorny Altai area located in Central Asia (south-western part of Siberia) near to the western cross of Russia, Mongolia and China boundaries. The guide-book was prepared for the 4th International Symposium on the IGCP Project 283 "Geodynamic evolution of Paleasian Ocean" convened in Novosibirsk (Russia) 15-18, June, 1993.

One of the most important results of this work was compilation of a Geodynamic Map of the Paleasian Ocean of 1:2,500,000 scale. The majority of geodynamic environments distinguished in the map are widespread within the territory of Gorny Altai. In the guide-book the authors tried to characterize a variety of these environments which reflect a long evolution of the Paleasian ocean during the Paleozoic. Thus, the guide-book may be considered as explanatory note to the Gorny-Altai part of the Geodynamic Map (Berzin et al., 1993). Since, not all the structural and compositional units have an uniform geodynamic interpretation, the materials present in the guide-book are a good subject for discussion.

Gorny Altai relates to the western part of Altai-Sayan folded area being one of the most complicated accretionary-collisional structures of South Siberia (fig.1). Four major stages of formation of the Altai-Sayan folded area can be distinguished:

- 1) Vendian-Cambrian island arc stage;
- 2) Ordovician-Silurian collisional stage;
- 3) Devonian-Carboniferous stage of an active margin;
- 4) Late Paleozoic-Mesozoic collisional stage of the Okhotsk-Mongolian

ocean.

The first three stages characterize the evolution of Paleasian Ocean. The fourth stage has been displayed after the Paleasian ocean closing, when a complicated Paleozoic structure of the region has formed. The youngest stage is characterized by manifestation of multi-amplitude variously oriented thrust

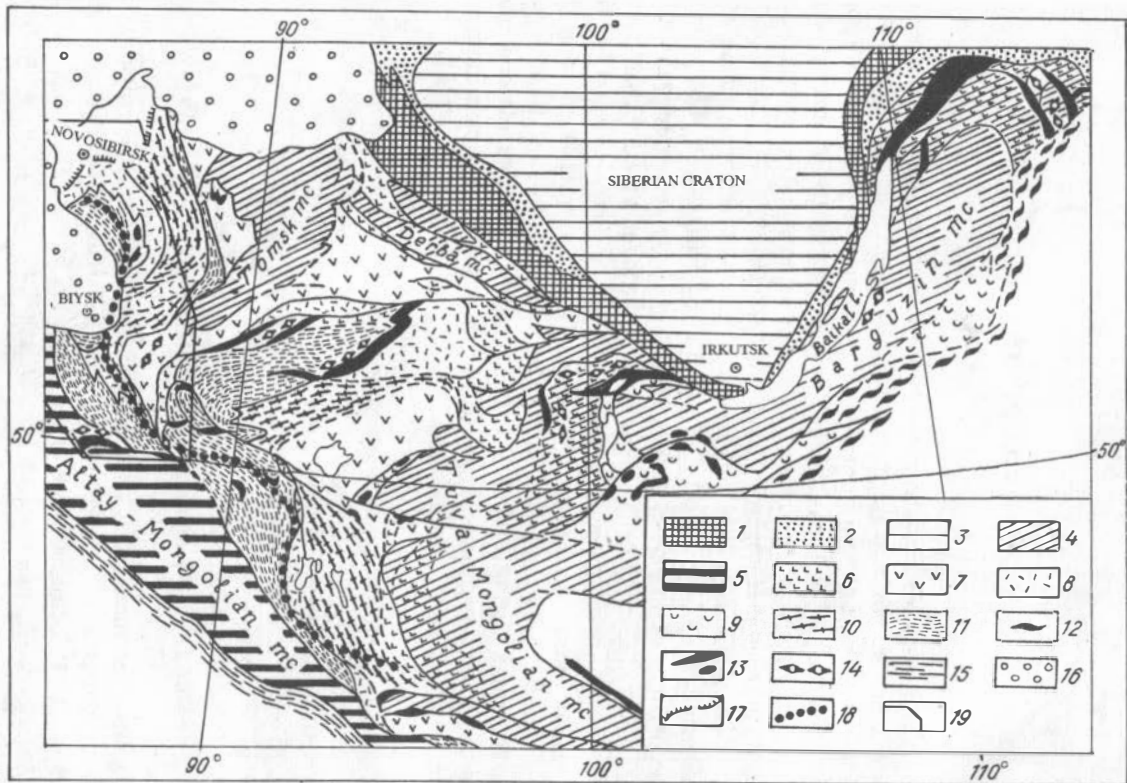


Fig. 1. Geodynamic complexes of South Siberia and West Mongolia (compiled by N.A. Berzin and N.L. Dobretsov):
1 - Basement of Siberian craton (AR-PR₂); 2 - Complexes of passive margin of craton and intercontinental rifts; 3 - Cover of craton (V-MZ); 4 - Microcontinents of Laurasian group; 5 - Altai-Mongolian microcontinent (part of Gondwana passive margin - PR₃-C); 6-9 - Island arc terranes: 6 - PR₃, 7 - V-C₁, 8 - C₁, 9 - C-O; 10 - Seamount and arc-related terranes (V-C₁); 11 - Accretional-collisional complexes (C-O); 12 - Collisional complex of the East Baikal type with granite metamorphic domes; 13 - Ophiolites including ultrabasites and serpentinite melange; 14 - Belts of high-pressure rocks (blueschists, eclogites, etc.); 15 - Hercynian Paleooceanic zone (O-S-D); 16 - MZ-KZ cover; 17 - Hercynian thrust; 18 - Boundary of Hercynian active margin; 19 - locations see fig.2-4.

and strike-slip dislocations of blocks squeezed between Kazakhstan, Siberia and Northern China continents. Late Paleozoic-Mesozoic collision of continents has created the modern mosaic-block structure of Altai-Sayan area. Only inside blocks the fragments of deformed Paleozoic structure are preserved which are connected with the folded areas of linear type. The deformations of every next stage of the Paleasian ocean development were superimposed on earlier formed structures. Therefore, study of Early Paleozoic structures and paleogeodynamic reconstructions was difficult to be carried out. Devonian-Early Carboniferous rocks of an active continental margin are less deformed.

Active continental margin stage

Figure 2 shows the main structural elements of the Devonian-Carboniferous active continental margin of Siberian continent divided by transverse and longitudinal thrusts into several blocks. Three systems of various age (D_1 - D_2^1 , D_2^2 and D_3 - C_1) consisting of the back rift zone rocks, volcanic-plutonic belts, volcanic terraces and accretionary prisms are well recognized. Typical feature of these systems is their eastern displacement towards the Paleasian ocean and left-side rotation of structures by 90° in time (Yolkin et al., 1993). During field trip the study of D_1 - D_2^1 and D_2^2 volcano-plutonic belts (Stops 9-14) is suggested, where the questions on comagmatic nature of volcanic and plutonic rocks, their subdivision and geodynamic nature will be discussed.

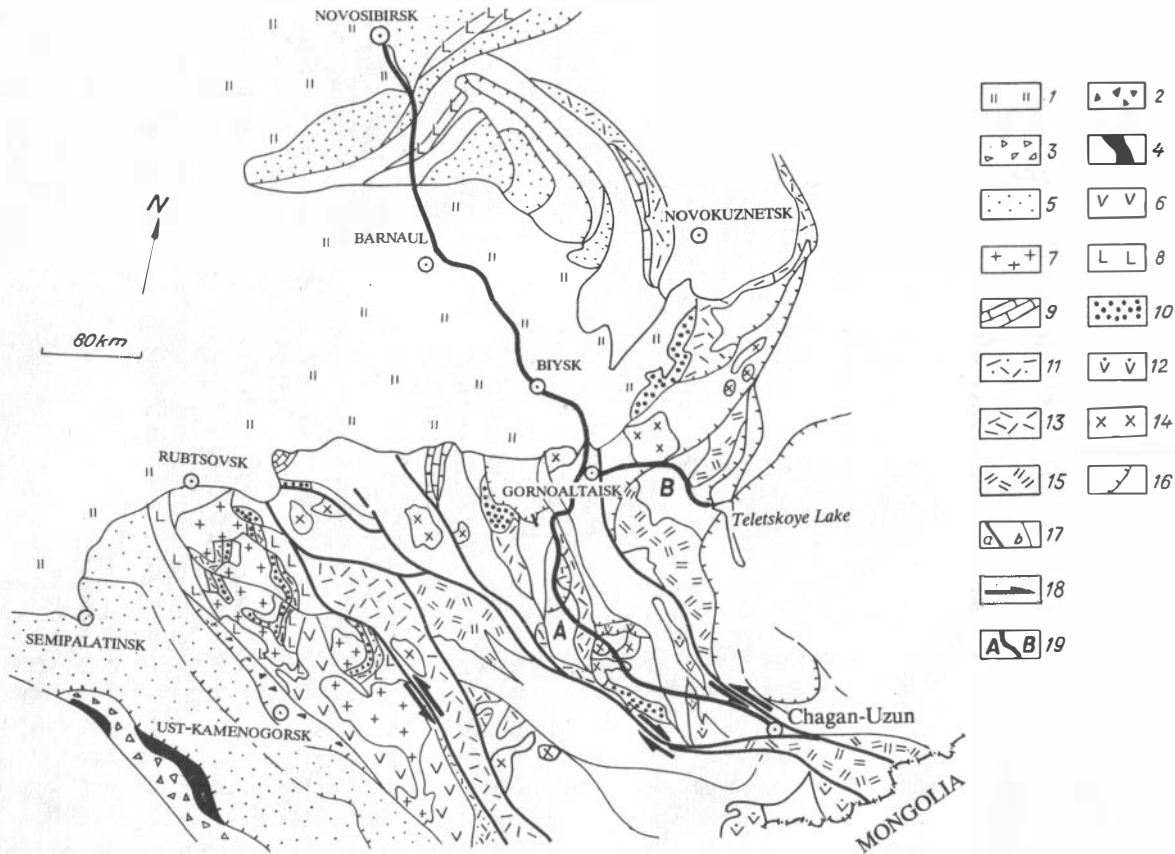


Fig. 2. Geodynamic complexes of the Devonian active margin stage on the territory of Gorny Altai and adjacent areas (compiled by M.M.Buslov).

1 - Neogene-Quaternary sediments of Biya-Barnaul depression; 2-4 - accretionary prism complexes; 2- Late Devonian, 3- Early Carboniferous, 4- Chara ophiolite belt consisting of serpentinite melange with ophiolite sheets and blocks (O_2-S_1 and D_{1-2}) and high pressure rocks (garnet-glaucophane and glaucophane schists, garnet amphibolites); 5- nonvolcanic terrain (D_3-C_1); 6-7 - volcano-plutonic belt (D_3-C_2); 6- predominantly andesite-dacite volcanic rocks (D_3-C_1), 7- granitoids (C_{1-2}), 8- basalt-rhyolite volcanic rocks and sediments ($D_2^2-D_3^1$) of the axial riftogenic environment; 9-10 - nonvolcanic terranes (D_1^2); 9- rifting carbonates-bearing terranes, 10- tuff-terrigeneous sediments; 11- undivided volcanic terrain (D_2); 12-14 - volcano-plutonic belt ($D_1^2-D_2$); 12- andesite-basalts, andesite and dacite volcanic rocks (D_1^2), 13- dacite-rhyolite volcanic rocks (D_2), 14- granitoids (D_{1-2}); 15- the complexes of back rift zones ($D_1^2-D_2$); basalt-rhyolite volcanic rocks, gabbro diabases and sediments; 16- thrusts; 17- strike-slip faults: main (a), other (b); 18- direction of block movement; 19- the line of A and B routes of the excursion.

Collisional stage

The Ordovician-Silurian collisional stage proceeded within the junction zone of Gorno-Altai and West Sayan blocks (fig.3). Various collisional complexes are widespread here: zonal granite-gneiss domes (the Kurai, Teletsk and Chulyshman domes), two-mica granites, volcanic molasse of the Erinad and Ulagan structures, nappe-imbricated structures with serpentinite melanges containing blocks and sheets of gabbros, basalts and siliceous rocks.

Far from the junction zone of the Gorno-Altai and West Sayan blocks the facial change of Ordovician-Silurian rocks from continental facies through coastal sea facies to marine rocks occurs. Ordovician-Silurian flysch is typical of the West Sayan block. Together with rocks of Early Paleozoic basement the flysch is thrust over collisional rocks.

During the field trip we suggest to study the Teletsk metamorphic complex (Stop B-9), Silurian deposits (Stop 15) and nappe-imbricated structures (Stops 22, 24). The question on the age and geodynamic nature of granite-metamorphic blocks is under discussion: Did they result from collision and following metamorphism of Paleozoic rocks or they are fragments of an ancient microcontinent or both cases?

Island arc stage

The Vendian-Cambrian island arc stage of Paleozoic ocean evolution is well

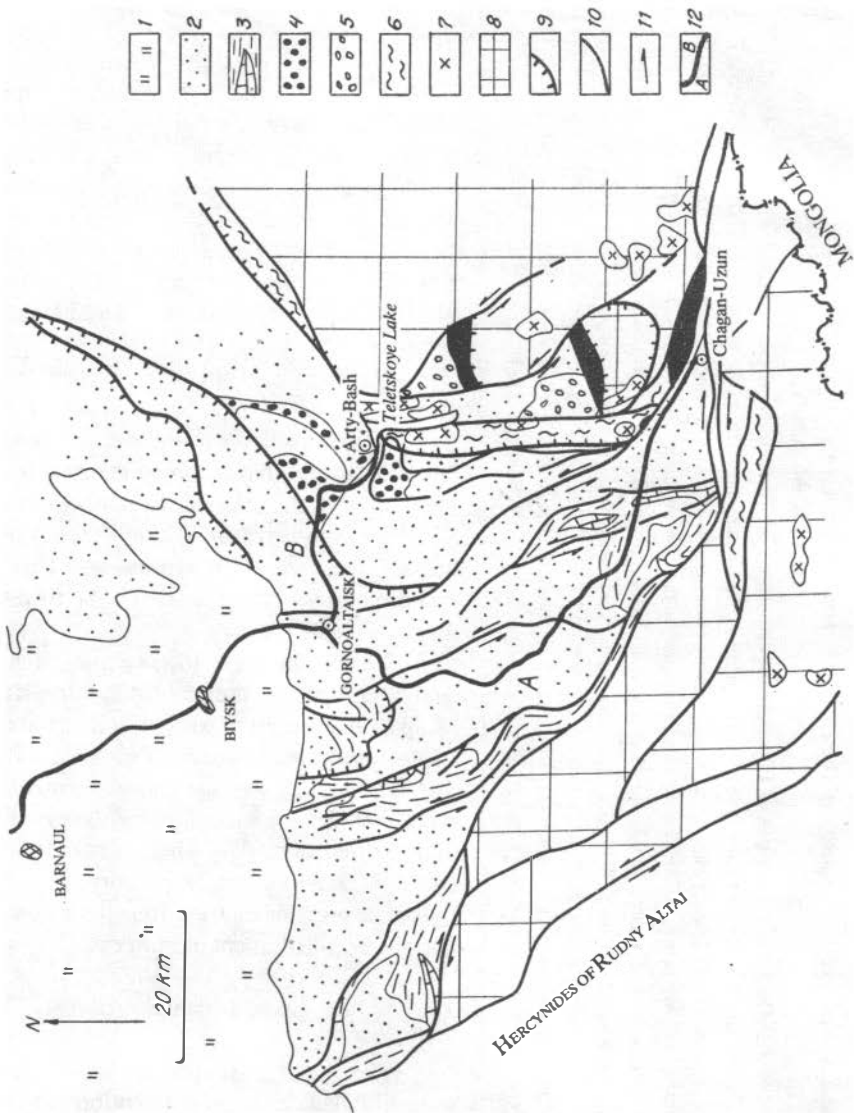


Fig. 3. Geodynamic complexes of the Ordovician-Silurian collisional stage on the territory of Gorny Altai (compiled by M.M.Buslov):

1 - Neogene-Quaternary sediments of Biya-Barnaul depression; 2-7 - Gorno-Altai block (terrane); 2 - undivided Early Caledonian rocks, 3-5 - collisional stage sedimentary complexes (O-S₁); 3 - grey marine carbonate-terrigenous deposits (O-S₁), 4 - coastal-sea red coarse rocks (O₁₋₃), 5 - volcanic molasse (O-S₁), 6-7 - granite-gneiss domes; 6 - zonal metamorphic series, 7 - granitoids; 8 - Early Caledonian rocks of Altai-Sayan terrane; 9 - thrusts; 10 - strike-slip faults; 11 - direction of block movement; 12 - A and B route lines.

fixed in the structural-compositional complexes of Gorno-Altai block (terrane) and has no analogues among other South Siberia terranes (fig.4). Inside Gorno-Altai terrane the following geodynamic units are distinguished (from west to east):

1. Primitive island arc composed of Vendian-Early Cambrian rocks of tholeiite-boninite composition with ophiolite affinity.

2. Accretionary wedge consisting of Early Cambrian olistostrome and basalts. Olistostrome appearance is comparable with the rocks of oceanic crust and paleoseamounts according to the set of fragments. Olistostrome includes large blocks of Vendian-Early Cambrian seamounts (Barnaul, Biya-Katun, Kadrin and Baratal seamounts), sheets of metaperidotites and serpentinite melanges with high pressure rocks (the Chagan-Uzun complex).

3. Ust-Syoma normal island arc is characterized with various Early-Middle Cambrian volcanic series. Stratigraphically upwards they are changed from sub-boninite to calc-alkaline. By lateral towards the ocean they are changed from shoshonite to tholeiite series. Tonalite-gabbro-diorite dikes, sills and plutons are typical of island arc, as well. Volcanic structures and plutons formed both within primitive island arc and the Lower Cambrian accretionary wedge.

4. Fore-arc and inter-arc troughs are filled with Middle-Late Cambrian flysch, olistostrome and breccias (Anui-Chuya zone).

In fig.5 the possible model of the development of the Early Paleozoic system of Gorny Altai is shown. Five stages are noted:

1. In the Vendian, when the Paleoasian Ocean reached maximum dimensions a subduction zone was formed near the Siberian continent. Its activity resulted in formation of ophiolites of the Uymen-Lebed-Kuznets primitive island arc superimposed on oceanic crust. Simultaneously, seamounts with basalts of subalkaline were formed in the central parts of Paleoasian Ocean.

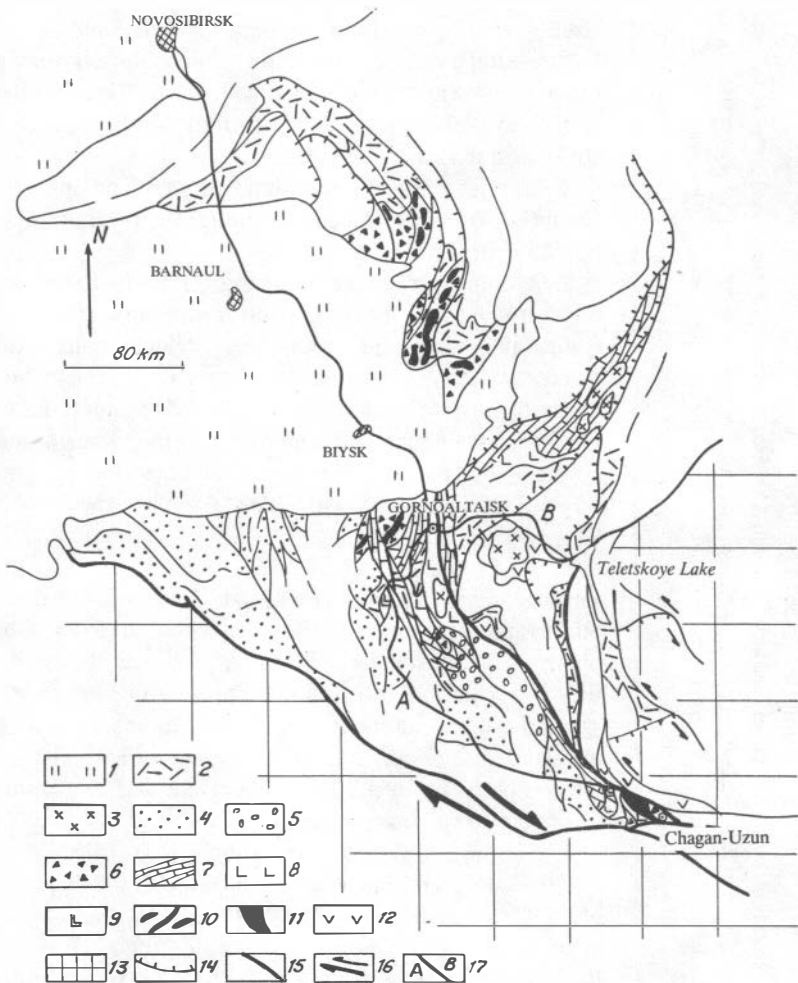


Fig. 4. Geodynamic complexes of the Vendian-Cambrian island arc stage on the territory of Gorny Altai and Salair (compiled by M.M.Buslov and N.L.Dobretsov):

1- Neogene-Quaternary sediments of Biya-Barnaul depression; 2-5 - the Cambrian complexes of normal island arc: 2- calc-alkaline volcanic rocks and sediments ($C_1^2C_3$), 3- plutons and massifs of gabbroids (C_2), 4-5 - complexes of troughs (C_{2-3}): 4 - forearc, 5 - interarc; 6-12 - the Vendian-Early Cambrian complexes of arc-trench system and accretionary prism: 6-

olistostrome (C_1^1), 7,8 - giant bodies of paleoseamounts: 7 - siliceous-carbonate cover, 8 - basalts; 9 - the sheets of sedimentary-basaltic rocks of oceanic crust, 10 - the zones of serpentinite melanges and schists, 11 - Chagan-Uzun ophiolite massif (sheets of metaperidotites, dikes and metabasalts, serpentinite melange with the blocks of eclogites and garnet amphibolites); 12 - Vendian-Early Cambrian rocks of primitive island arc with tholeiite-boninite type of magmatism; 13 - undivided rocks of Early Caledonides of Altai-Sayan terrane; 14 - thrusts; 15 - strike-slip faults; 16 - direction of block movement; 17 - A and B route lines.

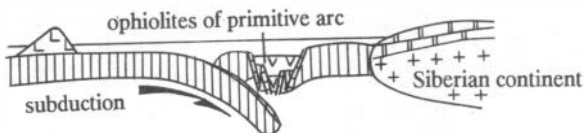
2. In the Vendian-Early Cambrian within a subduction zone high-pressure rocks have been formed, primitive island arc has developed up to central type volcanos, the formation of non-volcanic uplifts with the fragmental material of the upper layer of oceanic crust began. Volcanic seamounts (Biyakaton, Baratal, etc.) have been getting close to a subduction zone and overlain by a cover of siliceous-carbonate sediments.

3. In the middle of Early Cambrian in Gorny Altai the collision of paleoseamounts with island arc occurred resulting in the squeezing of subduction zone and the appearing of return matter currents in an accretionary wedge. The uplift of serpentinite melanges and high-pressure rocks to the surface of arc slope was a result of such collision. Seamounts become a part of accretionary wedge, the simultaneous with olistostrome formation "jumping" of subduction zone proceeding oceanwards.

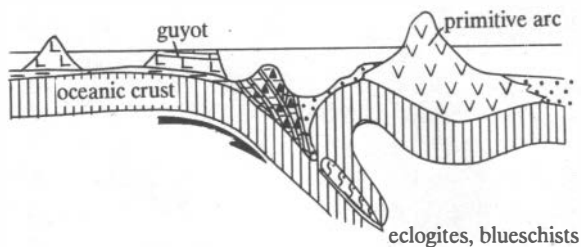
4. In the end of Early Cambrian-beginning of Middle Cambrian subduction processes resulted in the formation of volcanic-plutonic assemblages of normal island arc, for which a transitional type crust serves as a basement. This crust consists of accretionary wedge and pre-existing primitive island arc.

5. In the Middle-Late Cambrian subduction processes in Gorny Altai have ceased, and the paleo-trench of Anui-Chuya zone has been filled with coarse-grained material consisting of the destructing Early Cambrian olistostrome, accretionary wedge and rocks of seamounts, primitive, and normal island arcs.

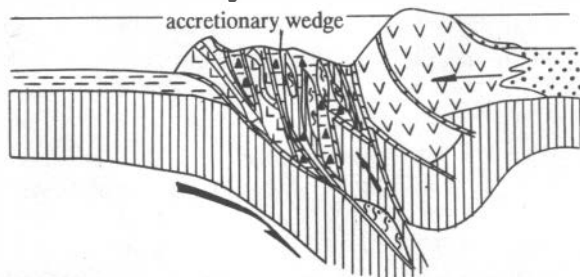
Major part of trip will be devoted to the study of Vendian-Cambrian rocks of island arc stage. Almost all its structural and compositional units are characterized in the guide-book. The question on the distinguishing of island arc ophiolites characterized by tholeiite-boninite magmatism, is most significant for discussion. Although these island arc ophiolites consist of all the



I stage (Vendian) - subduction. Formation of ophiolites with boninite-tholeiite magmatism.

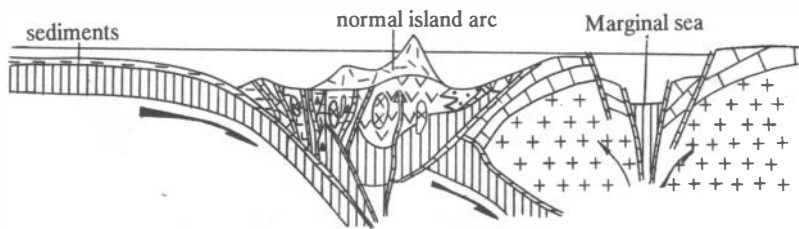


II stage (Vendian-Early Cambrian) - subduction. Formation of accretionary prism and subduction high pressure rocks.

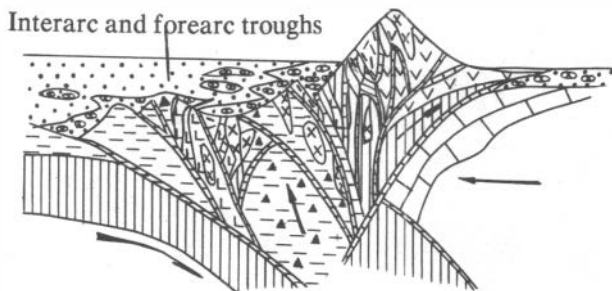


III stage (Early Cambrian) - collision of guyots with island arc. Closing of subduction zone and reverse flows in accretionary wedge.

constituent parts of oceanic and margin sea ophiolites, they differ from the latter in: 1) composition of magmatic rocks; 2) widespread dike-sill complexes but not dike-sheeted complexes; 3) thick volcanic-sedimentary sections where acid lavas and tuffs play a significant role; 4) structural position over subduction zone.



IV stage (Early-Middle Cambrian) - formation of a new subduction zone, accretionary prism and normal island arc with calc-alkaline magmatism.



V stage (Middle-Upper Cambrian) - collision of island arc with continent. Formation of molasses and flysch, forearc and interarc troughs.

Fig. 5. The model of Vendian-Cambrian arc-trench system of Gorny Altai (compiled by M.M.Buslov, comments see in the text).

DESCRIPTION OF FIELD TRIP

Day 1. Departure to Gorny Altai: Novosibirsk-Barnaul-Biysk-Gornoaltaisk - 450 km route. The second half of this day: study of the Early Cambrian accretionary prism of the northern part of Gorny Altai.

General review (stops 1-3)

First 100 km from Novosibirsk to the south our path crosses three geodynamic units of different age: 1) Middle Devonian-Early Carboniferous predominantly sedimentary complex; 2) Carboniferous-Permian molasse coal-bearing sequences of Gorlovsk basin; 3) Early Cambrian sedimentary-volcanic island arc rocks. However, rocks are poorly exposed to be seen only in some river-beds.

Middle Devonian-Early Carboniferous rock complex of Tom'-Kolyvan zone is widespread in two tectonic wedges at the piece of the road from Novosibirsk to Evsino Village (0-50 km) and near to Cherepanovo Town (70-85 km). Between these two points (50-70 km distance) the Carboniferous-Permian sequences of Gorlovsk basin are located. Hercynian terranes are thrust onto the Early Cambrian island arc rocks of the Salair zone which are crossed by our route over 80-100 km.

The Middle-Devonian rocks of Tom'-Kolyvan zone represent sandstones, mudstones, argillites, conglomerates, limestones and various volcanic rocks with their tuffs. Upwards, there are Late Devonian-Early Carboniferous sandstones and mudstones interpreted as the deposits of active margin.

The Late Carboniferous-Permian sediments of Gorlovsk basin consist of gravellites, sandstones, mudstones and coals similar to the same-age deposits of Kuzbass basin. Anthracite coals are used for the production of high-quality electrodes in the factory of Linyovo Village.

Early Cambrian rocks are a part of the Cambrian Salair island arc and consist of acid and andesitic volcanic rocks, conglomerates, sandstones, schists and limestones.

After 100 km path the route crosses Barnaul Neogene-Quaternary fore-mount depression (Steep Altai). We will cross Chumysh River near to Talmenka Village and Biya River in Biysk City. From Biysk the route goes along Chuya motorroad which crosses Steep and Gorny Altai for 600 km to continue in Mongolia.

Forty kilometers from Biysk after Srostki Village the road goes upwards and we can observe a nice panorama of wide flood-lands of Katun River lower reaches. In clear weather one can observe the whole view of Gorny Altai where the Bobyrgan Mountain is seen (absolute height is 1008 m) in the left bank of Katun River and is composed of Devonian granitoids, mostly.

After this point the road goes downwards along the largest river of Gorny Altai - Katun River. At 416 km of the route immediately after Surtaika Village

the Chuya motorroad goes close to the first large outcrop of Gorny Altai. Here we begin to study the geology of the northern part of region (fig.6). The height of mountains of this part of Gorny Altai reaches 800-1200 m. Commonly, the northern mountain slopes are covered with woods, the southern ones being opened for geological study. In the fig.7 the main geodynamic and structural units of region are shown. Here, the Early Cambrian accretionary prism penetrated with the dikes and gabbroid massifs of Early-Middle Cambrian island arc system and the volcano-plutonic belt of Devonian active continental margin are seen. Accretionary prism is composed of the sheets of Vendian volcanic, sedimentary-volcanic and siliceous-carbonate rocks of the Katun paleoseamount, serpentinitic schists and melanges with the large blocks of gabbro and the sheets of olistostromes. Geochemistry data for the magmatic rocks of accretionary prism are cited in table 1.

Stop 1. Located at 414-415 km of Chuya motorroad (fig.6,7) near to Surtaika Village. Here, a well-exposed rock precipice exposes the outcrops of Vendian amygdaloidal pillow-lavas of the Katun paleoseamount which have undergone greenschist metamorphism. The pillow sizes are 1-1.5 m length. The matrix is filled with siliceous-carbonate material. The central parts of pillows are composed of clinopyroxene metaporphyrites. Commonly, pyroxene is replaced by chlorite and epidote. Matrix mainly consists of actinolite, epidote, chlorite and albite. The rim of some pillows is rich in calcite amygdales. According to bulk and REE chemistry, lava is characterized as seamount subalkaline basalt (table 1,2 fig. 8-11).

Stop 2. Located at 456 km of Chuya motorroad in the outskirts of Souza Village (fig.6,7). The outcrops of Early Cambrian olistostrome can be observed. They generally consist of poorly graded sandstones and gravellites with the angular fragments of diabases, porphyrites and shales. Large blocks 1-5 m in diameter are composed of pyroxene porphyrites and diabases. According to bulk chemistry, they correspond to the destructive products of the basalts of the third layer of oceanic crust and paleoseamounts (table 1, fig. 8,9).

Stop 3. Located near to 455 km of Chuya motorroad. Here, the outcrops of the siliceous-carbonate rocks of Katun paleoseamount are found within the left and right banks of Katun River, near the bridge to Aya Lake. Underwater-slide siliceous-carbonate breccias relate to the slope facies of paleoseamount. The interbeds of black siliceous rocks contain the plots enriched in pyrite.

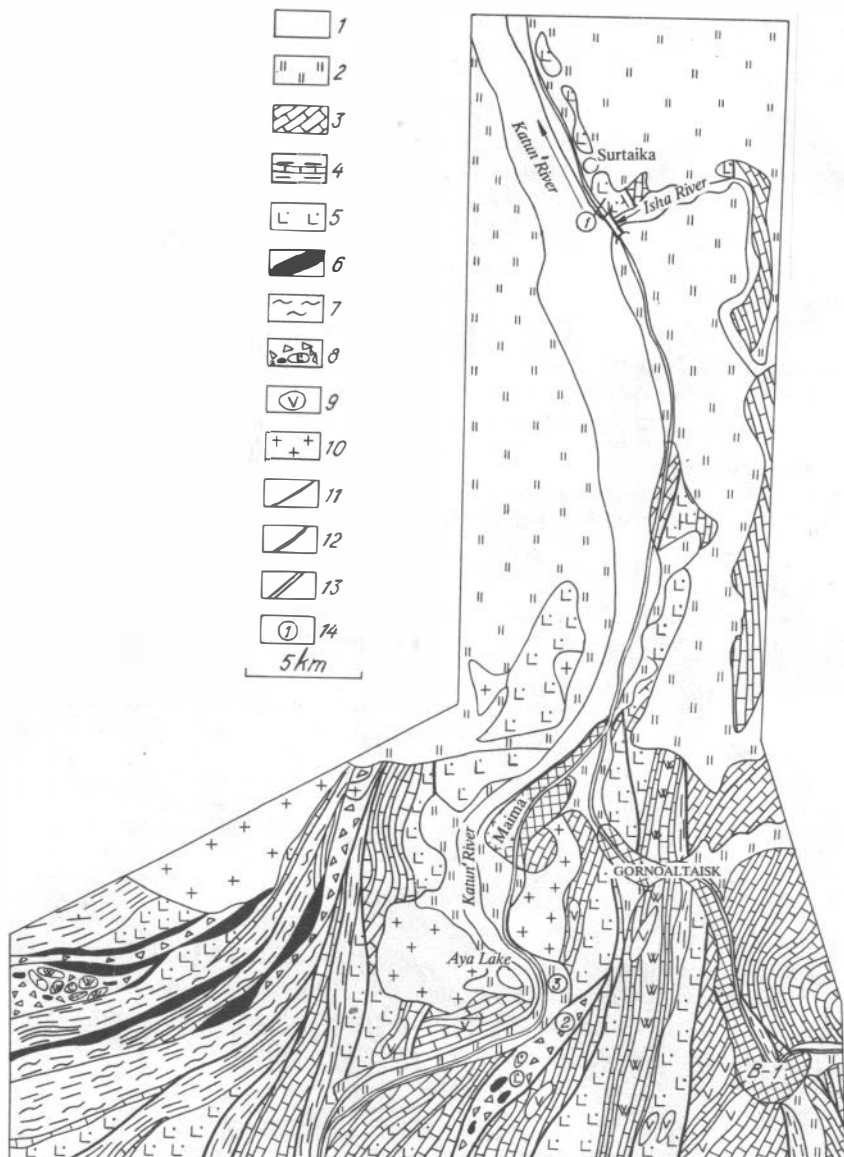


Fig. 7. Geodynamic complexes of the northern part of Gorny Altai (compiled by M.M.Buslov and N.L.Dobretsov):

1 - alluvium deposits of Katun and Ishi Rivers; 2 - Quaternary sediments of Barnaul foremountain depression; 3-8 - the complexes of Early Cambrian accretionary prism: 3-5 - Vendian rocks of Katun seamount: 3 - siliceous-carbonate, 4 - carbonate-terrigenous, 5 - basaltic rocks; 6 - serpentinite schists and melanges with gabbroid blocks; 7 - greenschists after terrigenous rocks; 8 - Early Cambrian olistostrome with blocks of serpentinites (a) and seamount rocks (b): W - siliceous, G - gabbroids, L - basalts, limestones; 9 - dikes and massifs of gabbro-diabases of Early-Middle Cambrian island arc; 10 - granitoids of Devonian active margin; 11 - lithological boundaries; 12 - faults boundaries; 13 - The Chuya motorroad line; 14 - Stops location.

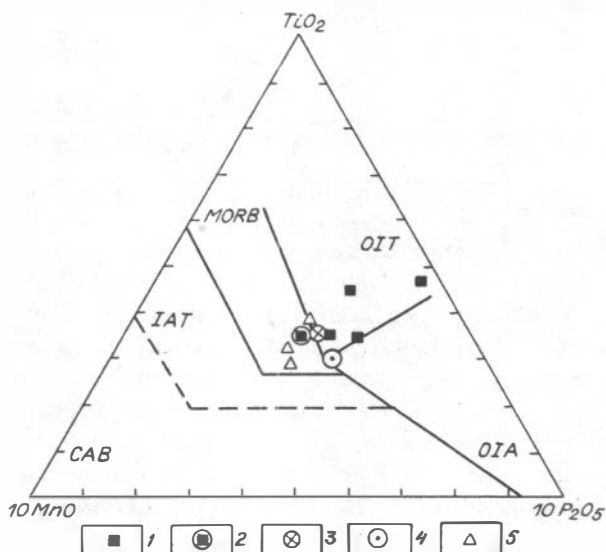


Fig. 8. The diagram of TiO_2 - $10MnO$ - $10P_2O_5$ for Gorny Altai rocks at a whole and for Stops 1 and 2 (compiled by M.M.Buslov):

1-4 - Katun seamount: 1 - pillow lavas of Stops 1, 2 - the average values for basalts ($n=17$) from the right bank of Katun River, between Siurtaika and Maima Villages, 3 - average values for basalts ($n=14$) from the left bank of Katun River to the south-west from Aya Lake (Kaimskaya suite), 4 - average values for subvolcanic bodies of gabbro-diabases from Kaimskaya suite; 5 - the fragments of magmatic rocks from olistostrome of Stop 2.

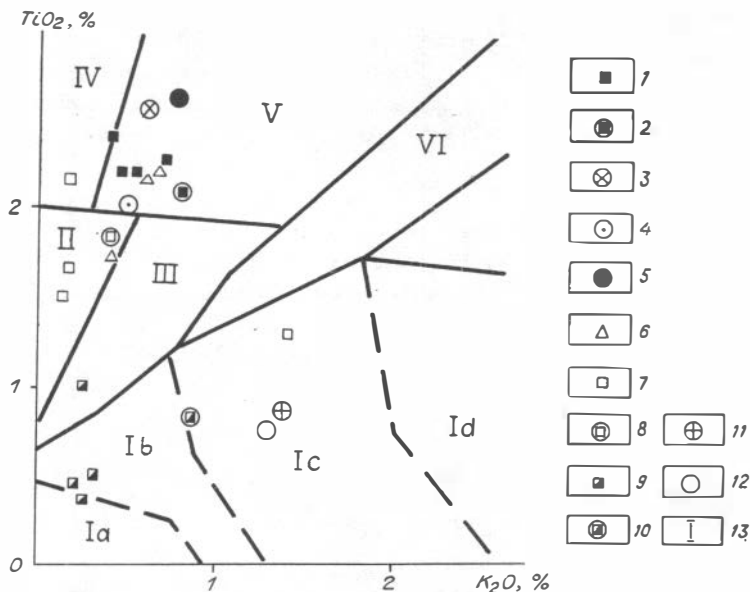


Fig. 9. The diagram of TiO_2 - K_2O for the rocks from the northern part of Gorny Altai at a whole and Stops 1, 3, 4, 6, 7 (compiled by V.A.Simonov and M.M.Buslov using the diagram of Yu.V. Mironov, 1991):

1-5 - Katun seamount: 1 - pillow lavas of Stop 1; 2 - average values for basalts ($n=17$) from the right bank of Katun River between Siurtaika and Maima Villages, 3 - average values for basalts ($n=14$) from the left bank of Katun River to the south-west from Aya Lake (Kaimskaya suite), 4 - average values for subvolcanic bodies of gabbro-diabases from Kaimskaya suite, 5 - average values for basalts of Manzherok suite ($n=30$) from the section Cheposh - Ust-Syoma of Stop 3; 6 - fragments of magmatic rocks from olistostrome of Stop 3; 7-8 - oceanic basalts Ulus-Cherga suite of the lower part of Cherga-Bulukhta section: 7 - volcanic rocks of Stop 6; 8 - average value ($n=14$); 9-10 - Ust-Syoma suite basalts of normal island arc from the upper part of Cherga-Bulukhta section: 9 - volcanic rocks of Stop 7; 10 - average value ($n=9$); 11-12 - Ust-Syoma basalts and dikes of gabbro-diabases from Cheposh - Ust-Syoma section of Stop 4: 11 - average values for basalts ($n=28$), 12 - average values for gabbro-diabase dikes ($n=20$); 13 - the fields of geodynamic environments for volcanic rocks from: I - island arc (Ia - boninites, Ib - tholeiites, Ic - calc-alkaline and Id - alkaline rocks); II - mid-oceanic ridge of back-arc spreading centers of intercontinental rifts; III - back-arc spreading centers and transform faults; IV - oceanic islands; V - oceanic islands and platform activation areas; VI - platform activation areas (flood basalts).

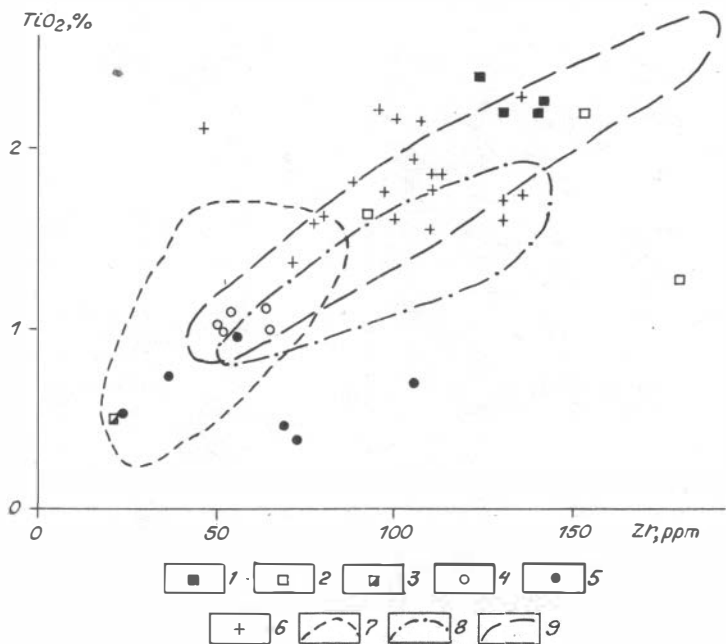


Fig. 10. Diagram TiO_2 -Zr for the rocks of the northern part (Stops 1, 6, 7) and south-eastern part (Stops 20, 21) of Gorny Altai (compiled by V.A.Simonov and M.M.Buslov):

1 - pillow lavas of Stop 1; 2 - basalts of Stop 6; 3 - basalts of Stop 7; 4 - pillow lavas of Stop 21; 5 - volcanic rock pebbles of Stop 20; 6 - amphibolites of Chagan-Uzun massif; 7-9 - boundaries of fields (Sharaskin & Zakariadze, 1982; Tarney & March, 1991; Saunders et al., 1980); 7 - island arc volcanic rocks, 8 - basalts of back-arc basins, 9- basalts of mid-oceanic ridges.

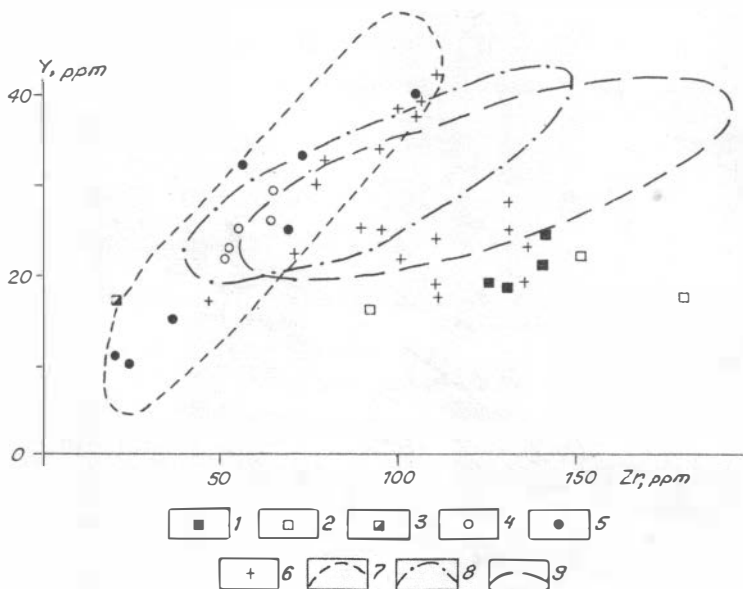


Fig. 11. Diagram of Y-Zr for rocks of the northern part (Stops 1, 6, 7) and southeastern part (Stops 20, 21) of Gorny Altai (compiled by V.A.Simonov and M.M.Buslov):

1 - pillow lavas of Stop 1; 2 - basalts of Stop 6; 3 - basalts of Stop 7; 4 - pillow lavas of Stop 21; 5 - volcanic rock pebbles of Stop 20; 6 - amphibolites of Chagan-Uzun massif; 7-9 - boundaries of fields (Sharaskin & Zakariadze, 1982; Tarney & March, 1991; Saunders et al., 1980): 7 - island arc volcanic rocks, 8 - basalts of back-arc basins, 9 - MORB.

Day 2. Characteristics of sedimentary-volcanic complexes of Early-Middle Cambrian arc-trench system. Study of composition and paleontological characteristics of the complexes mentioned and their underlying rocks of Early Cambrian accretionary prism.

Section Cheposh -Ust - Syoma (Stops 4-5)

Stop 4. Located 45 km from Stop 3 between Ust-Syoma and Cheposh Villages (fig. 12). Here, one of the most representative in Altai-Sayan area sections of Lower-Middle Cambrian island arc is observed. The lower horizons

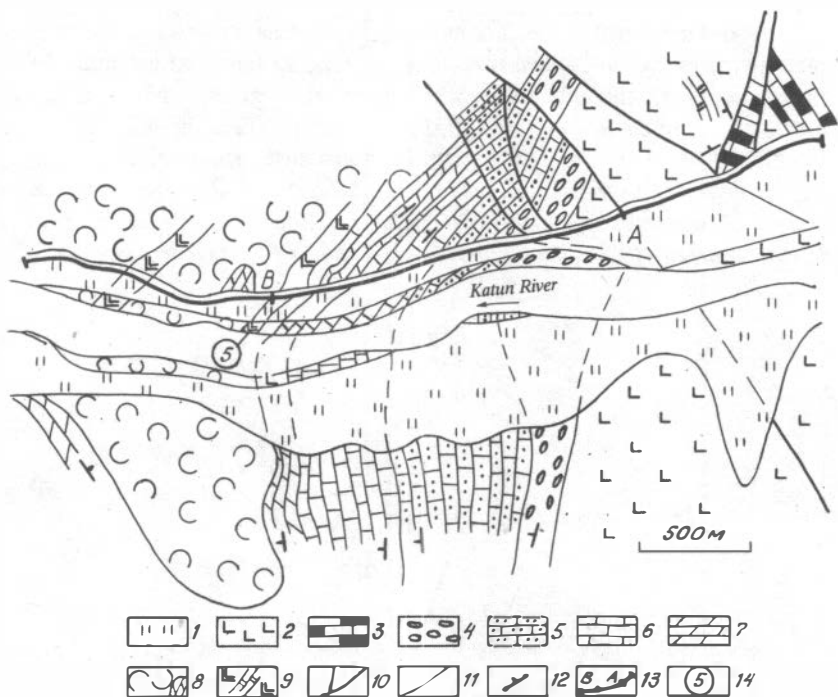


Fig. 12. The scheme of geological structure of a fragment of Early-Middle Cambrian normal island arc (the right bank of Katun River between Ust-Syoma and Cheposh Villages, Stops 4,5) (compiled by M.M. Buslov using materials of Repina & Romanenko, 1978):

1 - Quaternary deposits; 2-3 - Vendian rocks of Katun seamont: 2 - basalts of Manzherok suite, 3 - siliceous-carbonate rocks of Baratal suite; 4-9 - the Early-Middle Cambrian rocks of normal island arc: (4-5) - Shashkunar suite: 4 - conglomerates, 5 - sand-bearing limestones; 6 - limestones of Cheposh suite, 7 - terrigenous-carbonate Barangol suite, 8-9 - Ust-Syoma suite: 8 - andesite-basalt tuffs, greywackes with blocks of carbonate rocks, 9 - basic lavas; 10 - faults; 11 - stratigraphical contacts; 12 - direction of bedding plunge; 13 - the line of complete Cheposh - Ust-Syoma section and A - B section of Stop 4; 14 - location of Stop 5.

of section near Cheposh Village represent a fragment of Early Cambrian accretionary prism composed of the siliceous-carbonate sequence (Baratal

suite) and volcanic sequence (Manzherok suite) of Katun paleoseamant.

The Manzherok suite is composed of diabases, pyroxene basalts and their pyroclastics, dolomites, limestones, cherts, siliceous schists and shales. Basalts relate to tholeiite series with increased alkalinity analogous to the basalts of oceanic islands (table 3, fig.9, 13). Dolomites and limestones contain Vendian stromatolites and microphytolites: *Algotactis. sp. Ambigolamellatus sp., sp., Radiusus cf. sphaericus Z.Zhur., R. cf. badius Z.Zhur. Stratifera sp., - Osagia cf. composita Z.Zhur., O. aff. badius (Z.Zhur.), O.st. slobini Milst., O. cf.tenuilamellata Reitl., Nubecularites algonkiensis Posp., Conophyton sp.*

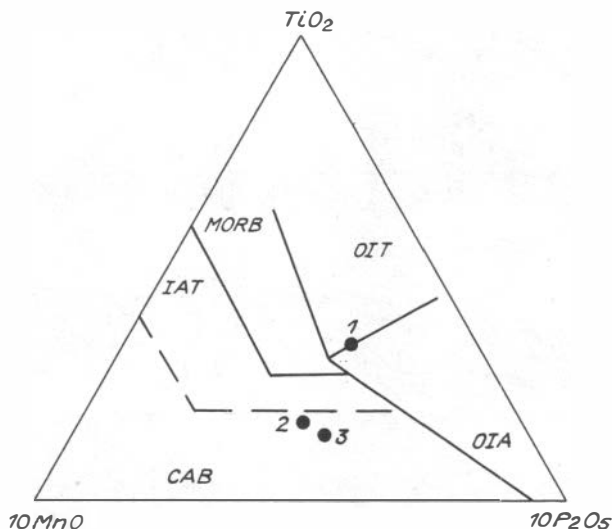


Fig.13. Bulk composition of magmatic rocks of Manzherok and Ust-Syoma suites in the diagram $TiO_2-10MnO-10P_2O_5$ for Stop 4. The points and numbers indicate on the average value for magmatic rocks:

1 - basaltic lavas of Manzherok suite, 2 - basaltic lavas and 3 - dikes of Ust-Syoma suite (compiled by M.M.Buslov comparable with fig.5).

Manzherok suite is connected with Baratal suite by gradual transitions. Transitional rock pockets consists of tuff-sandstones, large-block tuff-breccias and lavabreccias with the fragments of pyroxenites, diabases, limestones and dolomites.

The Baratal suite represents dolomites, dolomitized limestones, quartzites, cherts and somewhere carbonate schists and shales. Carbonate rocks contain stromatolites and microphytolites: *Algotactis kabirsaensis* Posp., *Ambigolamellatus* sp., *Radiosus* cf. *sphaericus* Z.Zhur., *R.* cf. *badius* Z.Zhur., *Osagia* sp., *O* cf. *tenuilamellata* Reitl., *Conophyton* sp., *Occultus* sp., *Jasenia* sp.

Stromatolites and microphyllites indicate the Vendian age of Manzherok and Baratal suites.

To the south-east in the basin of Edigan River (the right tributary of Katun River) among the rocks of Katun seamount there are tectonic sheets of Early Cambrian olistostrome. It is composed of chlorite and siliceous-chlorite schists, calc-sandstones and calc-gravellites and breccias with the fragments of stromatolite dolomites, limestones, porphyrites and phosphorites. Vendian species are found in stromatolite fragments: *Spongiostroma* cf. *kaizasensis* Posp., *Algotactis* sp., *Stromatactis* sp. This type stromatolite dolomites and limestones are widespread among the rocks of Baratal and Manzherok suites of Katun seamount. Siliceous-chlorite schists composing the olistostrome matrix contain spicules of Early Cambrian sponges (Afonin, 1976).

Lower-Middle Cambrian sedimentary-volcanic rocks relate to normal island arc. Through basal conglomerates they unconformably overlie the rocks of Katun seamount. Sedimentary-volcanic section in the right bank of Katun River is following (Repina & Romanenko, 1978):

1. Shashkunar suite with basal conglomerates of 250 m thickness. The pebbles of conglomerates include quartzites, volcanic rocks, schists and limestones. In limestone pebbles from the right bank of Katun River stromatolites and microphytolites are found: *Occultus* sp., *Stromatactis palaeozoicus* Posp., *Gleocapsella* sp., *Paleomicrocystis* sp., *Renalcis* sp., trilobites, radiolarians, and spicules of sponges. In the upper horizons of conglomerates pebbles become fine, the interlayers of bedded sandstones (from coarse to fine-grained with carbonate cement) which pass into sand-bearing limestones and finally into homogeneous grey, dark grey and black plated limestones are found.

The thickness of Shashkunar suite - 400-500 m. After I.T.Zhuravleva limestones contain the relics of Archaeocyata: *Archaeolynthus* sp., *Vologdinocyathus* sp., *Ethmophyllum* cf. *caveaquadratum* Vologd., *Squamosocyathus* cf. *caveaquadratus* (Vologd.); Trilobites: *Parapagetia katunia* Rep., *P. limbata* Rep., *P. paleoformis* E.Roman., *P.* sp., *Miraculaspis picta* E.Roman., *Serrodiscus fossuliferus* Rep., *S. levis* Rep., *S.* cf. *spinulosus* Rasetti, *S.* ? sp., *S. lepidus* E.Roman., *Parapagetia* sp., *II*, *Stigmatiscus* ? sp.,

Semadiscus sollinnis E. Roman., *Neopagetina infirma* Jegor., *Neocobboldia altaica* Polet., *Pagetia altaica* Polet., *P.katunica* Polet., *Ladadiscus limbatus* Pokr., *L. sp.*, *Tannudiscus altus* Rep., *Calodiscus mirus* E. Roman., *C. sp.* *Bergeroniellus certus* Jegor., *B.sp.*, *Laticephalus ? sp.*, *Bonnia sp.*, *B. cf. prima* Pokr., *Eoptychoparia sp.*, *Antagmidae gen. indet.*, *Alokistocaridae gen. indet.*

Composition of the Shashkunar suite organic remnants allows comparison of host deposits and analogous deposits in the other sections of Gorny Altai and to refer them to the layers with *Parapagetia-Serrodiscus*. Shashkunar suite is believed to have the same age with the rocks of Lower Cambrian Sanashtykgol horizon of Altai-Sayan folded area.

2. The Cheposh suite is composed of grey and light grey limestones having planar texture in the lower part and massive texture in the upper part.

Four levels characterized with a definite complex of organic remnants are distinguished in the Cheposh suite deposits (upwards) (fig.14):

2-1. Grey and dark-grey banded limestones. In the base of the suite there are: *Stromatactis paleozoicus* Posp., *Ambigolamellatus sp.*, *Osagia sp.*, bad-preserved remnants of *Trilobites* and *Brachiopods*. Five meters upwards the suite base one limestone interlayer contains the remnants of *Trilobites* *Onchocephalina sp.* The upper part of package contains trilobites: *Bergeroniellus certus* Jegor., *Bergeroniaspis sp.*, *Onchocephalina aff. partenus* Rep., *O. cf. plana* Rep., *O. aff. flabilis* Rep., *O. cf. accuminata* Rep., *Laminurus cf. insuetus* Rep., *Binodaspis cf. prima* Pokr., *Edelsteinaspis sp.*, *Redlichina sp.*, *Bathyriscellus tersus* E. Roman.; The remnants of *Archeaeocyata-Ethmophyllum Meek* are rare; algae: *Renalcis sp.*; brachiopods: *Kutorgina paucicostata* Aks., *K. sp.*, *Nisusia sp.*; bivalve mollusk: *Cambridium sp.*

2-2. Massive grey limestones with high content of algae remnants.

Microphitolite remnants observed: *Osagia cf. irregularis* Reitl., *Ambigolamellatus cf. horridus* Z. Zhur., *O.cf. poletaevae* Krasn. Also, there are *Archeocyata* remnants: *Retecyathus sp.* In thin-section the tests of *Trilobites* together with *Archeaeocyata* are found.

2-3. Light-grey, massive, marble-like limestones.

In the base of package the *Archeaeocyata* remnants are found: *Archeocyathus cf. kuzmini* (Vologd.), *Claruscyathus sp.*; stromatolites: *Palaeomicrocystis ? sp.*; algae: *Renalcis cf. granosus* Vologd., *Botominella ? sp.*; trilobites: *Parapoliella ? sp.*, *Onchocephalina cf. partenus* Rep., *O. cf. plana* Rep., *O. aff. flabilis* Rep., *O.sp. II*, *Bathyriscellus tersus* E. Rom. *Solontzella sp.*; brachiopods: *Kutorgina sp.*, *Kreticostata* Aks. Stratigraphically upwards *Archeaeocyata* remnants are found: *Tegerocyathus sp.*, *Ethmophyllum sp.*;

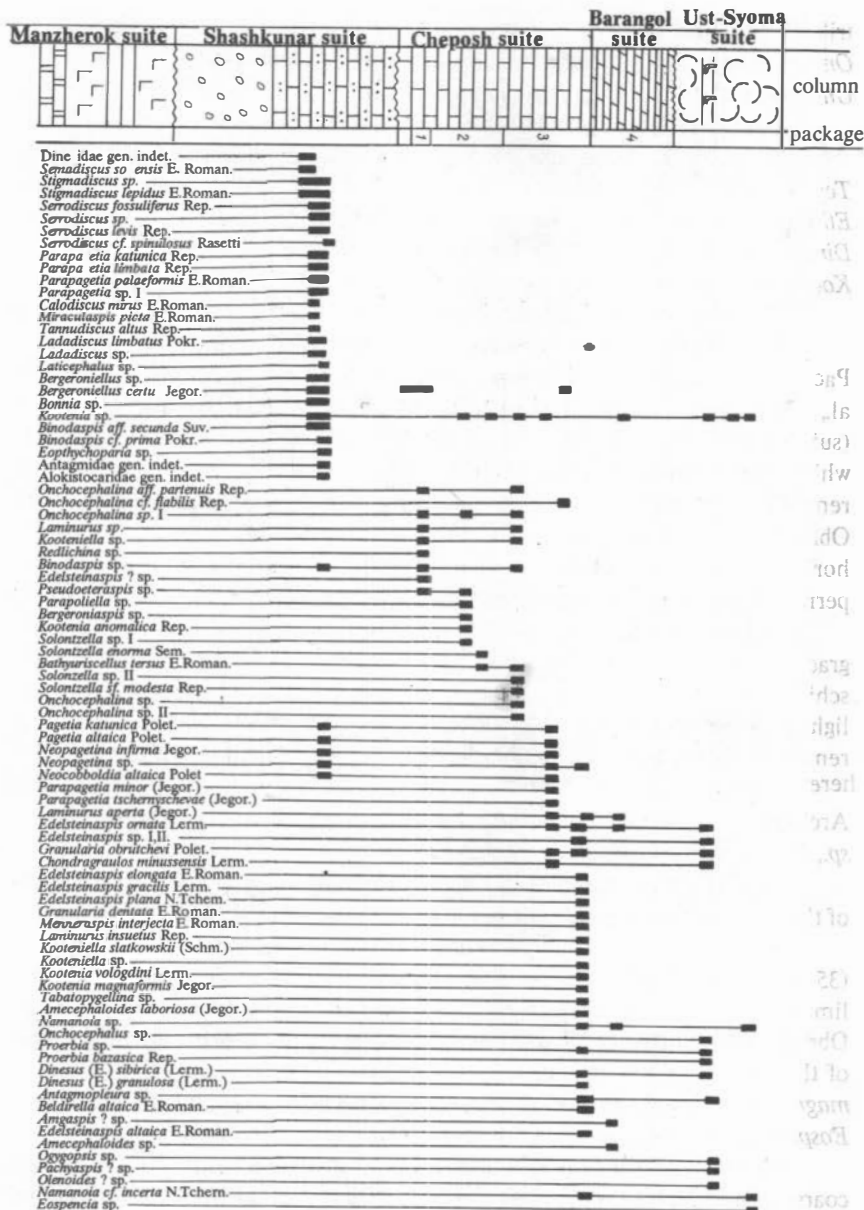


Fig.14. Distribution of trilobite remnants throughout the Cheposh - Ust-Syoma section (Stop 4) in the right bank of Katun River (see captions to fig.12) (Repina & Romanenko, 1978).

trilobites: *Kootenia anomalica* Rep., *Bathyuriscellus tersus* E.Roman., *Onchocephalina* sp., *Ptychopariidae* gen. indet., *Solontzella enormis* Sem., *Onchocephalina* cf. *flabilis* Rep., *Kooteniella* sp.

2-4. Massive, grey and dark-grey, marble-like limestones.

In 10-15 m from the base package the Archaeocyata are found: *Tegerocyathus* aff. *edelsteini* (Vologd.), *T.* aff. *abacanensis* (Vologd.), *Ethmophyllum* sp.; algae: *Proaulopora* sp., *Epiphyton* sp., *Renalcis* sp.; trilobites: *Dinesus* sp., *Kooteniella* cf. *slatkowskii* (Schm.), *Laminurus* sp., *Namanoia* sp., *Kootenia* sp., *Bergeroniellus certus* Jegor.

The total thickness of Cheposh suite is 450-500 m.

Deposits in a section from the upper horizons of Package 1 to the top of Package 3 contain a typical fauna complex of Solontsovsk horizon (Repina et al., 1964) - the layers with *Onchocephalina* can be considered as a separate unit (subdivision). The deposits of package 4 contain trilobite remnants (fig.14) which differ significantly from trilobites of previous complex due to essential renewal of species and genera set. They could be correlated with the deposits of Obruchev horizon of the Early Cambrian in other regions and with the Elansk horizon of Siberian platform. The characteristic features of this complex permit to distinguish the layers with *Edelsteinaspis-Kooteniella*.

3. The Barangol suite is connected with its underlying Cheposh suite by gradual transitions and composed of grey and dark-grey marls, mudstones, schists, tuffs and lavabreccias of pyroxene porphyrites with lenses of schists and light-grey limestones. The suite thickness does not exceed 200 m. The fauna remnants belong to lenses and blocks of limestones. Microphitolites are found here: *Renalcis* sp., *Proaulopora* sp., *Ambigolamellatus* sp., *Osagia* sp., *Renalcis* sp., Archaeocyata: *Tegerocyathus* sp., *Ajacycyathus* sp.; Trilobites: *Gaphuraspis* ? sp., *Brachipods*: *Kutorgina* sp., *Wimanella* sp.

At a whole the complex of organic remnants of Barangol suite is typical of the layers with *Edelsteinaspis-Kooteniella* of Obruchev horizon.

4. Ust-Syoma suite unconformably overlies the Barangol suite. The thick (35 m) horizon of lavabreccia is located in the base of suite. The blocks of limestones from lavabreccias contain the numerous fauna remnants of Obruchev horizon of the Early Cambrian. Besides the above trilobites typical of the layer with *Edelsteinaspis-Kooteniella*, here the *Oleoides* ? sp., *Kootenia magnaforms* Jegor., *Namanoia* cf. *incerta* N.Tchern., N., *abunda* E.Roman., *Eospencia* sp., *Ogygopsis* sp., *Chondramonocare* sp. I, Ch. sp II were found.

Stratigraphically upwards the suite is made up with predominating coarse-grained tuffs, lavabreccias and clastolites with giant blocks of limestones

and marls somewhere containing Lower Cambrian fauna. Towards Ust-Syoma Village the coarse-grained greywackes and tuff-like rocks appear. The basaltic lavas have subordinate significance (up to 10-20%) and represent pyroxene-plagioclase, pyroxene and plagioclase porphyrites mainly related to the lower parts of suite section.

The majority of volcanic rocks have middle-coarse porphyry and sometimes aphanite texture. Porphyry grains compose up to 30-50% of the rock volume. Pyroxene is enstatite and clinopyroxene varying from diopside to augite. According to petrochemistry characteristics, the volcanogenic rocks of Ust-Syoma suite differ from Manzherok suite rocks being related to calc-alkaline and boninite series of island arcs (table 3, fig.9, 13, 15).

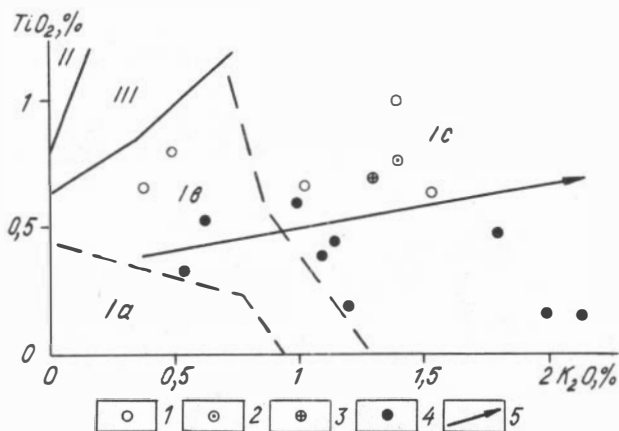


Fig.15. Diagram of TiO_2 - K_2O for Early-Middle Cambrian rocks and melt inclusions from clinopyroxenes of Cheposh - Ust-Syoma section (Stops 4,5) (compiled by V.A.Simonov using the diagram of Yu.V.Mironov, 1991).

1- basalts and porphyrites of Ust-Syoma suite; 2- average composition for Ust-Syoma suite basalts; 3- average composition for diabase dikes co-magmatic to Ust-Syoma suite (see table 3); 4- homogenized melt inclusions in clinopyroxenes from porphyrites of Ust-Syoma suite; 5- compositional trend for rocks and melt inclusions in island arc assemblages of Teletskoye Lake district (see Route B text); 6- magmatic rock fields from: I- island arcs (Ia- boninites, Ib- tholeiites, Ic- calc-alkaline); II- mid-oceanic ridge, back-arc spreading centers and transform faults; III- back-arc spreading centers and transform faults.

Vendian and Early-Middle Cambrian rocks along the Katun River right bank are crossed by numerous dikes of gabbro-diabases and diabases up to several meters thickness. According to composition the dikes are co-magmatic to sub-boninites of Ust-Syoma suite (table 3, fig.9, 13, 15) and characterize the magmatism of the initial stages of island arc development.

Stop 5. Located in the right bank of Katun River (fig. 12). The outcrops of basal lavabreccias of Ust-Syoma suite are found here. The central part of lava flow represents clinopyroxene porphyrites. Bulk composition of lava is cited in table 3, number 10. The edges of pyroxene crystals are often replaced with hornblende and chlorite. Non-altered porphyritic grains of clinopyroxenes are found, as well. They contain a lot of primary melt inclusions. Chemical compositions of three clinopyroxene crystals are cited in table 4. According to the content of main oxides the crystals reveal compositional zoning. From the center to the edge of U/S-92-3 crystal a significant increase of Si, Ti, Al, Cr, Fe, Mn and Mg is observed. Only Ca-content decreases.

Poor in Ti pyroxenes are enriched in Mg. In the diagram $\text{SiO}_2/100$ - TiO_2 - Na_2O they fall on the field of pyroxenes from boninites of the modern primitive ensimatic island arcs in the western part of Pacific Ocean (fig.16).

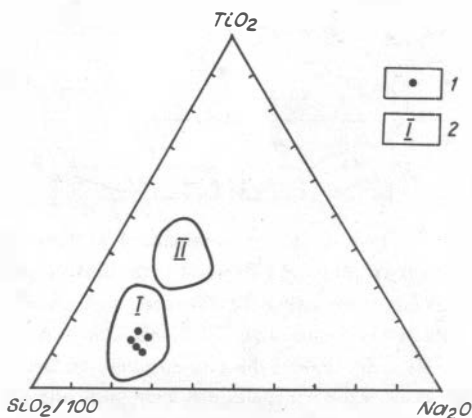


Fig.16. Diagram $\text{SiO}_2/100$ - TiO_2 - Na_2O for clinopyroxenes from sub-boninite lava of Ust-Syoma suite (Stop 5) (compiled by V.A.Simonov using the data Peive (Ed.), 1980; Bogatikov (Ed.), 1985; Meen, 1987; Vysotsky, 1989; Dobretsov (Ed.), 1991b; Tsameryan et al., 1991).

1- pyroxenes of Ust-Syoma suite; 2-I - the fields of pyroxene composition: 2-I - from boninites of Pacific ocean, 2-II - from oceanic and island arc tholeiites.

In the diagram $\text{TiO}_2\text{-K}_2\text{O}$ (fig.15) all the compositions of homogenized melt inclusions in clinopyroxenes (table 5) fall in the island arc fields and exhibit a trend from tholeiites (nearby boninite field) to calc-alkaline series. A good correlation between bulk compositions and melt inclusions data is noted. Only decreased Ti content in inclusions compared to its content in a rock should be mentioned. Concerning the formation of Ust-Syoma suite porphyrites in the initial stages of island arc systems, the conclusions made using peculiarities of clinopyroxene composition, were confirmed. According to melt inclusions in clinopyroxenes a complete path of island arc development was traced: from sub-boninite through tholeiite to calc-alkaline series. Thus, the data obtained after study of melt inclusions composition in clinopyroxenes together with the data on minerals and rocks testify to the evolution of island arc magma of Ust-Syoma suite have essential similarities with the Vendian-Cambrian island arc rocks in Teletskoye Lake district (see description of Route B).

Generally, lava flow (Stop 5) which belongs to boninite series rocks illustrates magmatism of the initial stage of normal island arc formation appeared on the Cambrian accretionary prism.

Section Cherga-Bulukhta (Stops 6-8)

Located in the Bulukhta River and Cherga River basins to the west from Cherga Village. Here, Cherga-Bulukhta section (fig.17) consists of three terranes which belong to: 1) third layer of oceanic crust or back-arc basin; 2) normal island arc and 3) fore-arc trough. Their relationships are commonly interpreted as stratigraphic, but as it is seen in fig.10, it can represent a tectonic combination of three terranes which characterize the various zones of island arc.

Basaltic-sedimentary sequence of Lower Cambrian oceanic crust consists of the interlayering pillow-lavas of pyroxene and plagioclase basalts, tuffs, tuff sandstones, siliceous rocks, shales and limestones. In limestone the bad-preserved Archaeocyata and Trilobites are found: *Dinesidae*, *Dorypygidae* and *Agnostidae* which are comparable with those from the Lower Cambrian Elansk horizon of Siberian platform (Volkov, 1966). Basalts of this sequence are comparable with MORB, but taking into account the big thickness of sedimentary sequence and occurrence of tuffogenous rocks, they can represent a complex typical of back-arc basin. The basaltic-sedimentary sequence with angular unconformity is overlain by lavabreccias of the Middle Cambrian Ust-

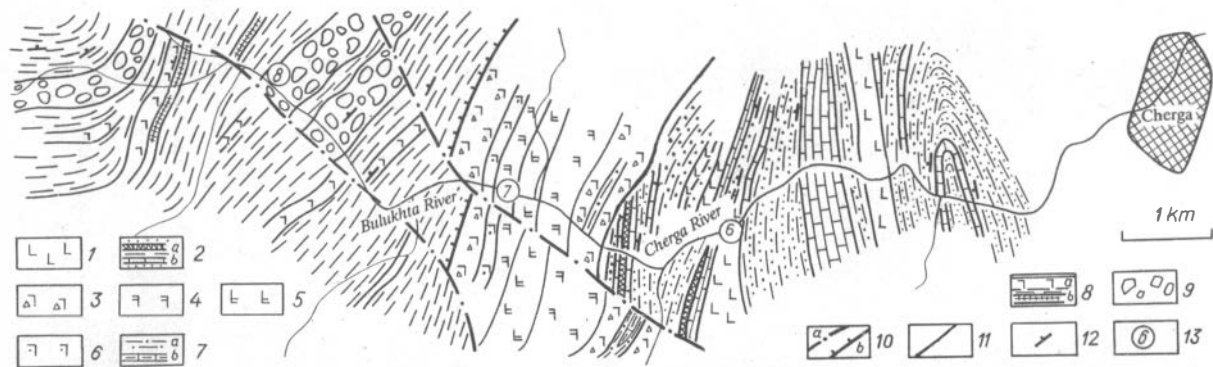


Fig.17. Geodynamic complexes of Bulukhta and Cherga River basins (Stops 6, 7, 8) (compiled by M.M.Buslov using materials of V.V.Volkov, 1966):

1, 2 - basaltic-sedimentary Usul-Cherga suite of Early Cambrian oceanic crust: 1 - pillow-lavas of pyroxene basalts, 2 - sandstone-mudstone rocks with horizons of cherts (a) and limestones with Early Cambrian fauna (b); 3-7 - Middle Cambrian rocks of normal island arc: 3-5 - lavabreccias: 3 - coarse porphyry, 4 - aphyric, 5 - fine porphyry; 6 - volcanic sandstones, 7 - horizons of clayish rock (a) and limestones (b); 8-9 - Middle-Late Cambrian rocks of fore-arc trough: 8 - polymict and volcanic sandstones, mudstones and tuffs with horizons of andesite-basaltic lavas (a) and cherts (b), 9 - olistostrome; 10 - faults: strike-slips (a) and thrusts (b); 11 - boundaries of stratigraphical (?) overlying of Ust-Syoma suite island arc rocks over oceanic rocks of Ulus-Cherga suite; 12 - direction of bedding plunge; 13 - location of observation points.

Syoma suite relating to normal island arc. The basal horizon of Ust-Syoma suite of 100 m thickness consists of the fragments of basaltic porphyrites and lying below basaltic-sedimentary sequence: siliceous and sand-schist rocks and marble-like limestones.

The Ust-Syoma suite is predominantly composed of basaltic lavabreccias: pyroxene, pyroxene-plagioclase and plagioclase basalts, aphyric basalts and rarely andesite-basalts and dacites. Basalts have spilitic or amygdaloidal texture. The thickness of some horizons of lavabreccias changes from n meters to $10 \cdot n$ meters.

Somewhere, basaltic lavas are crossed by sills and dikes of gabbro-diabases which fragments are often included in breccias. Lavas are interlayering with basaltic and andesite-basaltic tuffs, siliceous rocks, mudstones and volcanic sandstones.

Together, the basaltic-sedimentary and volcanic sequences form a single tectonic sheet, over which the rocks of Middle-Late Cambrian fore-arc trough are thrust. They represent siliceous and clayish-siliceous rocks, sandstones, olistostromes, breccias and sometimes lavas of pyroxene-plagioclase porphyrites and their tuffs.

Stop 6. Located 4 km from Cherga Village (fig.17) to the west, on the left bank of Cherga River. Here, rock cliff exposes a boundary between two lava flows from the Lower Cambrian basaltic-sedimentary sequence (table 6). Lava flows represent pillow-lavas in which the pillows have 1-2 m length. Lava rocks were metamorphosed in greenschist facies. The eastern lava flow is composed of amygdaloidal pyroxene basalt. The pseudomorphs after pyroxene filled with epidote and chlorite are wide spread (sample 6-1). Marginal part of the western lava flow is amygdaloidal plagioclase basalt, which towards the center of lava bed is changed to hyalocrystalline plagioclase dolerite (sample 6-4). Amygdales of 1 cm in diameter are filled by calcite. The boundary between flows is made up with breccia of metabasalt. Breccia consists of epidote-chlorite matrix with the fragments of marble-like limestones and plagioclase metabasalts (sample 6-2).

The chemical and geochemical characteristics of basalts from the lower part of Bulukhta-Cherga cross-section is cited in table 6. In the diagrams (fig.18 and 19) they fall in the MORB field and partly in the field of oceanic island basalts.

The central part of pillow from the western lava flow (sample 6-3) contains less Si, Ti, Al, Fe, alkalies, P, REE and more Mn, Mg and Ca compared with the marginal part. Lavabreccia (sample 6-2) is intensively

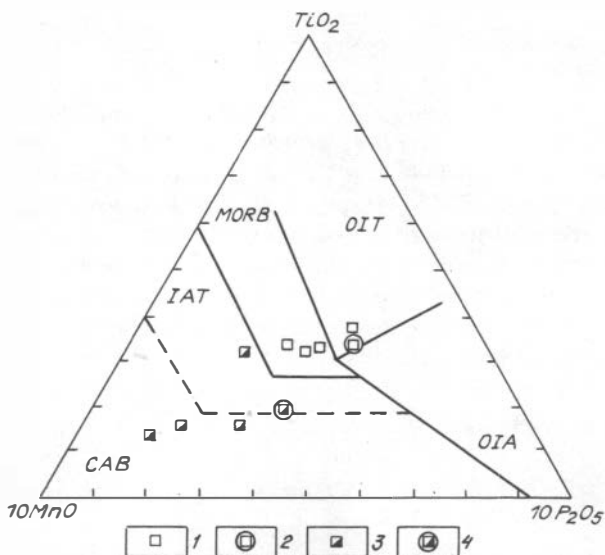


Fig.18. Diagram of TiO_2 - $10MnO$ - $10P_2O_5$ for basalts of Stops 6,7, Cherga-Bulukhta section (compiled by M.M.Buslov comparable with fig.8,13):

1 - oceanic basalts of Ulus-Cherga suite (Stop 6), 2 - average value for basalts ($n=14$) of Ulus-Cherga suite; 3 - island arc basalts of Ust-Syoma suite (Stop 7); 4 - average value for Ust-Syoma suite basalts.

enriched in K, Rb and Zr and contains less Na, Mg, Fe, Ti and Sr compared with the main flow body. According to trace element contents (Y, Zr) the rocks of the western lava flow correspond to MORB (fig. 10, 11).

Commonly, the oceanic characteristics predominate in basalts of the lower part of Bulukhta-Cherga section (that is N-MORB type basalts). Together with sedimentary rocks they are considered as the Early Cambrian fragment of the third layer of oceanic crust of marginal sea, which was put into the Early Cambrian accretionary prism during the last stages of its formation.

Stop 7. Located in 3 km from Stop 6 in the left bank of Bulukhta River (fig.17). Here, rock cliff exposes lavabreccia belonging to Middle Cambrian island arc. Major and trace element concentrations of lava flow are shown in table 4.

The major volume of lava is composed of plagioclase porphyrite (samples 7-1 and 7-2) in which a block of diabase (samples 7-1a) of 1 m length is included. The marginal parts of lava flow are composed of lavabreccias (sample 7-3). The lava rocks containing a lot of magnetite grains have undergone dynamometamorphism and chloritization.

According to chemical and geochemical data, the basalts from Stop 7 significantly differ from oceanic basalts of Stop 6. In the diagrams $\text{TiO}_2\text{-K}_2\text{O}$ (fig.9) and $\text{TiO}_2\text{-10MnO-10P}_2\text{O}_5$ (fig.18) they fall in the field of island arc basalts. Data on trace element concentrations (fig.10,11) confirm the island arc type of basalts.

Stop 8. Located in 4 km from Stop 7 (fig. 17). Near to the bridge over Bulukhta River there are outcrops of olistostromes. Debris is mainly composed of siliceous-carbonate rocks likely of Baratal suite; the well-rounded pebbles of basaltoids, granitoids and limestones with Archaeocyata are found, as well.

ROUTE A

Syoma Pass - Chiketaman Pass - Aktash Village - Chagan-Uzun Village

Day 3. Trip path is divided into two routes: A and B. Route A continues along Chuya motorroad up to Kurai zone in the south-eastern part of Gorny Altai. Route B returns to Gornoaltaisk and goes to the east for Teletskoye Lake in the north-eastern part of Gorny Altai.

General review (stops 9-15)

The route's length is about 300 km. The route crosses the rhythmically bedded sand-schistose rocks of Middle-Upper Cambrian Anui-Chuya fore-arc through, the Ordovician-Silurian terrigenous-carbonate sequences formed in the collisional stage and the Devonian magmatic rocks of active margin.

Composition and structure of the Devonian active margin volcanic complex can be observed in the left bank of Ursul River from Tyekta Village to Ongudai Village. From 595 to 640 km of Chuya motorroad the sediments, volcanic rocks, tuffs, and rocks of the vent facies of Devonian volcanos are exposed. Here, they form the eastern part of a large syncline fold complicated by second order folds and faults (fig.19).

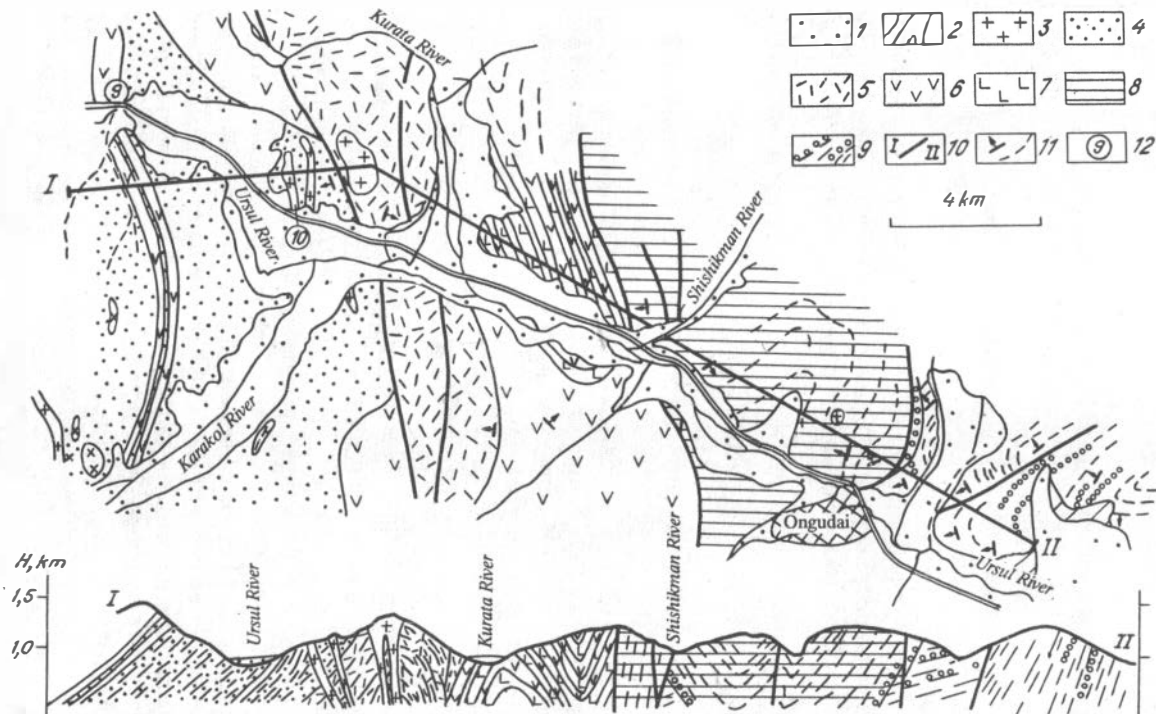


Fig.19. The scheme of geological structure of volcanic part of Hercynian active margin of Ursul River basin (Stops 9,10) (Polyakov (Ed.), 1986):

1 - Quaternary deposits; 2 - gabbro-diabases of Charysh intrusive complex. Kuratin volcanic complex: 3 - dacite porphyries, spherolites and micro granites (bodies of vent and subvolcanic facies); Kuratin suite (D₂): 4 - sandstones and mudstones, 5 - tuffs (D₁), 6 - rhyolite-dacite lavas, 7 - andesite lavas; Ongudai suite (D₁): 8 - andesite-basaltic and andesite lavas; Karakudiyur suite: 9 - sandstones, conglomerates and mudstones; 10 - faults; 11 - bedding elements; 12 - location of Stops 9, 10.

Volcanic complex of Hercynian active margin (stops 9-10)

Devonian volcanics relates to two complexes of various age: Early Devonian Ongudai andesite complex and Middle Devonian Kuratin rhyolite-dacite complex.

The rocks of the lower Ongudai complex are widespread along the motorroad from Shishikman Village to Ongudai Village. Within this part of the motorroad the lavas of pyroxene porphyrites together with andesitic pyroclastic rocks form the Ongudai suite. The rocks of Ongudai suite were folded into asymmetric fold which axis is steeply dipping to the south-west. The limbs of this fold are made up with rocks of various facies: pyroclastic rocks predominate in the north-western limb - coarse-grained andesitic tuffs and lavabreccias, the lava flows occur in the south-eastern limb. The thickness of Ongudai suite is 2500m.

The Kuratin complex is composed of the rocks of Kuratin suite and hypabyssal intrusions which are divided into vent and subsurface intrusive bodies. The rocks of Kuratin suite are subdivided into three subsuites in which volcanic rocks are irregularly developed: they almost completely compose the lower subsuite, predominate in the middle subsuite and rare in the upper subsuite. About 70% of total rocks volume of 4500 m section relate to volcanic rocks. Upwards, andesite rocks and tuffs are changed with acid rocks which almost completely make up the upper parts of a section, whereas the andesitic porphyrites are absent. Acid pyroclastic deposits are widespread in the middle part of Kuratin suite.

The rocks of Kuratin suite are crumpled into numerous complicated and steep additional folds which appearance makes an impression about the giant thickness of the whole suite.

Within the right bank of Kurata River a volcano vent passes through the pyroclastic deposits of the middle subsuite of Kuratin suite. The major body forms a neck reaching 300-500 m in diameter. To the west the smaller lense-like bodies are situated. All of them represent the extrusive rocks which texture changes with the depth of occurrence: the tops of necks are felsite and spherolite varieties of rhyolite-dacite porphyries, the lower parts of the same bodies are crystalline microgranite-porphyries and granophyries. There is a zonation on the plane: the central parts of bodies are composed of rhyolite porphyries, the peripheral ones composed of spherolites and quartz-feldspar dacite porphyries. The periphery of necks also contain composite fluidal and breccia spherolite porphyries and alkaline quartz rhyolite-dacite porphyries.

Subvolcanic intrusions are located near to vent bodies and some are far from them. All of them have small dimensions: from few meters to first hundreds meters. Compared with vent facies bodies the subvolcanic intrusions have more homogeneous structure and rock composition. They have fluidal and taxitic textures and no predominate zonation. The dacite porphyries and microdiorite porphyrites are mainly developed.

There are four groups of Devonian volcanic rocks having the common comagmatic petrochemical features (table 7): 1) The earliest lavas composing the Early Devonian Ongudai suite correspond to andesite-basalts; 2) the next group of volcanic rocks represents andesites; 3) most spread rock group of the second half of Middle Devonian (Kuratin suite) has dacite composition; 4) the youngest subvolcanic bodies have rhyolite composition.

Stop 9. Located near 612 km of the Chuya motorroad. The outcrops of the upper sedimentary sequence of Kuratin suite are exposed in the left bank of Ursul River. The sequence is composed of interbedding dark-grey and black calc-sandstones, shales, marls and limestones. Terrigenous rocks contain Franian Brachiopods (Late Devonian) defined by R.T.Gratsianova: *Productella subaculeata* Murch., *Cyrtospirifer achmet* Nal., *C. tentaculum* (Vern.), *C. schelonicus* Nal., *Lamellispirifer ales* (Khalf.), *Anathyris supraphalaena* Khalf., *Retzia tshernyschewi* Peetz; Bryozoans: *Fistulipora subsphaerica* Nekh., *Amplexopora devonica* Nekh., *Batostomella tshuensis* Nekh., *Fenestella buratinensts* Krasnop., *F. pioneri* Krasnop., *Hemitrypa devonica* Nekh., *Petalotrypa perforata* Nekh., *Reteporina carinata* Krasnop., *R. carinostriata* Nekh., *Semicoscium altaicum* Nekh., *S. bugusunicum* Nekh., *Isotrypa tuberculata* Nekh., *Goniocladia antiqua* Nekh.

Terrigenous rocks have western dipping ($50-60^{\circ}$) and contain two cleavage systems: 1) Dipping azimuth 290° , dipping angle 75° and 2) dipping azimuth 100° , dipping angle 15° . The first cleavage system occurs only after schists with surface traces of ripple. Rocks include abundant pyrite grains. Stratigraphically upwards dacite and subvolcanic rhyolite bodies are seen.

Stop 10. Located 6 km to the east from Stop 9. Here, the outcrops of subvolcanic rhyolite porphyry (sample K-1) are found among the Kurai suite sandstones. Porphyry represents a green-grey dense rock with cryptocrystalline matrix in which there are some grains of quartz, rose orthoclase and plagioclase. Orthoclase is used to be replaced with albite.

The plutonic rocks of Hercynian active margin are most widespread in the Chiketaman pass district. The Word "Chiketaman" means "plane sole" translating from Altaian language. Height of the pass reaches 1800 m. A panorama of the central part of Gorny Altai is well observed.

The granitoids are named as the Yaloman group. From the north to the south the Chuya motorroad crosses Chiketaman, Kadrin, Yaloman and Ust-Chuya plutons (fig.20). All these plutons form a single areal available for study. They intrude into the Cambrian, Ordovician and Lower Silurian terrigenous deposits and, somewhere, Middle Devonian sedimentary-volcanic rocks.

The first detail investigations of this group plutons were made by Yu.A. Kuznetsov (1936, 1939). He united them into the granodiorite-tonalite complex of Carboniferous age. Yu.A. Kuznetsov described xenoliths and phenomena of wall rock re-working around the Yaloman group plutons. There was revealed a lot of various hybrid quartz diorites, tonalites and other granitoids of endocontact zone being an unique assemblage of rocks which are characterized by unusual combination of basic zonal plagioclases with abundant quartz (labrador tonalites, labrador quartz monzonites and other "basic" granitoid varieties). Later Yu.A.Kuznetsov (1964) considered granodiorite-tonalite complex of the Central Altai as an example of autochthonous batholith formations and suggested that these plutons were formed due to magmatic replacement of wall rocks.

Nowadays, some geologists (Kononov, 1969; Izokh et al., 1987) consider the Yaloman group plutons as the multi-phase igneous rock series which correlates well with the Carboniferous (C_1 - C_2) gabbro(diorite)-granite series of adjacent East Kazakhstan region. There are 4 phases in their evolution: 1) gabbro-diorite phase (gabbro, quartz, quartz-bearing and quartz-free diorites and tonalites); 2) granodiorite phase (granodiorites and tonalites); 3) adamellite phase (adamellites passing into essentially plagioclase granites, granodiorites, and quartz monzonites); 4) alaskite phase (alaskites, leucogranites and leucoadamellites).

However, there are lot of data that in these plutons at least two rock series are combined: Devonian and Late Carboniferous-Permian. The Devonian series includes the rocks of gabbro-diorite and granodiorite phases, the Carboniferous-Permian series includes the rocks of adamellite and alaskite phases, somewhere the rocks of diorite-granodiorite phases.

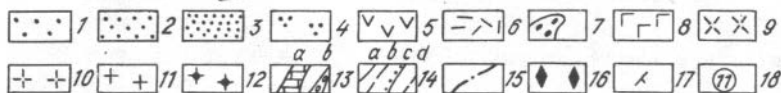
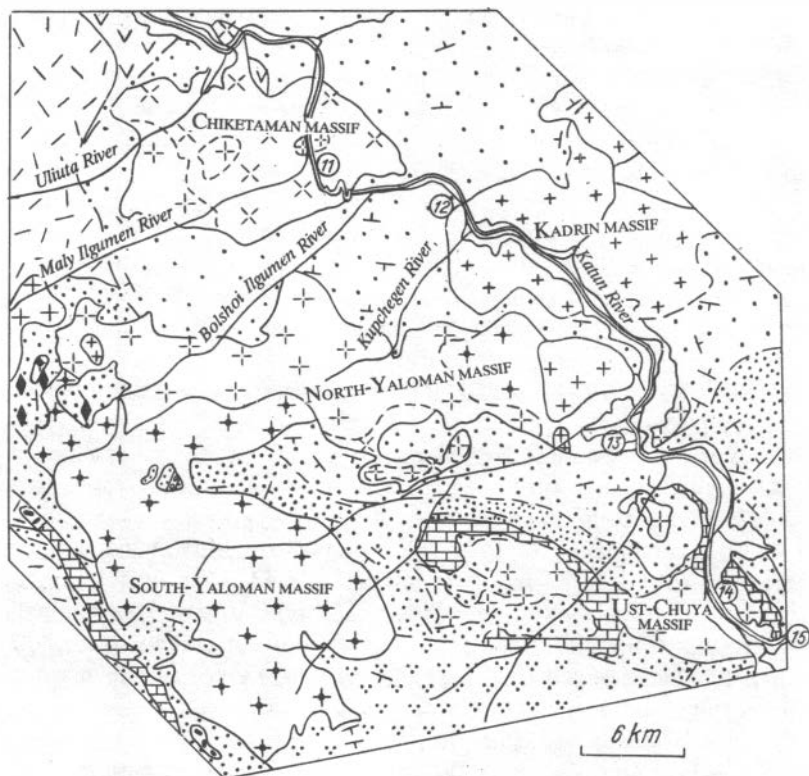


Fig.20. The geological structure scheme of plutonic part of Hercynian active margin (compiled by M.M.Buslov using materials of Dobretsov (Ed.), 1991a): 1 - Middle-Upper Cambrian flysch-like sequence (Gorno-Altai series); 2 - Middle-Upper Ordovician limestone-terrigenous deposits; 3 - Lower Silurian terrigenous-limestone deposits; 4 - Lower Devonian red terrigenous deposits; 5 - Lower Devonian andesites, basalts, their tuffs, sandstones and mudstones (Ongudai suite); 6 - Middle Devonian rhyolites, dacites, their tuffs, sandstones and mudstones (Kuratin suite); 7 - subvolcanic rhyolites and dacites of Middle Devonian Kuratin complex; 8 - Early Devonian pre-granite hornblende gabbro; 9-10 - Early-Middle Devonian quartz diorites and biotite-hornblende tonalites (9) and granodiorites (10); 11 - Carboniferous granites and adamellites; 12 - Permian alaskites and leucogranites; 13 - marking horizons of Lower Silurian limestones (a) and conglomerates (b); 14 - geological boundaries traced (a), supposed (b), discordant (c), petrographical (d); 15 - faults; 16 - magnetite-bearing skarns; 17 - bedding elements; 18 - Stops location.

The rocks of diorite group of Chiketaman, Kadrin and Yaloman plutons (together) occupy about 12% of total area, the rocks of granodiorite group - 25%, adamellites - 60% and alaskites - 3%. In the Chiketaman pluton composed mainly of tonalites, quartz diorites and granodiorites, the rocks of diorite group and granodiorite group occupy about 23% and 77% of total area, correspondingly.

In Yaloman pluton which rock assemblage is close to Kadrin pluton, there are following relationships: diorites - 4%, granodiorites - 23%, adamellites - 70%, alaskites - 3%.

Within the intrusive bodies of every above listed rock group the dike-like bodies composed of fine-grained and porphyry-like varieties are found. In diorites they represent quartz diorite porphyries, microdiorites and diorite-aplites, in granodiorites they are granodiorite-porphyries, microgranodiorites and granodiorite-aplites. In the later adamellites they are plagiogranite porphyries, granite porphyries, granite-aplites and pegmatites, in alaskites they are granite porphyries, quartz porphyries and alaskite-aplites. The amount of these dike-like bodies is higher in later intrusions having reached almost 50% of an area of alaskite bodies. The occurrence of numerous pegmatite and aplite veins and dikes is typical of later intrusions, as well.

In diorite and granodiorite intrusions there are xenoliths up to several meters. There are hornfelses, diorite-like rocks and fine-grained taxite diorites. Xenoliths which composition is different from wall rock have angular shape with clear boundaries along which a rim of K-feldspar is often developed. Xenoliths of the approximate to wall rock composition have round shape and diffused outlines. Often xenoliths are enriched in biotite and hornblende. The granodiorites of the second group often contain xenoliths of quartz diorites of the first group. Generally, such situation and multi-phase intrusion show a typical picture of syntaxis-mixing of basic and acid magmas.

The rocks of later intrusions are two-feldspar biotite and biotite-hornblende granites (adamellites) and their related granodiorites and quartz monzonites. They consist of zonal oligoclase and andesine, quartz, microcline-pertite, oligoclase-pertite, biotite and hornblende. Monzonite-like rocks occupy about 30% of the Yaloman complex area. They include the rounded xenoliths of 5-20 cm in diameter representing hornfelses, quartz diorites and granodiorites.

Leucogranites and alaskites of the forth group form separate small bodies and are commonly accompanied by aplite dikes of microcline-pertite-quartz varieties with little amount of biotite and oligoclase.

Petrochemical peculiarities of quartz diorite, tonalite and melanocratic granodiorite intrusions reveal the increased aluminium and sodium contents. The increased aluminium and potassium are typical of granodiorites and granites of the second and third phases. Leucogranites and alaskites have increased alkalinity and clear potassium over sodium predomination (table 8,9).

In the diagram of de La Roche (fig. 21) the possible diorite-granodiorites of Yaloman complex form a trend which confirms the evolution of its various groups and their relation to the Devonian volcanogenic rocks of Ongudai and Kuratin suites.

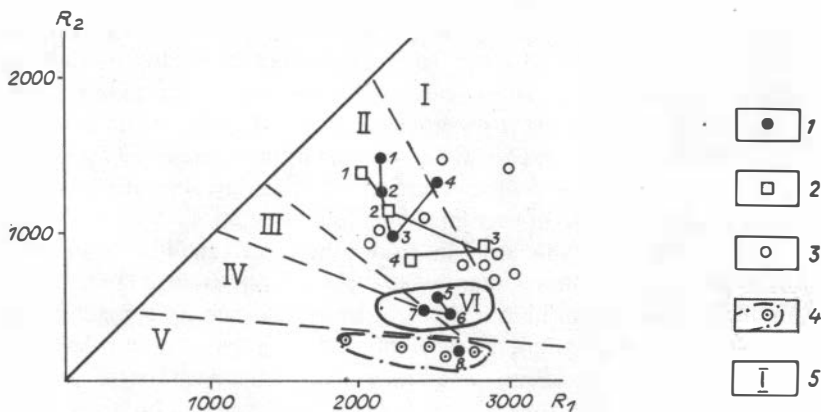


Fig.21. A display of selected granitoid compositions of Yaloman plutons in the de La Roche R_1 - R_2 multicationic diagram (La Roche, 1977; Batchelor & Bowden, 1985) (compiled by M.M.Buslov):

1-2 - points of average values for rocks from Yaloman plutons: 1 - total, 2 - Chiketaman massif (numbers correspond to rock varieties, table 8: 1-4 - Chiketaman Devonian complex, 5-8 - Late Carboniferous-Early Permian Yaloman complex); 3-4 - volcanic rocks of the Middle Devonian Ongudai and Kuratin suites: 3 - basalts, andesite-basalts and andesites, 4 - subalkaline rhyolites; 5 - rock groups: I - mantle plagiogranite, II - destructive active plate margin, III - Caledonian "permitted" granites (post-collision uplift), IV - subalkaline plutons (later orogenic), V - alkaline/peralkaline magmatism of A-type (post-orogenic), VI - anatexitic magmatism (syn-orogenic). The numbered groups I-VI relate to the tectonomagmatic divisions postulated by Pitcher (1979, 1982).

So, the early groups of diorites and granodiorites correspond to active margin related magmatic rocks (field 11). Their comagmatic rocks are the Early Devonian basalt, andesite-basalt and andesite lavas of Ongudai suite and the Middle Devonian andesites and dacites of Kuratin suite.

The later adamellites of the third group correspond to the anatectic granites of field 6 and have no analogues among Devonian volcanic rocks. The rocks of adamellite group cut through Devonian rocks. The youngest alaskites relate to A-type post-orogenic granites.

In the diagram SiO_2 vs oxides (fig.22) and " $\text{Al}_2\text{O}_3/(\text{Na}_2\text{O}+\text{K}_2\text{O})$ mol vs $\text{Al}_2\text{O}_3/(\text{Na}_2\text{O}+\text{K}_2\text{O}+\text{CaO})$ mol" obtained by Maniar and Piccoli (1989) (fig. 23) the Chiketaman Devonian granitoids (diorites and granodiorites) fall in the field of continental margin granitoids. But, the younger granites, dikes of alkaline aplite-granites and aplites correspond to the field of continental-collision granites. In the same diagram the granitoids of Kadrin massif are located between island arc and continental-margin granitoids. The later aplite dikes fall in the field of continental-margin granitoids, as well. On one side, the position of Yaloman complex granitoids in the diagrams of de La Roche (fig.21) and Maniar and Piccoli (fig.22, 23) confirms the multi-stage process of their formation (accepted by many scientists), but on the other side the problem on correct joining of various granitoid plutons formed in different geodynamic environment into a single complex arises.

The age of Yaloman group bodies was not established distinctly. Many geoscientists continue to consider all the rocks as Carboniferous-Permian, since the majority of radiological dates correspond to this time interval (table 10). Taking into account the high deformation of early rock groups and their petrochemical correlation with the Devonian volcanic rocks of Ongudai and Kuratin suites, we can consider the age of early diorites and granodiorites as Early-Middle Devonian, but their relation to Chiketaman complex is the topic of current discussion. According to geologic and geochronologic data, adamellites, alaskites and some diorites-granodiorites have been formed in Late Carboniferous-Early Permian and relate to Kadrin complex.

Polymetallic skarn mineralization and quartz-molibdenite-sheelite ores are connected with Kadrin complex. Within the area of plutons and their wall rocks there are widespread basic and composite dikes being referred to the Terehta Early Mesozoic complex of still not clear age. Their characteristic feature is north-western and submeridional strike.

Thus, the geologic, radiological and petrochemistry data cited allow us to distinguish two groups of the granitoids of Yaloman complex various in age

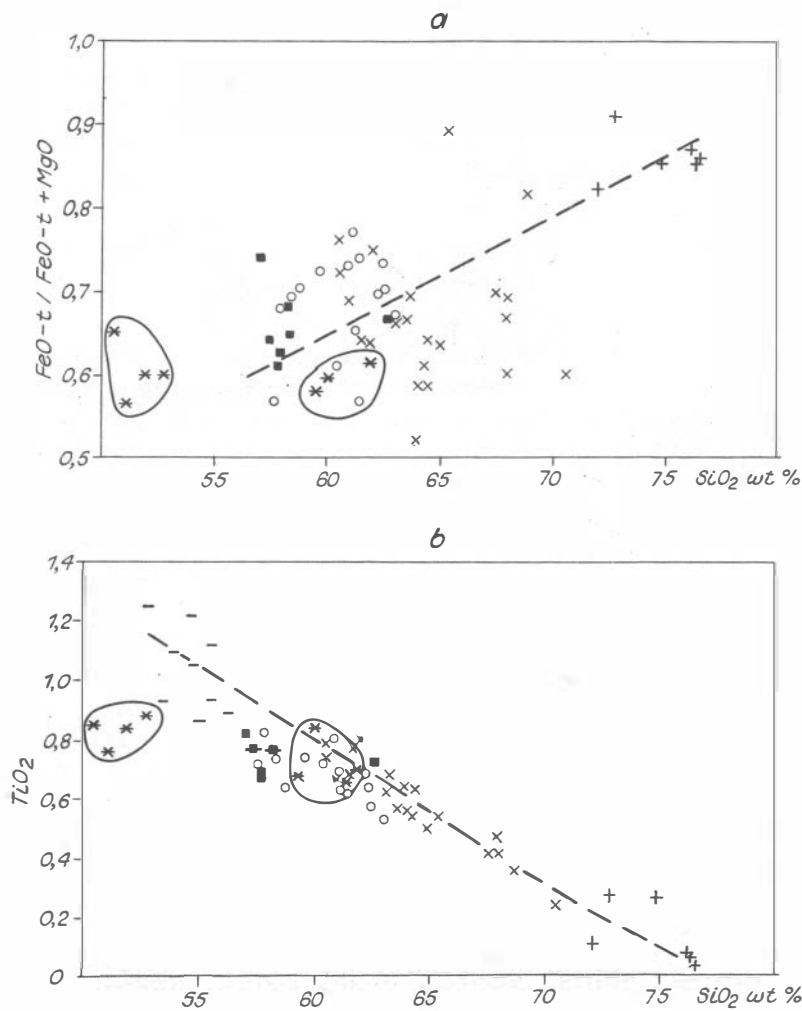
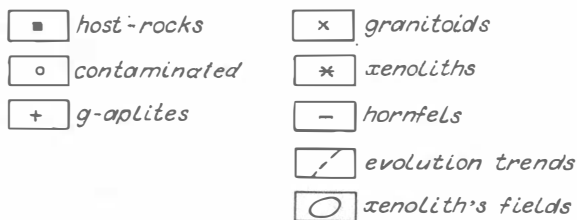
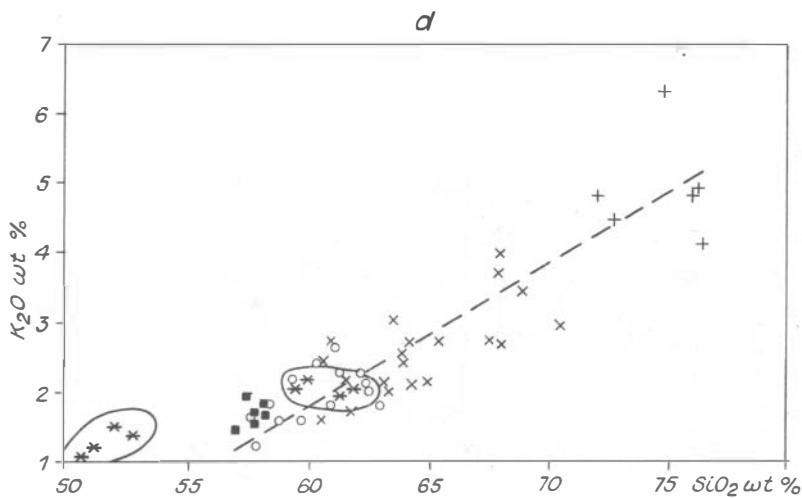
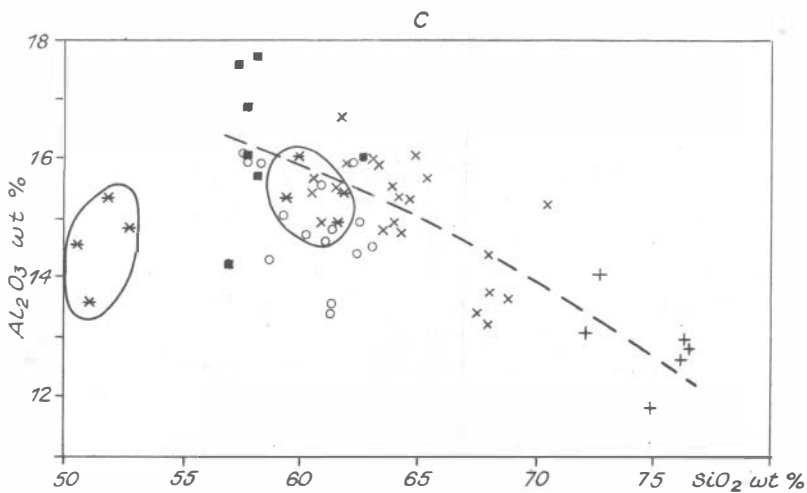
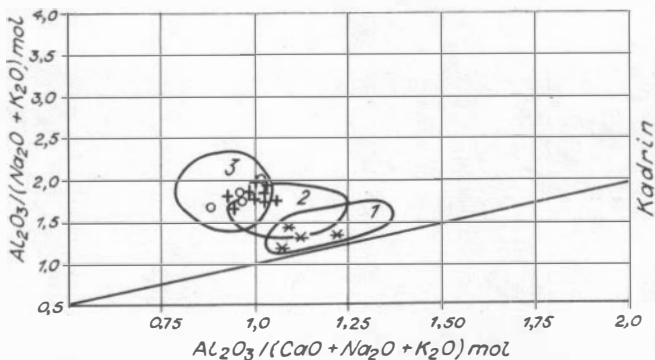
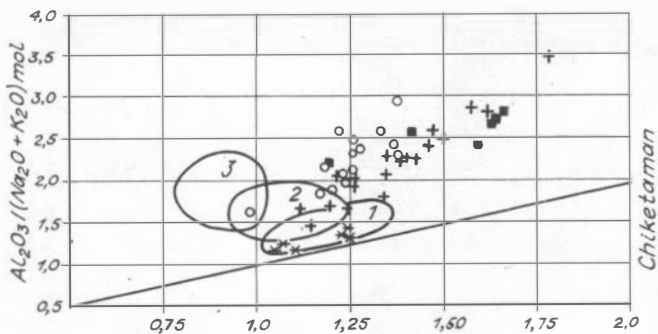


Fig.22. Chiketaman granitoids evolution diagrams "oxides vs SiO_2 " (compiled by N.F.Krasov, 1993).





1-3 - The fields determined by Maniar and Piccoli (1989) for granitoids of 1: continental collision, 2-continental arc, 3- island arc

Fig.23. Yaloman granitoid complex. Diagrams A/NK vs A/CNK (compiled by N.F.Krasov, 1993).

and geodynamic position: 1) Early-Middle Devonian continental-margin diorite-granodiorite group and 2) Late Carboniferous-Early Permian continent-collisional adamellite-alaskite group.

Stop 11. Chiketaman pluton is the first met. (fig. 21). Its tonalites and biotite-hornblende granodiorites are exposed in the left bank of Ursul River between 632 km (Ongudai Village) and 642 km (Uliuta Village) of the

motorroad. Their contact with Cambrian-Ordovician rocks converted into hornfels can be observed in the right bank of Maly Ilgumen River. Here, hornfels sandstones and schists intruded by quartz diorites, monzonites, and granodiorites are found. Farther, these rock outcrops are met up to Khabarovka Village where an uplift to Chiketaman pass begins.

Along all the motorroad through Chiketaman pass tonalites and subordinate quartz diorites and granodiorites are found. They are filled with the numerous xenoliths of variously metamorphosed rocks and abundant secondary coarse-grained biotite-hornblende rocks. Composition and texture of melanocratic component are highly variable. There are abrupt and gradual transitions between different rock varieties. Predominate tonalites and other rocks of pluton are cut by later aplite dikes which in turn together with earlier granitoids are cut by the numerous submeridional dikes of diabases, diabase porphyrites, spessartites and other rocks of the Early Mesozoic Tereka complex of various structure and composition. Unlike the later dikes the granitoids have shistose and cataclastic texture.

At the top of Chiketaman pass (absolute elevation 1800m) tonalites are cut by a series of diabase, diorite-porphyry and porphyry dikes. To the north from the top of pass tonalites are cut by a composite meridional dike (2m thickness). Its edge part is composed of diorite-porphyrites and central part of granite-porphyries passing into granodiorite-porphyries. The latter contain xenoliths of gabbro-diabases and diabase porphyrites. While going down the pass such dikes are found every 5-30 m. Near the southern contact of pluton a zone of vein hydrothermal rocks (up to 1 m thickness) made up of quartz-aksinite aggregate is observed in quartz diorites.

Then, at the 666 km of motorroad there exposed a contact of tonalites and quartz diorites of Chiketaman pluton with biotite hornfels formed after the sandstones and schists of Middle-Upper Cambrian Gornoaltai series. Hornfels are changed gradually to less metamorphosed terrigenous rocks of this series. Observation of the Chiketaman massif granitoids revealed the xenoliths of melanocratic rocks being of high interest. In the diagrams (fig.22,23) there are two distinct groups of xenoliths: 1) metasedimentary and 2) metabasite. The first one belongs to the common trend of Chiketaman granitoids and is located among the Cambrian wall rock points taken far from the massif. The second group is distinguished in the area of basic rocks and differs from a common trend of granitoid rock evolution in Al_2O_3 , TiO_2 , K_2O contents and $FeOt/(FeOt + MgO)$ ratio and belong to derivation of basic magma.

Stop 12. After Chiketaman pass the road goes along the left bank of Bolshoy Ilgumen River. Near the mill of Kupchegen Village the south-western contact of the Carboniferous-Permian granitoids of Kadrin pluton, which is composed mainly of various granites (often adamellites), is exposed. The endocontact zone of their interaction with the host Cambrian-Ordovician flysch-like deposits is composed of quartz diorites and biotite-hornblende granodiorites including the abundant xenoliths of altered wall rocks and biotite and biotite-hornblende schlieres new-formed in the place of these xenoliths. Far from the contact granodiorites are changed by biotite-hornblende granites crossed by the dikes of pegmatites, aplites, fine-grained granites, and micro granites and later basic dikes of diabases and diabase porphyrites of Terekta complex.

At 679 km (the junction place of Bolshoy Ilgumen and Katun Rivers) the Chuya motorroad goes upwards the left bank of Katun River rounding the numerous vertical rocks called "bom". Carboniferous-Permian adamellites of the north-eastern margin of Yaloman pluton and its wall rocks are exposed here. Korkechu and Urkosh "boms" are composed of Middle-Upper Cambrian sand-schist deposits and their related biotite hornfelses and crossed by regionally extend basic dikes. Kupchegen and Bichektu-Kaya "boms" are composed of quartz diorites intruding through the Cambrian-Upper Ordovician hornfels and skarn rocks.

Stop 13. Airy-Tash "bom" (695 km) is composed of the Devonian biotite-hornblende granodiorites of Yaloman pluton which are changed to monzonites cut by thin aplite dikes. Granodiorites include hornblende and biotite-hornblende schlieres and altered diorite-like xenoliths. The later dikes of felsite and spherolite porphyries, diorite porphyrites and diabases of Terekta complex are found, as well.

Kyngyrara "bom" (696-967 km) exposes the north-eastern contact of Yaloman pluton with Upper Ordovician deposits. Endocontact zone presents Devonian biotite granites with xenoliths of altered wall limestones, schists, and sandstones crossed by the submeridional dikes of Terekta complex. The granites crossed by dikes have cataclized and schistose texture. Also, dikes cross the wall rocks transformed into spot-like feldspar hornfelses.

Stop 14. Near Inya Village the Chuya motorroad passes on the right bank of Katun River. 5 km from village near to Chuya and Katun Rivers junction there is Devonian Ust-Chuya tonalite-granodiorite pluton (about 40 square km area) which together with accompanying fine granite bodies forms the south-eastern part of Yaloman areal-pluton. The Ust-Chuyta pluton is

composed of tonalites, quartz diorites, granodiorites, and monzonites. They are crossed by thin irregular bodies and dikes of fine-grained rocks of the second group varying from granite to granodiorite.

Stop 15. Located near to junction place of Chuya and Katun Rivers where the numerous terraces of many tens meters over the modern water level are observed. Terrace deposits overlie the Early-Silurian carbonate-terrigenous deposits. Together with Ordovician sediments they represent a subplatform cover of the Gorno-Altai micro continent's block. The thickness of Ordovician marine sequences (sandstones, mudstones, marls) reaches 4.5-6 km. Silurian rocks transgressively overlie Ordovician rocks and represent the coastal-sea sediments (rift limestones, conglomerates, sandstones, marls and mudstones). The thickness of Early Silurian deposits reaches 1.5-2 km. Here, a body of riftogenic limestones with Llandoveryan and Wenlockian coral fauna is located. Tabulates and Helyoritides are defined: *Palaeofavosites simplex Tcherr.*, *Multisolenia tortuosa Fritz.*, *Mesofavosites obliquus Sokolov var. maior Sok.*, *Favosites lichenarioides Sokolov, etc.*

Days 4 and 5. Geodynamic complexes of Vendian-Cambrian and Devonian continental margins, nappe-imbricated, strike-slip and strike-slip-thrust dislocations of south-eastern part of Gorny Altai.

General review (stops 16-25)

South-eastern part of Gorny Altai has mountainous relief of Alpine type. Here, the inter-mount depressions (Kurai and Chuya depressions, 1500-1900 m) and high-mount plateau (Chulyshman Plateau, etc. 1800-2000 m) alternate with ridges (Kurai, Sailugam, North-Chuya and South-Chuya Ridges - 2000-4506 m). The highest point is Belukha Mtn. of South-Chuya ridge. Belukha Mtn. (4506 m) is the highest top of Siberia. The North-Chuya and South-Chuya Ridges are covered with gletschers being the relics of the last glaciation occurred 11,000 y.y. ago.

The structure of south-eastern part of Gorny Altai includes several terranes and sutures. According to age and genesis they are divided into Cambrian periocenic and Ordovician-Early Silurian pericontinental groups (fig.24). Terranes and sutures are broken with the cross inner-continental strike-slip faults and overthrusts of Late Paleozoic-Mesozoic age. Middle-Cambrian suture fixes the stages of "soft" collision of Baratal terrane

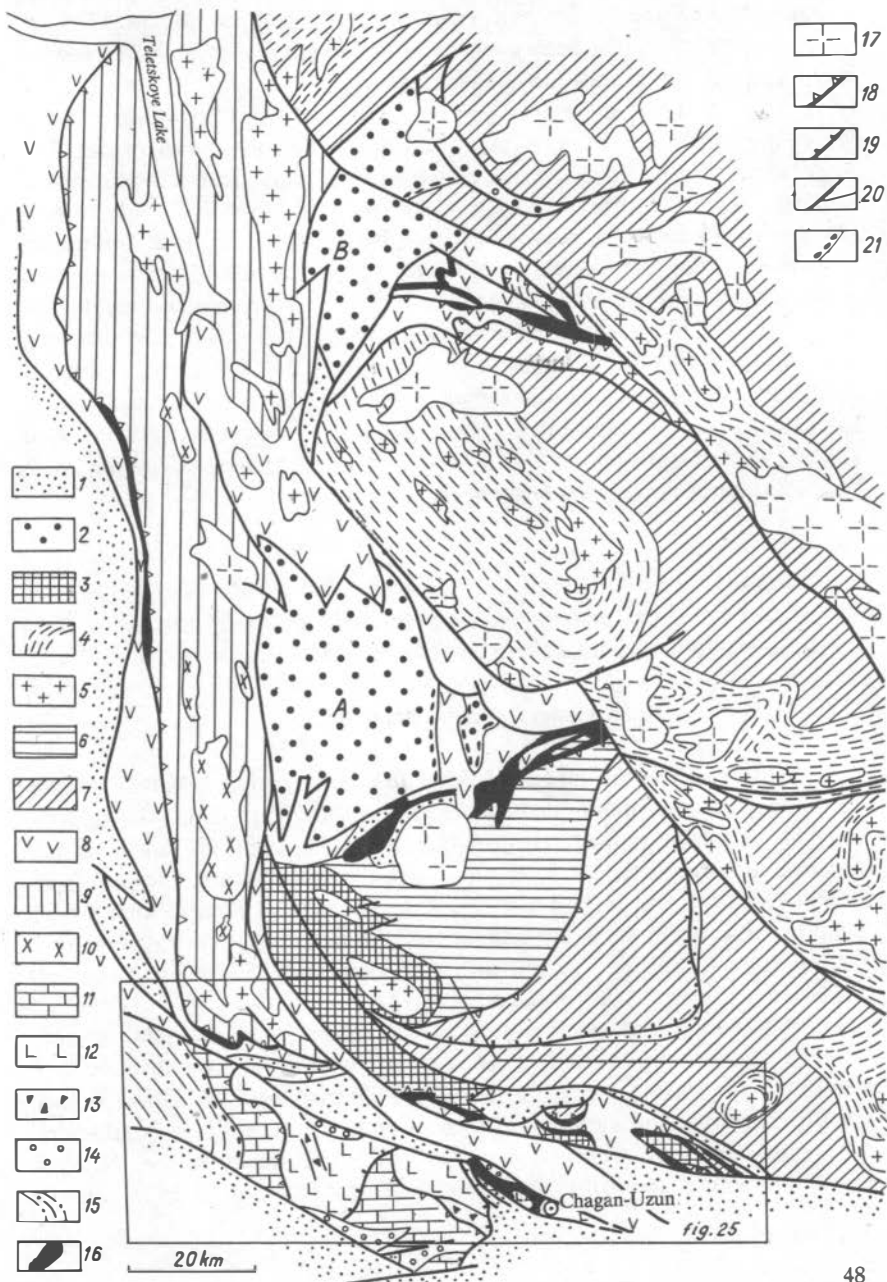


Fig.24. Main geodynamic complexes and structural elements of the south-eastern part of Gorny Altai (compiled by M.M.Buslov):

1 - The Devonian rocks of active continental margin; 2-5 - Middle Paleozoic collisional complexes of pericontinental suture zones: 2- Ordovician-Early Silurian volcanic molasse of Ulogan (A) and Erinad (B) structures; 3-5 - zonal granite-gneiss domes: 3 - garnet-sillimanite-cordierite subzone rocks, 4 - biotite subzone rocks, 5 - Early Ordovician two-mica granites; 6, 7 - West Sayan terrane: 6 - Vendian-Early Cambrian sedimentary-volcanic rocks, 7 - Early-Middle Cambrian flysch of fore-arc trough; 8-10 - Gorno-Altai terrane: 8-10 - island arc rocks: 8 - undivided rocks of the Vendian-Early Cambrian primitive island arc and Early-Middle Cambrian normal island arc, 9, 10 - island arc rocks metamorphosed during collisional stage: metamorphic rocks (9) and Middle Cambrian granitoids (10); 11-15 - Early Cambrian accretionary prism: 11-12 - Baratal terrane: siliceous-carbonate rocks (11), sedimentary-volcanic rocks (12); 13 - olistostrome; 14 - olistostromes and molasse of Middle-Late Cambrian inter-arc trough; 15 - flysch of the Middle-Late Cambrian fore-arc trough; 16 - ophiolites: sheets of peridotites, gabbro, serpentinite melanges; 17 - post-collisional Carboniferous granites; 18 - Early Paleozoic thrusts; 19, 20 - Late Paleozoic-Mesozoic faults: thrusts, reverse thrusts (19), strike-slips and reverse strike-slips (20); 21 - basal conglomerates.

(seamount system) with terranes composing the remnants of primitive island arc. The collision of island arc with seamounts (Kurai terrane) promoted high speed uplift to the surface and preservation of high pressure subducted rocks (eclogites, blueschists and garnet amphibolites) and meta-peridotites of Chagan-Uzun complex.

Ordovician-Early Silurian suture was formed due to "rigid" collision of Gorno-Altai micro continent with Cambrian island arc and West Sayan micro continental blocks. Their collision was accompanied with formation of nappe-imblicated structures, Ordovician-Early Silurian volcanic molasse (Ulogan and Erinad structures), zonal granite-gneiss domes and batholiths with an ancient peak of isotopic dates about 450-510 Ma (table 11). The younger peaks of values between 250 and 370 Ma characterizes the repeated metamorphism and rock melting in the conditions of Devonian and Late Paleozoic active margin being accompanied by strike-slip and thrust deformations. Final stage occurred due to collision of Siberian and Kazakhstan continents resulting from the Permian closing of Paleasian Ocean.

The route of trip lies through Kurai region of the south-eastern part of Gorny Altai. There, all the noted above groups of terranes and blocks are spatially combined to provide the variety and complexity of the region's

geological structure. The paleodynamic complexes of Vendian-Early Cambrian primitive island arc (Kurai terrane), Early Cambrian accretionary prism (with the fragments of Baratal seamount, ophiolites and high pressure rocks), Early-Middle Cambrian normal island arc and Middle-Late Cambrian fore-arc and inter-arc troughs are distinguished there (fig.25)* Moreover, the rocks of Devonian active continental margin present with the rocks of volcanic belt, back rifts and various granites are wide spread in Kurai zone, as well.

Kurai terrane of Vendian-Early Cambrian primitive island arc

The fragments of Vendian-Early Cambrian primitive and Cambrian normal island arc compose the south and central parts of Kurai ridge. They form the folded nappe-imbricated structure (fig.25, section A-B). Generally, the structure is dipping to the north-east. Its upper structural level is the zonal epidote-amphibolite facies metamorphic rocks considered as Kurai complex. It forms a tectonic nappe in which sole the serpentinite schists and melanges are available. Under this structural group the thick (up to several km thickness) zone of tectonic sheets composed of the fragments of island arc ophiolites occurs: 1) layered Mezhtuyaryk pyroxene-gabbro complex; 2) parallel dike complex; 3) sub-intrusive dike-sill complex; 4) Vendian-Lower Cambrian effusive-tuff Balkhash suite. The Cambrian carbonate-terrigenous black shales and turbidites compose the imbricated structure, as well. They could serve as sedimentary cover of ophiolites and replace them towards the marginal sea along lateral.

The sheets mentioned above alternate with the sheets of Lower-Middle Cambrian andesite and calcgreywacke and tuff-terrigenous turbidites being the fragments of normal island arc.

Meshtuyaryk layered complex belonging to the structure of two giant tectonic sheets up to 1km thickness consists of serpentinites, wherlites, clinopyroxenites with cumulative structure and layered lower gabbro. Gabbro contains gabbro-pegmatite lenses and xenoliths of clinopyroxenites making up a magmatic breccia. The rocks of layered complex are intruded by the dikes of quartz diorites and plagiogranites often forming a magmatic breccia, as well. The similar interrelations were described in the late members of the gabbroid complex of Oman ophiolites (Nicolas, 1989). Parallel dikes and dike-sill complex closely associate with volcanic-terrigenous rocks forming the upper part of complicated assemblage. They include diabases, gabbro-diabases, gabbro and pyroxenite porphyrites of boninite series (Simonov & Kuznetsov, 1991).

* Look through inset.

Commonly, the rocks of primitive arc are divided into two series (table 12). In the diagram TiO_2 - 10MnO - $10\text{P}_2\text{O}_5$ basalts characterize only the fields of tholeiite and calc-alkaline series of island arcs (fig.26). In the diagram TiO_2 - K_2O (fig.27) the Vendian-Early Cambrian magmatic rocks have two distinct trends. The first trend is characterized with low contents of potassium and wide variations of titanium (fields III-IVa). Under titanium content decrease the rock compositions consequently fall in the fields of oceanic island basalts - mid-oceanic rift basalts - tholeiites of back-arc spreading. The second trend is characterized with relatively low content of titanium with the increasing content of potassium while passing from boninites to tholeiites of island arcs and to calc-alkaline rocks.

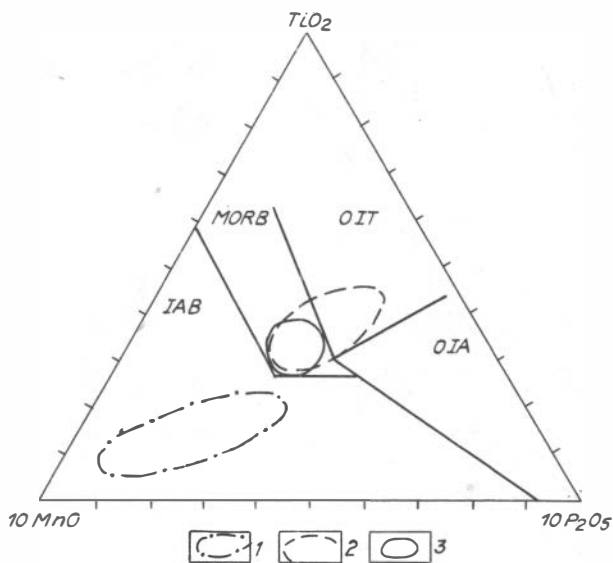


Fig.26. The diagram TiO_2 - 10MnO - $10\text{P}_2\text{O}_5$ for basalts and metamorphic rocks of Kurai zone (compiled by M.M.Buslov):

1 - Vendian-Early Cambrian basalts of primitive island arc; 2 - Vendian-Early Cambrian basalts of Baratal terrane; 3 - eclogites, garnet amphibolites and barroisite-actinolite schists from the sheets of accretionary prism.

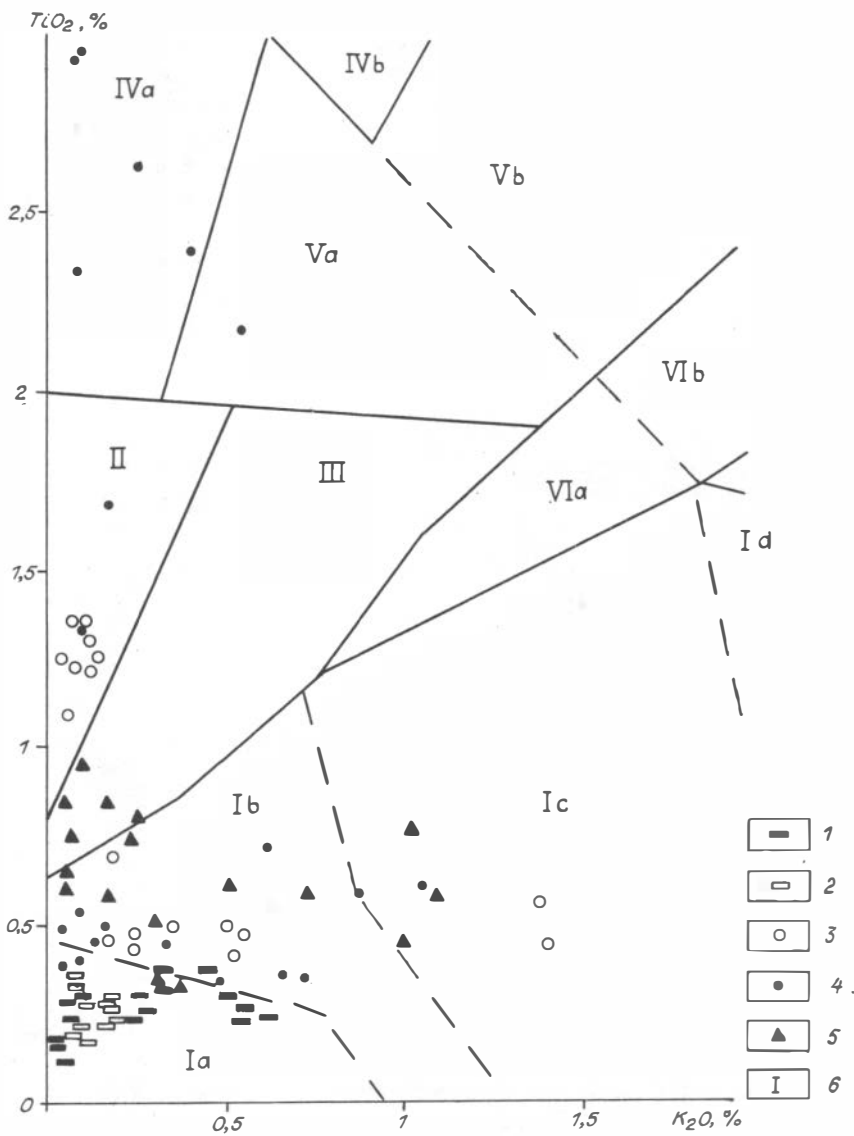


Fig.27. The diagram TiO_2-K_2O for the rocks of Vendian-Early Cambrian ophiolites of the primitive island arc of Kurai ridge (compiled by V.A.Simonov using the diagram of Yu.V.Mironov, 1991):

1 - boninite series; 2 - composition of homogenized melt inclusions from clinopyroxene phenocrysts from boninites; 3 - lavas; 4 - sheeted-dike complex; 5 - dike-sill complex; 6 - fields of volcanic rocks: I - island arcs (Ia - boninites, Ib - tholeiites, Ic - calc-alkaline, Id - alkaline rocks); II - mid-oceanic ridges, back-arc spreading centers and intercontinental rifts; III- back-arc spreading centers and transform faults; IV - oceanic islands (IVa - tholeiites, IVb - subalkaline rocks); V - oceanic islands and platform activation areas (Va - tholeiites, Vb - subalkaline rocks); VI - platform activation areas (VIa - tholeiites, VIb - subalkaline rocks).

The diagram compiled using the concentrations of REE and Zr, Y, which are likely stable under metamorphic processes, confirm the results obtained while considering the distribution of titanium and potassium. The two rock series are distinguished clearly: 1) with high contents of Ti, Na and Zr are oceanic rocks falling in the fields of mid-oceanic ridge basalts; 2) rocks with the low contents of the noted elements fall near to the field of the Marian arc boninites represent the primitive island arc rocks (fig.28, table 13).

Study of clinopyroxenes and chrome-spinels from boninites of Kurai ridge (fig. 29, 30, table 14) showed that their chemistry correlates with mineral compositions from boninites of the other ophiolite associations (ophiolites of Maly Caucasus and East Sayan) and from boninites of modern island arc systems of Pacific Ocean. Particularly, clinopyroxenes are characterized with low contents of Ti and Na (fig.30), increased Cr_2O_3 (0.4-0.6) and variable FeO (2.5-5%, table 14). The increased Cr and non-constant Fe/Mg ratio (fig.30) are typical of chromites.

Generally, the geochemical investigations give enough information to reconstruct the paleogeodynamic environments for formation of Kurai ridge ophiolites. The evolution of magmatic processes from the initial formation of oceanic crust within spreading centers of mid-oceanic ridges to the following development of the magmatic processes of hot-spots (oceanic islands) is traced distinctly. Simultaneously or later (?) over oceanic crust the "young" primitive island arc with boninites is formed. It is consequently transformed into the normal island arc system with the tholeiite series changed to calc-alkaline series.

The typical boninites form both the separate flows among lava sequence

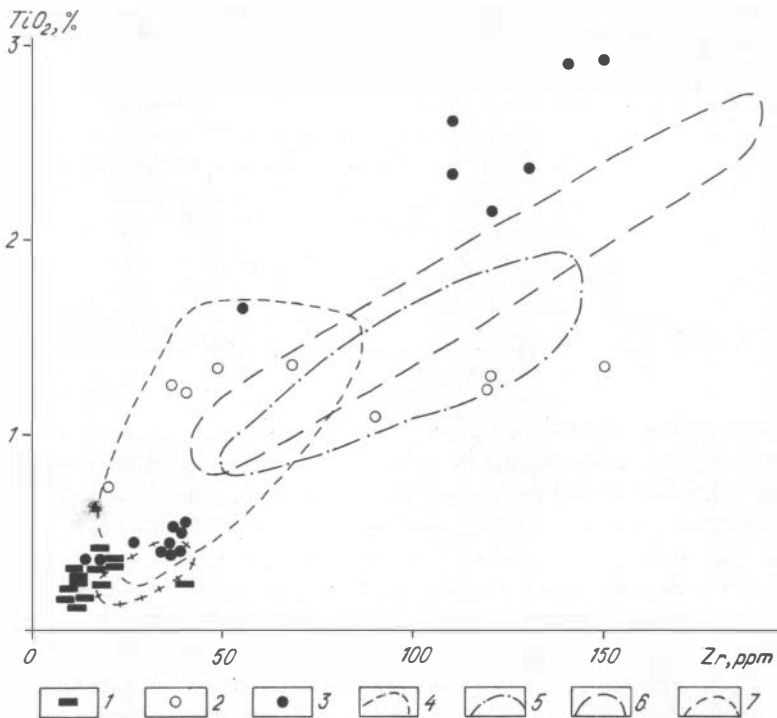


Fig.28. Diagram TiO_2 -Zr for rocks of the Vendian-Early Cambrian ophiolites of the primitive island arc of Kurai ridge (compiled by V.A.Simonov and M.M.Buslov):

1 - dikes and lavas of boninite series; 2 - lavas; 3 - sheeted-dike complex; 4-7 - boundaries of fields: 4 - volcanic rocks of island arcs; 5 - back-arc basin basalts (Sharaskin & Zakariadze, 1982; Tarnery & March, 1991); 6 - mid-oceanic ridge basalts (Saunders et al., 1980; Tarney & March, 1991); 7 - Boninites of Marian arc (Tarney & March, 1991).

and thin (about 0.5m) dike zonal bodies with clear fine-grained contacts and large crystals of fresh pyroxenes in the center. More thick (up to 5m and more) boninite dikes belong to sheeted dike complexes. Boninites fill the sill bodies between the beds of tuff rocks and compose the magmatic breccias within near-contact zones of lava flows associated with piroclastics, as well.

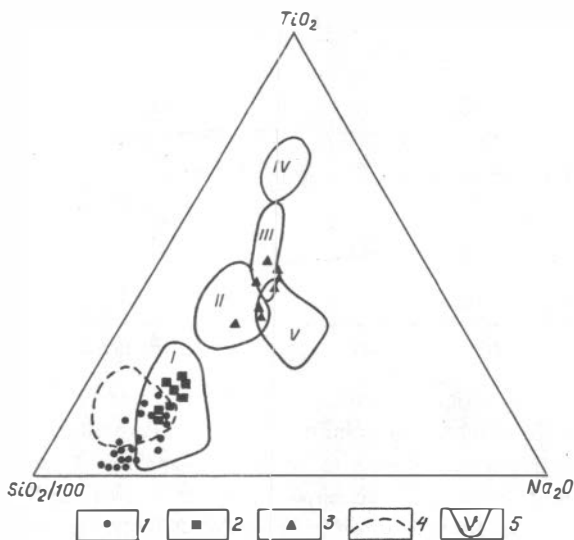


Fig.29. Diagram $\text{SiO}_2/100\text{-TiO}_2\text{-Na}_2\text{O}$ for clinopyroxenes from Vendian-Early Cambrian magmatic rocks in primitive island arc (compiled by V.A.Simonov): 1 - pyroxenes from Kurai ridge boninites; 2 - pyroxenes from Biya River porphyrites; 3 - pyroxenes from Teletzkoye Lake porphyrites; 4-5 - clinopyroxene compositional fields: 4 - from Maly Caucasus boninites (Tsameryan, 1991), 5-I - from Pacific boninites (Peive A.V.(Ed.), 1980; Vysotsky, 1989; Dobretsov N.L (Ed.), 1991b); 5-II - from oceanic and island arc tholeiites; 5 - III,IV - from oceanic basalts of subalkaline (III) and alkaline (IV) series (Tsameryan et al., 1991); 5-V - from the rocks of shoshonite series (Bogatikov O.A. (Ed.), 1985; Meen, 1987).

Comparing the chemical composition of some pyroxene porphyrites of Gorny Altai with rock compositions of different boninite series (table 15) we showed that they are similar according to the majority of petrogenic components (SiO_2 , TiO_2 , Al_2O_3 , CaO , Na_2O , K_2O). The contents of MgO in pyroxene porphyrites for Gorny Altai ophiolites coincide with the average values for boninites at a whole and for boninites of Marian trench and Bonin islands. High Cr contents (up to 1050 g/t) in Gorny Altai porphyrites correspond to the data on boninites of Marian trench, Bonin islands and boninites at a whole. In the diagram $\text{Ti/Cr} - \text{Ni}$ (fig.31) the porphyrites studied fall on the field of boninite series. Also, the composition of homogenized melt

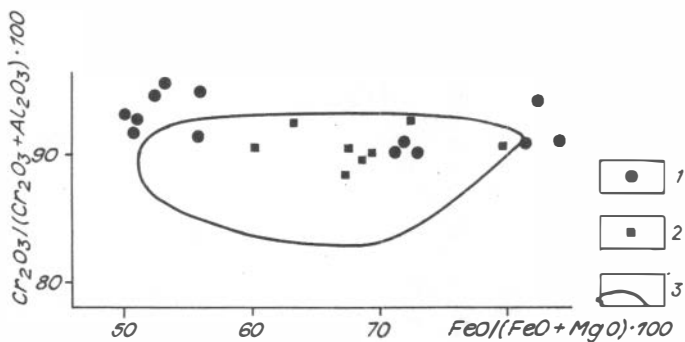


Fig.30. Composition of chrome-spinels from boninites of Vendian-Early Cambrian Kurai terrane of primitive island arc (compiled by V.A.Simonov): 1, 2 - chrome-spinels from Kurai ridge boninites (1) and from East Sayan boninites (2) (Sklyarov, 1990); 3 - field of chrome-spinel composition from Marian trench boninites, Tongue arc and Idzu-Bonin trench (after: Peive (Ed.), 1980; Vysotsky, 1989; Dobretsov (Ed.), 1991b).

inclusions in clinopyroxenes (fig.29, table 14) clearly enough corresponds to oninite series. Thus, according to chemistry the pyroxene porphyrites of Gorny Altai correspond to the rocks of boninite series of folded areas and the modern ensimatic arcs of the western Pacific.

The comparison of composition of volatile components in Gorny Altai boninites with the data on fresh boninites in Tongue trench (table 16) was carried out. They are close in H_2O differing in other gases (CO_2 , H_2 , CO). The total amount of gases in Gorny Altai boninites is higher in 3-4 time than that in Tongue rocks, the relation between the volatiles being rather close. The existing differences could occur due to the minerals of various metamorphism degree were analyzed (fresh orthopyroxenes in Tongue rocks and clinopyroxenes of Gorny Altai substituted by amphibole).

Early Cambrian accretionary prism

Early Cambrian accretionary prism (fig.24,25) consists of the sheets of Baratal terrane (various in composition and dimensions) composed of sedimentary-basaltic layer of oceanic crust and formed over it rocks of seamount, Chagan-Uzun oceanic ophiolites, serpentinite melanges, sheets and

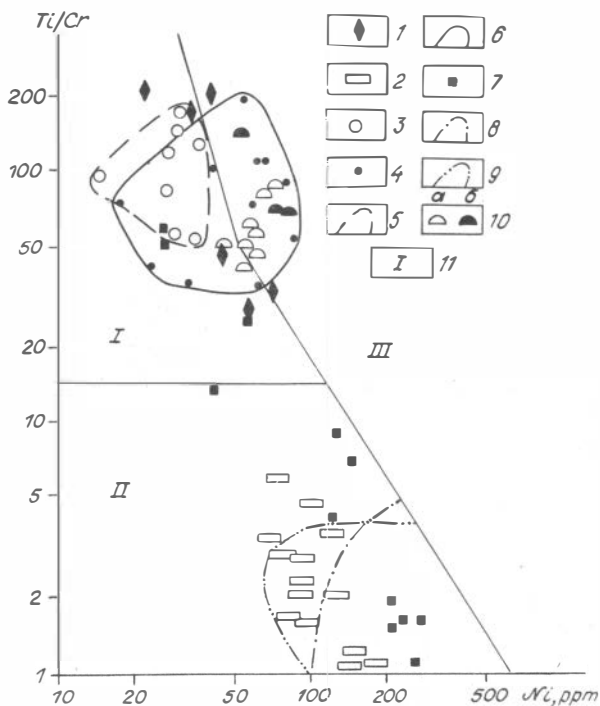


Fig.31. Diagram Ti/Cr - Ni for Vendian-Early Cambrian dikes, volcanic and metamorphic rocks of the Kurai zone of Gorny Altai (compiled by V.A.Simonov):

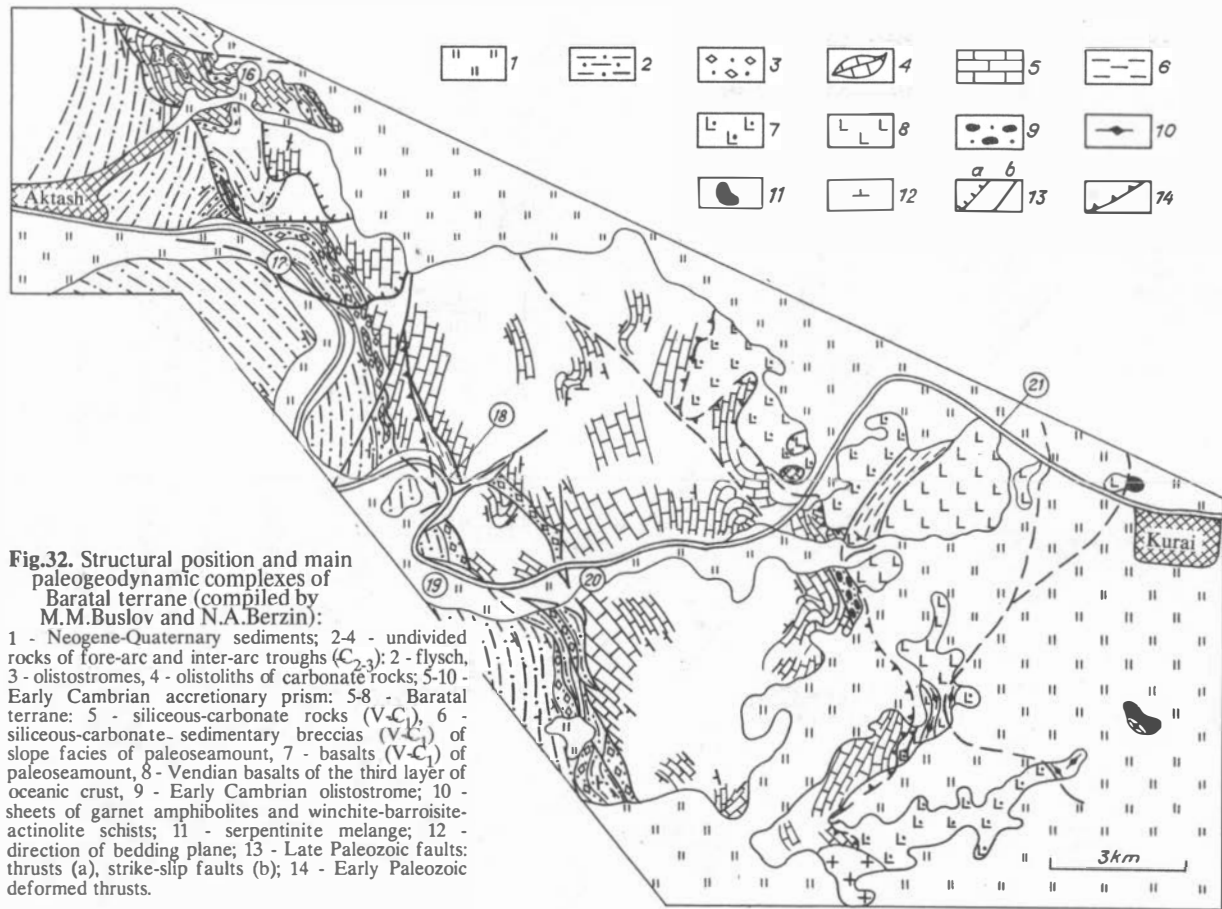
1 - gabbro dikes of Chagan-Uzun ultrabasite massif; 2-6 - ophiolites of primitive island arc of Kurai zone: 2 - boninites, 3 - volcanic rocks, 4 - dikes, 5 - field of volcanic rocks, 6 - field of dikes; 7 - rocks of boninite-marianite series from East Sayan ophiolites (Dobretsov et al., 1985); 8 - field of boninites from Bonin Islands of Marian trench; 9 - field of boninites from Mongolian ophiolites; 10 - garnet amphibolites (a) and eclogites (b) of Chagan-Uzun massif; 11 - areas of island arc and oceanic series (8, 9, 11 - according to Kepezhinskias et al., 1985; Kepezhinskias et al., 1987; Beccaluva et al., 1980; Beccaluva et al., 1983): I - moderate titaniferous tholeiite series of island arcs, II - low titaniferous (boninite, etc.) series of island arcs, III - high titaniferous tholeiite series of mid-oceanic ridges, marginal seas and seamounts.

small blocks of eclogites, garnet amphibolites and barroisite-actinolite schists. Barroisite-actinolite schists often occur near the base of sheets of Baratal terrane basalts as separate lenses. All the rocks mentioned alternate with Early Cambrian sheets of olistostromes.

The sheets and bodies of serpentinite melanges are folded dipping to the south-west in opposite direction than the nappe-imblicated structure of Kurai ridge (fig.25).

Baratal terrane includes various lateral and vertical facies of seamount and their underlying oceanic crust basalts (fig.32). Within separate sheets its upper terrigenous-siliceous-carbonate part (Baratal suite) and lower sedimentary-basaltic part (Sagalak suite and Arydzhan suite similar to Manzherok suite at Stops 1-4) can be fixed. The volcanics of the oceanic plate lay at the basement of Baratal seamount.

Bulk composition of the volcanic rocks of Baratal terrane and metamorphic rocks are cited in table 17. In the diagram $TiO_2-10MnO-10P_2O_5$ (fig.26) the basalts of Arydzhan and Sagalak suites form a single field with the values changing from mid-ocean ridge basalts to basalts of oceanic islands. According to TiO_2-K_2O relation the Arydzhan suite basalts correspond to mid-ocean ridge basalts (field II) , but the Sagalak suite basalts belong to basalts of back-arc basins (field III) partly falling in field V of oceanic islands (fig.33). Amphibolites from the sole of Arydzhan suite mainly correspond to MORB basalts (field II) stretching towards field IV of tholeiites from oceanic islands due to the higher TiO_2 content. In the diagram TiO_2-Zr basalts completely correspond to MORB basalts and partly to marginal sea basalts (fig.34). Generally, according to structural position, set of rock formations, geochemical and petrochemical characteristics the Baratal terrane may be considered as paleoseamount with a fragment of oceanic crust in the basement. In the beginning of Early Cambrian the terrane together with adjacent part of oceanic lithosphere (Chagan-Uzun) was entered into subduction zone where some of its rocks were metamorphosed. In the end of Early Cambrian Baratal terrane squeezed a subduction zone and collided with the Kurai fragment of primitive island arc. Due to collision and return current in an accretionary wedge the metamorphosed parts of oceanic crust (Chagan-Uzun ophiolites, eclogites and garnet amphibolites) were quickly uplifted to surface to be included in collision-accretionary wedge according to the model of Dobretsov & Kirdyashkin (1993). According to geochemical and petrochemical characteristics the high pressure rocks are analogous to seamount rocks, that is to MORB and oceanic island basalts (table 18, fig.31, 33, 34).



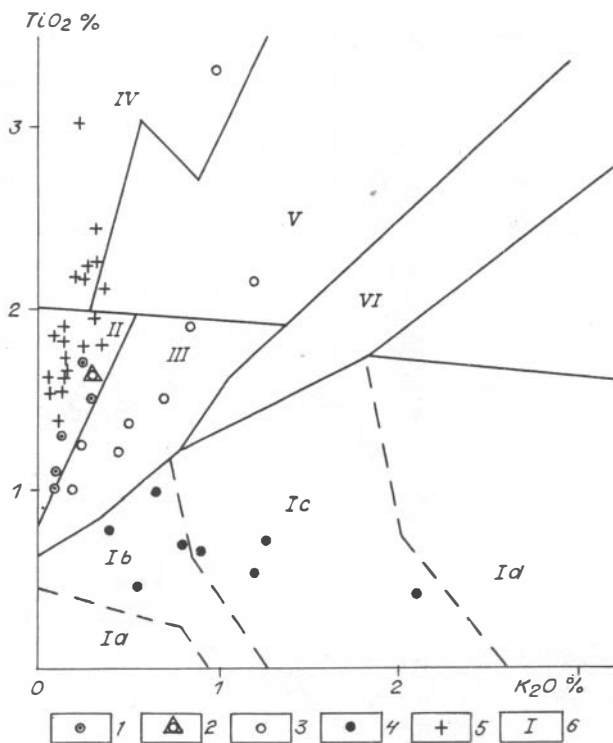


Fig.33. Diagram TiO_2 - K_2O for the rocks from Stops 20,21 and amphibolites of Chagan-Uzun massif and Baratal terrane (compiled by V.A.Simonov using the diagram of Yu.V.Mironov, 1991):

1 - volcanic rocks of Arydzhan suite of Stop 21; 2 - average values for volcanic rocks of Arydzhan suite after N.I.Gusev analyses; 3 - volcanic rocks of Sagalak suite (Gusev, 1991); 4 - volcanic rocks in pebbles, Stop 20; 5 - amphibolites; 6 - fields of volcanic rocks from: I - island arcs (Ia - boninites, Ib - tholeiites, Ic - calc-alkaline rocks, Id - alkaline rocks), II - mid-oceanic ridges, back-arc spreading centers and intercontinental rifts; III - back-arc spreading centers and transform faults; IV - oceanic islands (IVa - tholeiites, IVb - subalkaline rocks); V - oceanic islands and platform activation areas (Va - tholeiites, Vb - subalkaline rocks); VI - platform activation areas (VIa - tholeiites, VIb - subalkaline rocks).

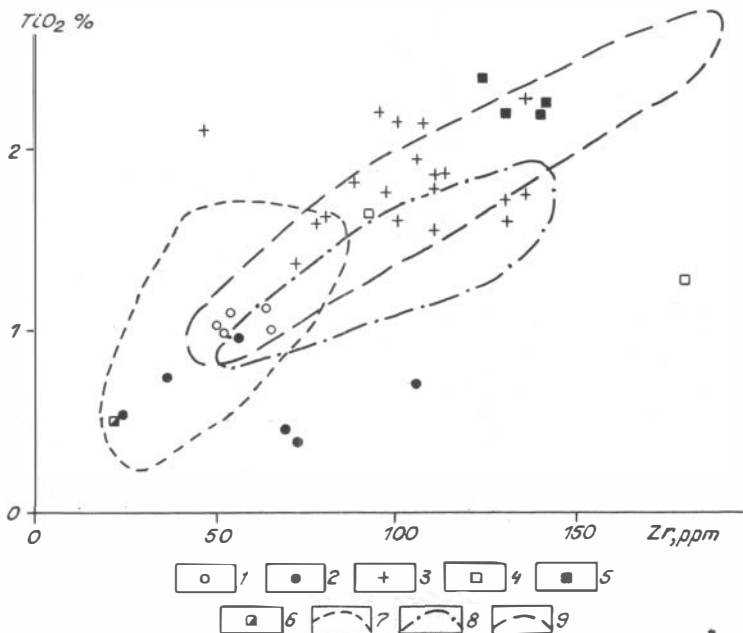


Fig.34. Diagram TiO_2 -Zr for pyroxene porphyrites of Arydzhan suite (Stop 21), volcanic pebbles (Stop 20) and amphibolites of Chagan-Uzun massif (compiled by V.A.Simonov and M.M.Buslov):

1 - lavas of pyroxene porphyrites (Stop 21); 2 - volcanic rock pebbles (Stop 20); 3 - amphibolites of Chagan-Uzun massif; 4 - volcanic rocks (Stop 6, the lower part of Bulukhrta-Cherga section); 5 - volcanic rocks of Stop 1 (Surtaika Vil.); 6 - volcanic rocks of Stop 7 (the upper part of Bulukhrta-Cherga section); 7-9 - boundaries of fields: 7 - volcanic rocks of island arcs, 8 - back-arc basin basalts (Sharaskin & Zakariadze, 1982; Tarney & March, 1991), 9 - MORB (Saunders, 1980; Tarney & March, 1991).

Olistostrome of accretionary prism is commonly present with gravellites with various content of fragments of cherts, limestones and basalts analogous to the rocks of Baratal terrane. The same rocks sometimes form chaotic accumulations of various blocks with dimensions up to several meters sometimes observed as well-rounded pebbles.

Fore-arc and inter-arc troughs

Anui-Chuya fore-arc trough makes up the vast areas of outcrops to the west from Baratal terrane to be composed of Middle-Upper Cambrian flysch-type sediments. Near to accretionary prism the trough sequences overlie Baratal terrane through basal conglomerates.

Middle-Upper Cambrian rocks of inter-arc trough are predominantly olistostrome breccias and conglomerates which were preserved within separate tectonic wedges inside the accretionary prism (fig.35).

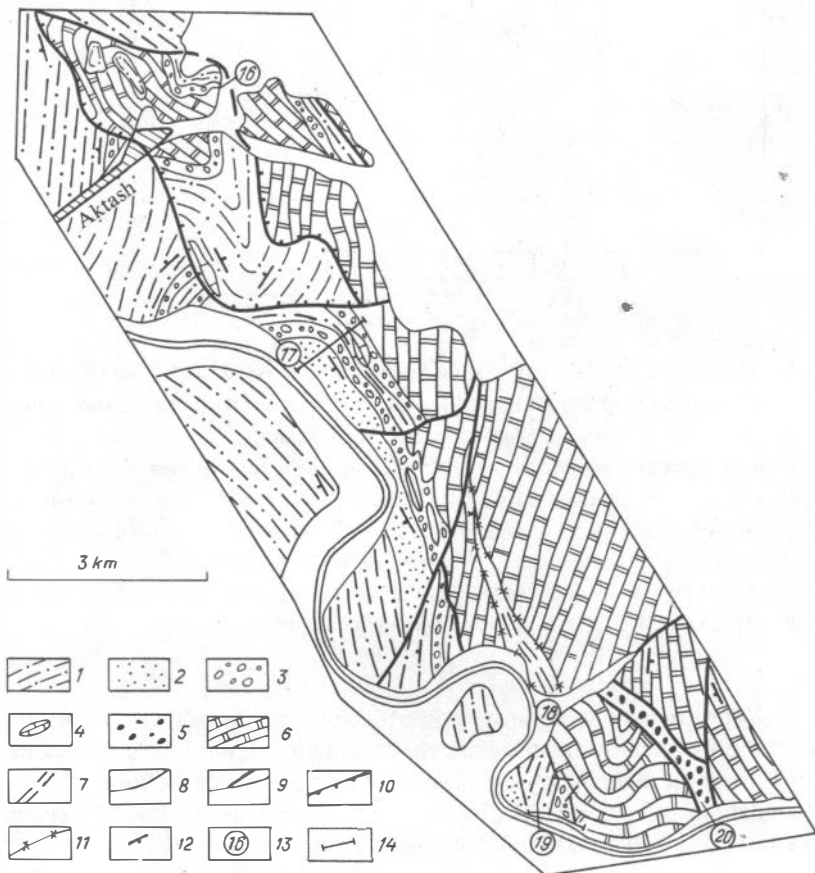


Fig.35. Geological scheme of the rocks of fore-arc trough, inter-arc trough and accretionary prism in Kurai zone of Gorny Altai (compiled by M.M.Buslov): 1-4 - Middle-Upper Cambrian rocks of the marginal part of Anui-Chuya fore-arc trough: 1 - sand-bearing rhythmically bedded shales, 2 - massive sandstones, 3-4 - olistostromes (3) with bodies of siliceous-carbonate olistoliths (4); 5 - olistostromes of fore-arc trough; 6,7 - Vendian paleoseamount: 6 - siliceous-carbonate Baratal series; 7 - volcanic sandstones; 8 - lithological boundaries; 9,10 - Late Paleozoic faults: reverse strike-slip faults (9) and reverse thrusts (10); 11 - tectonic melange along Early Paleozoic faults; 12 - bedding elements; 13-14 - location of observation points (13) and section (14).

In the piece of Chuya Motorroad from Aktash Village to Baratal Ravine the Middle-Upper Cambrian flysch-like sequence (Gornoaltaisk series) and its relation to siliceous-carbonate deposits of Baratal seamount can be observed. The sequence consists mainly of polymict and quartz-plagioclase sandstones and mudstones, and argillites, carbonate-clayish and siliceous deposits, as well. Often the rocks carry the features of rhythm bedding. The sand-schist sequence contains coarse-fragment rocks: olistostromes, conglomerates, breccias, sandstones and gravellites composing the lense-like bodies and packages up to several hundreds meters thickness with non-constant strike.

Coarse debris are generally bad-rounded products of accretionary prism destruction, rarely well-rounded pebbles of the rocks of Cambrian normal island arc. Inter-arc trough is composed of fragments of both accretionary prism and island arc.

Day 4. From Aktash Village (stop 16) along Chuya Motorroad during 1 day at a distance of 17 km the following objects will be demonstrated: the fragments of Baratal seamount section and adjacent from the west Cambrian fore-arc trough with the fragments of seamount and Cambrian normal island arc.

Stop 16. North-eastern outskirts of Aktash Village (fig.25 and 35). Stratigraphic overlying of Middle-Upper Cambrian rocks of Anui-Chuya fore-arc trough on the Vendian-Early Cambrian siliceous-carbonate rocks of Baratal seamount. The thickness of basal coarse-grained package on a distance of 1 km rarely changes from 2 to 200 m to the west towards deep-water part of the Anui-Chuya trough. The surface of Baratal seamount over which the coarse material beds is rough. Often outcrops of cherts are observed. Rough fragments are present with marble-like grey and black limestones and dolomites (with

inclusions and interlayers of cherts), black, green and red cherts. Somewhere, beds of sandstones and mudstones are similar to the products of intra-formation rewashing. Over conglomerate-breccias there are sandstones and mudstones which contain interlayers and lenses of coarse-grained debris.

Stop 17. Located near to Chuya motorroad 3 km to the south-east from Aktash Village (fig.25 and 35). The upper horizons of rock cliff expose a location of two siliceous-carbonate olistoliths among sand-mudstone deposits. Their thickness reaches $n \cdot 10$ m with the length more than 200 m. All the rock varieties from the lower parts of the section (I-I) of Middle-Upper Cambrian sequence are found in the block fragments near to the motorroad and the sole of rock cliffs. This sequence is present here with four steep-bedding packages (upwards):

1. Directly close to the Chuya motorroad the polymict coarse-grained sandstones with rare inclusions of triangle fragments of carbonate rocks and chert are exposed 120 m.

2. Polymict sandstones interlayering with mudstones. Among them bodies of irregular shape, bands and lenses of conglomerates, breccias and olistostromes are found to compose 50% of total volume. Their thickness - $n \cdot m$, length - $n \cdot 10$ m. They are composed of variously rounded fragments of marble-like limestones, oncolite limestones, dolomites, cherts, sometimes Early Cambrian limestones with *Archaeocyatha*, well-rounded ellipse-like pebbles of plagiogranites and polymict gravellites. Position of fragments in lenses resembles a zonation: in the center there are large blocks of olistoliths surrounded with smaller bodies. Olistoliths composed of limestones have the plane shape with splinted end to be present with oval bodies up to 20 m length 200 m.

3. Grey and dark-green roughly graded polymict sandstones and gravellites. In them the variously rounded fragments of marble-like limestones, dolomites and cherts up to several centimeters length are situated chaotically 35 m.

4. Grey carbonate shales containing sporadically dispersed inclusions of extend olistoliths and more fine siliceous-carbonate fragments oriented conformly to layering. The visible width of the largest olistolith reaches 8 m 50 m.

Further, the rocks of Baratal series are exposed. Two kilometers southwards within the upper reaches of Menka River water-fall along the same contact the stratigraphic overlying of basal coarse-grained trough sequence on the siliceous-carbonate rocks of Baratal seamount similar to described in Stop 1 is observed.

Stop 18. Located 9 km along the motorroad from Stop 17 within the right bank of Baratal Log mouth (fig. 25 and 35). The imbricated structure mapped among Vendian-Early Cambrian siliceous-carbonate rocks of Baratal seamount is present with volcanogenic sandstones and tectonic melanges between the siliceous-carbonate and terrigenous sheets. The matrix of melange is mainly composed of mylonitized terrigenous rocks. The blocks and fragments in melange of different dimensions (up to $n \cdot 10$ m) consist of cherts and carbonate rocks. Terrigenous rocks of the central part of a plate are present with volcanogenic greywackes corresponding to MORB basalts by composition (fig.36).

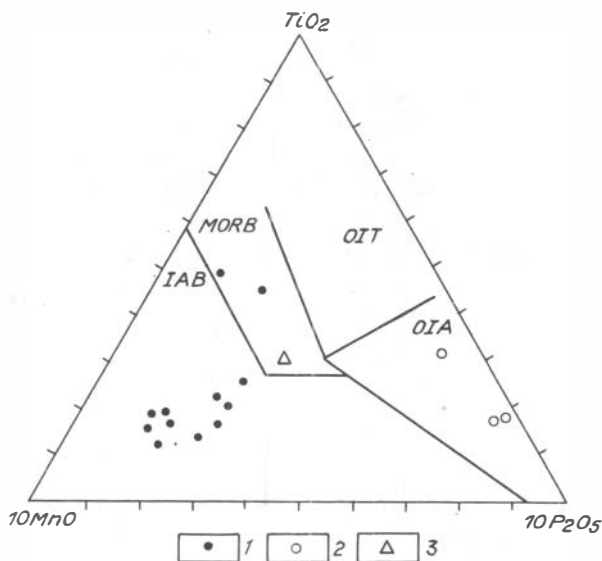


Fig.36. Bulk compositions of volcanic rock fragments from different terranes of Kurai zone (compiled by M.M.Buslov):

1 - pebbles of pyroxene porphyrites from conglomerates of inter-arc trough (Stop 20); 2 - pebbles of basalts from the Early Cambrian olistostrome of accretionary prism; 3 - sandstones of the third layer of oceanic crust (Stop 18).

Stop 19. Located 2 km from Stop 18. The flysch-like rocks of Gornoaltaiskaya series of Anui-Chuya trough containing in the basement coarse-grained rocks are exposed in rock cliffs of the Chuya River left bank. The fragment of series in II-II section consists of the following units dipping to the west-north-west at 60-80° angle (downwards):

1. Sand-mudstone rhythmic-layered unit. The thickness of rhythms from n*10 centimeters up to 250 m.
2. Mudstone unit with rare interbeds of sandstones and gravellites 250 m.
3. Olistostrome-conglomerate unit consisting of the fragments of cherts, dolomites and limestones of Baratal series. Terrigenous material includes variously rounded small and giant pebbles, olistoliths up to several meters length chaotically situated among gravellites and coarse-grained siliceous-carbonate and quartz-plagioclase sandstones. Somewhere there are interbeds of grey-green finegrained sandstones and mudstones. The sequence is intensively dislocated180 m.

Further the siliceous-carbonate rocks of Baratal series are exposed to be overthrust on the rocks of Gornoaltaiskaya series under 60-70° angle.

Stop 20. Located 3 km from Stop 19. Giant conglomerates of inter-arc trough make up tectonic sheet inside the outcrops of siliceous-carbonate rocks of Baratal seamount. The strata of this conglomerates are dipping to the north-east under 50-70° angle. Stratigraphically upwards 1.5 km from the basis they are substituted by siliceous-carbonate olistostrome. Boulders and pebbles in conglomerates form the strata various in composition due to the supply of terrigenous material into the trough from both non-volcanic and volcanic island arcs. Boulder conglomerates carried from non-volcanic island arc are usually composed of poor-rounded fragments of cherts and carbonate rocks, pebbles of basalts, amphibolites, rarely serpentinites and carbonate-siliceous gravellites. Boulder conglomerates carried from volcanic island arc contain well-rounded fragments of magmatic rocks of different composition, pyroxenites, gabbro, gabbro-diabases, diabases, potassium and sodium granitoids (somewhere transformed into cataclasites and mylonites), siliceous rocks, limestones with *Archaeocyatha*, terrigenous rocks and quartz-sericite schists.

In the table 19 there is bulk composition of the pebbles of magmatic rocks from conglomerates of inter-arc trough. Their composition corresponds to composition of the rocks from oceanic islands and island arc (fig. 33, 34, 36) both.

Day 5. We would like to demonstrate the eastern part of Kurai zone including the part of Baratal seamount (Stops 21, 22), Chagan-Uzun ophiolites with eclogites (Stops 25A), boninite volcanics and dikes of Vendian-Cambrian primitive island arc (Stops 23). The whole length of the route - 60 km; 30 km from Aktash Village to Stop 21 and 30 km to Chagan Uzun.

Stop 21. Located 11 km from Stop 20 at the left bank of Taldytiurgun River (fig. 25, 35). Pillow lavas and pillow breccias of the third layer of oceanic crust are present with breccia-like pyroxenite porphyrites (table 17, fig. 26, 33, 34).

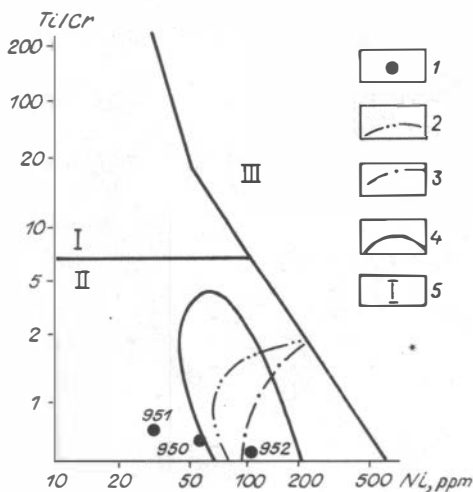
Upwards the section to the south-west among lavas there are interlayers of deep-water cherts and limestones which further are situated with olistostrome-breccia sequence. It consists of marl matrix involving various fragments (up to n·10 centimeters) of cherts and carbonate rocks to represent the slope facies of Baratal seamount.

Stop 22. Outskirts of Kurai Village. Devonian lavas of quartz porphyries of active continental margin. Observation of major geological complexes and structural elements of Kurai zone (fig.25). Panorama includes Baratal terrane, fragments of primitive island arc, Kurai metamorphic complex, Late Paleozoic-Mesozoic sequences and strike-slip deformations.

Stop 23. Located 21 km from Kurai Village. Lava, dike-sill and turbidite complexes belong to the primitive island arc. Lavas and intruded magmatic rocks relate to tholeiite-boninite series (table 20, fig.37). Commonly, turbidites consist of the fragments of pyroxenes and plagioclases.

Fig.37. Diagram Ti/Cr - Ni for the lava flow (Stop 23) (compiled by M.M.Buslov):

1 - different parts of the massive lava flow (950 and 951 - central part, 952 - marginal part); 2 - field of boninites for Bonin Islands of Marian Trench; 3 - field of boninites of ophiolites of Mongolia; 4 - field of boninites of Kurai terrane; 5 - series: I - moderate titaniferous tholeiite series of island arcs, II - low titaniferous boninite series of island arcs, III - high titaniferous tholeiite series of mid-oceanic ridges, marginal seas and seamounts (2, 3, 5 after data of Kepezhinskas et al., 1985; Kepezhinskas et al., 1987; Beccaluva et al., 1980; Beccaluva et al., 1983).



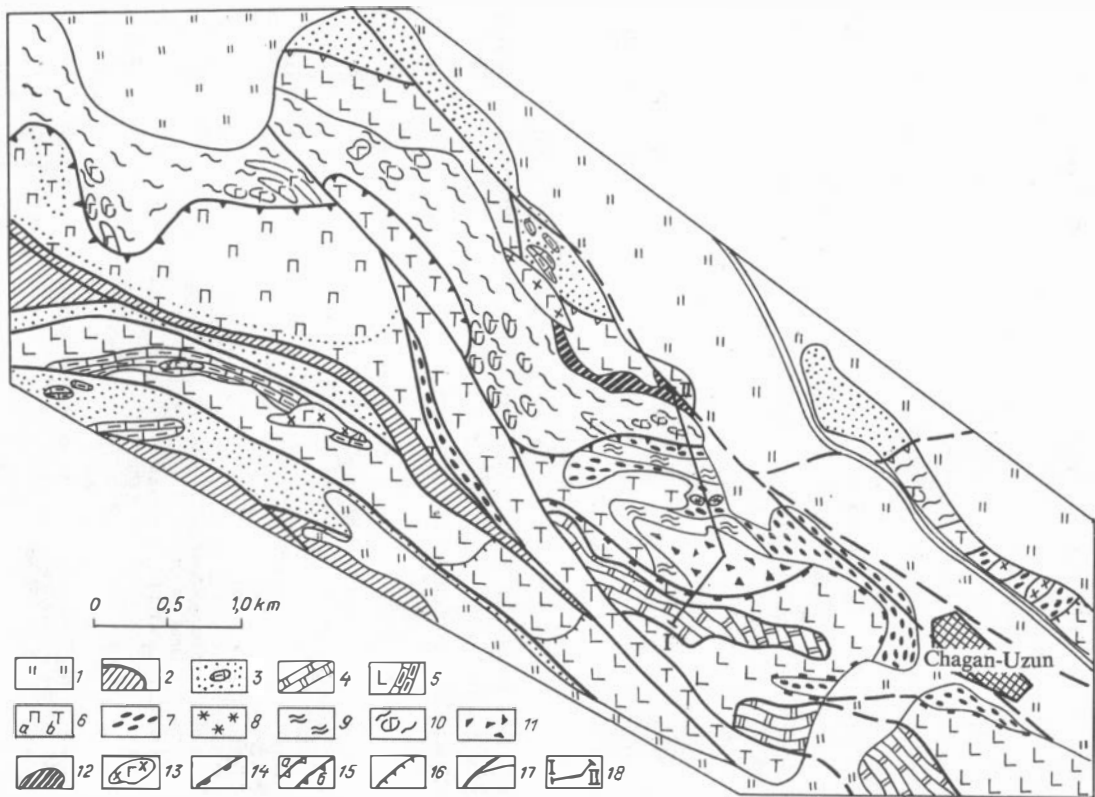


Fig. 38. The structure of accretionary prism of Chagan-Uzun ultrabasite massif (compiled by M.M. Buslov and N.L. Dobretsov using materials of P.P. Kuznetsov, 1980):

1 - Neogene-Quaternary deposits; 2 - Devonian sedimentary-volcanogenic rocks; 3 - calc-greywacke turbidites and andesites of the Middle Cambrian normal island arc; 4-12 -- Early Cambrian accretionary prism including: 4-5 - Vendian-Early Cambrian rocks of Baratal seamount; 4 - siliceous-carbonate rocks, 5 - sedimentary-volcanogenic rocks; 6-12 - Chagan-Uzun ophiolite massif; 6 - peridotites (a) and massive serpentinites (b), 7 - serpentinite melange; 8-9 - blocks and sheets of metamorphic rocks with eclogites and garnet amphibolites (8) and greenschists (9); 10 - schistose and massive serpentinites with gabbro dikes; 11 - Early Cambrian olistostrome; 12 - amphibolites at the sole of Chagan-Uzun massif; 13 - Devonian gabbro-dabase dikes; 14 - roof thrust of Baratal paleoseamount; 15 - floor thrusts of the lower (a) and upper (b) sheets of Chagan-Uzun massif; 16 - other thrusts; 17 - Late Paleozoic reverse thrusts; 18 - route line.

Stop 24. Located 6 km from Stop 23. Observation of imbricated structures of the Vendian primitive island arc and accretionary prism (Kurai and Saliugem Ridges) (fig.25).

Stop 25A. Located at the left bank of Chuya River, 1-2 km down the current from Chagan-Uzun Village. Study the fragment of the section of accretionary prism (fig.38). The following units are distinguished (up-downwards, section I-II):

1. Siliceous-carbonate nappe of Baratal seamount is exposed as several deformed steps. Its visible thickness reaches first hundreds meters. In their basis there is tectonic melange consisting of greenschist matrix which contains the fine fragments and blocks of limestones and cherts.

2. Sheet of metabasalts. They are present with schists, boudins and lenses. Its thickness varies from $n \cdot 10$ to $n \cdot 100$ meters.

3. Olistostrome. Its rocks have undergone cataclasis to be present with interlayering siliceous-carbonate gravellites, siliceous-clayish and marl schists. The fragments are composed of poor-graded dolomites, limestones and cherts up to first centimeters in dimension. Thickness reaches first $n \cdot 10$ meters.

4. Upper sheets of Chagan-Uzun ophiolite massif is made up of ultrabasites represent fresh peridotites in the upper horizon and massive serpentinites in the lower horizon (table 21). Serpentine melange sheets with inclusions of blocks massive serpentinites, eclogites and garnet amphibolites are located within the basis of the sheet considered. Thickness of sheets reaches 200 m. The largest bodies are composed of garnet

amphibolites containing eclogite relics. Among metamorphic rocks the lenses and interlayers of cherts are found. High pressure rocks have undergone greenschist diaphthoresis which is regularly exhibited at the marginal parts of bodies.

A series of rocks from greenschist diaphthorites (with relics of garnet) to garnet amphibolites (with relics of eclogites) is illustrated in fig.38. The samples were selected with 10-15 m interval out of the upper metamorphic sheet of I-II section along the route from the south to the north. Bulk composition and trace element concentrations for these samples are cited in table 22.

5. The lower sheet of Chagan-Uzun massif is composed of massive and schistose serpentinites which contain boudins and deformed dikes of gabbro and gabbro-diabases. The outside zones of these bodies are made up with rodingites. Below, there are rocks with geochemical characteristics of oceanic island basalts (table 22). At the contact we can clearly see the metamorphic sole of Chagan-Uzun massif composed of garnet-free amphibolites ($P=2-3$ kbar, $T=500^{\circ}\text{C}$). Its thickness reaches $n \cdot 100$ m. Far from the contact amphibolites gradually pass into well-known basaltic porphyrites.

Along the strike to the east the rocks of Chagan-Uzun massif are transformed into melange within the right bank of Chuya River.

The rocks of the upper sheets including eclogites (table 23) and garnet amphibolites are high pressure (13-14 kbar), the rocks of the lower sheets containing metagabbro, rodingites and garnet-free amphibolites correspond to lower pressure rocks (2-3 kbar). We can suggest that the upper sheets with eclogites are a subducted complex (the hanging wall of subduction zone ?), the amphibolites from the lower sheet formed under ascending movement of hot ophiolites to the surface and reached their hot contact with basalts of Baratal seamount (Dobretsov et al., 1992).

The composition of minerals from eclogites are cited in table 23. Clinopyroxenes in diagram Al - (Fe+Mn+Mg) - Fe fall onto the field of glaucophane schists, being closely associated with pyroxenes from low-temperature eclogites (Dobretsov et al., 1992).

The amphiboles from eclogites have the increased Ca content from center to edges of mineral grains due to the regressive metamorphism with pressure decreasing. In diagram $\text{Mg}/(\text{Fe}+\text{Mg})$ - $\text{Ca}/(\text{Ca}+\text{Na})$ (fig.39) the composition points of amphiboles from Chagan-Uzun eclogites fall onto the field of barroisite-actinolite group.

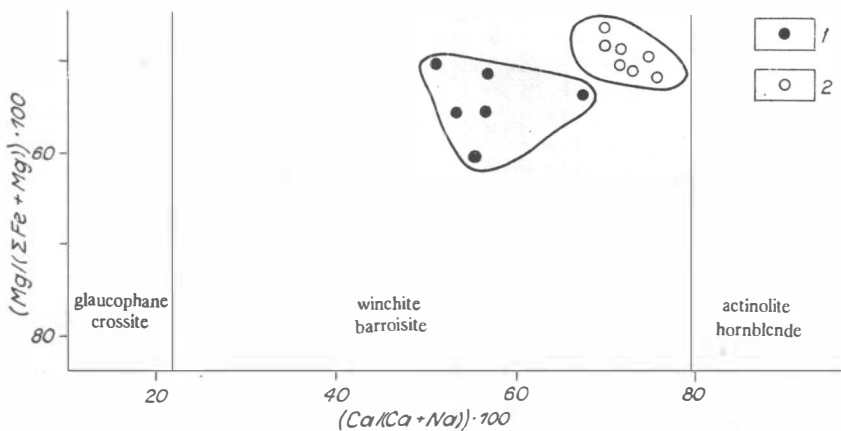


Fig.39. Composition of amphiboles from metamorphic rocks of Kurai zone (compiled by M.M.Buslov and V.A.Simonov):

1 - from eclogites of Chagan-Uzun massif; 2 - from amphibolites of accretionary prism.

The majority of analyses of garnet amphibolites and eclogites of Chagan-Uzun massif correspond to MORB and, somewhere, to basalts of oceanic islands (table 22, fig.31,33,34). According to Ti and Cr/Ni interrelation (fig.31) the analyses of gabbro dikes from the lower sheet of Chagan-Uzun massif fall at the boundary between the fields of oceanic and island arc series to cross slightly the field of dikes from Kurai primitive island arc. It can evidence their co-magmatic nature. In the diagram $TiO_2 - FeO/(FeO+MgO)$ (fig.40) the gabbro dikes from the upper sheet of ultramafics of Chagan-Uzun massif partly correspond to moderate titaniferous island arc rocks or to oceanic trend.

Thus, the following conclusions can be made using the analysis of geological structure of Stop 25 region.

Chagan-Uzun ophiolites are the fragment of oceanic lithosphere. It is confirmed by their structural position in the sole of accretionary wedge where they appeared from subduction zone being intensively tectonized and metamorphosed. According to chemistry and geochemistry of REE garnet amphibolites and amphibolites correspond to N-type of basalts of mid-oceanic ridges. Island arc moderate titaniferous dikes of Chagan-Uzun ultramafics mark the stage of the uplift of ultramafic sheet out from the subduction zone and its junction to the sole of island arc where it was penetrated with those

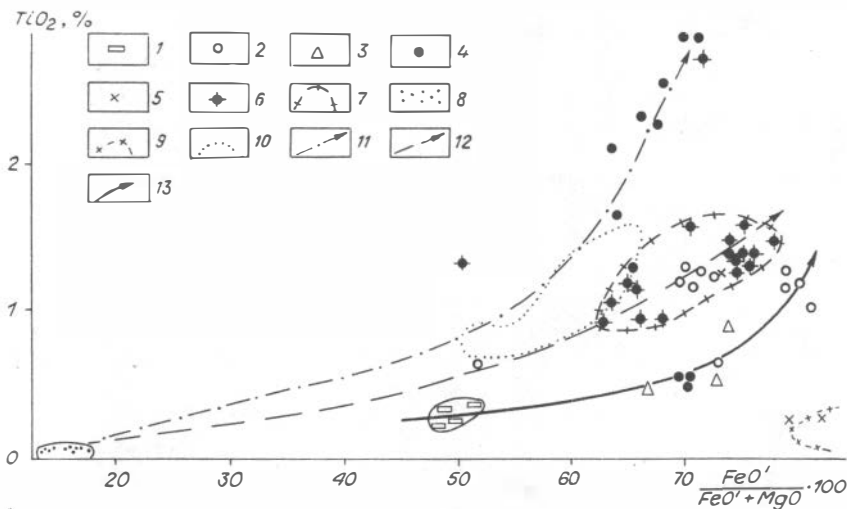


Fig.40. Diagram TiO_2 -FeO/(FeO+MgO) for magmatic rocks of Kurai zone (compiled by V.A.Simonov).

1-9 - magmatic rocks of Vendian-Cambrian primitive island arc: 1- boninites, 2 - aphyric lavas, 3 - sills, 4 - dikes, 5 - granitoids, 6-7 - dikes cutting peridotites of Chagan-Uzun massif (6) and field of dikes (7); 8 - harzburgites of Chagan-Uzun massif; 9 - Troodos granitoid field; 10 - field of MORB-type of Red Sea bottom; 11-13 - trends: 11 - oceanic, 12 - island arc, 13 - boninite.

dikes. The subduction of oceanic lithosphere proceeded beneath the primitive island arc of Gorny Altai zone.

Stop 25B. Located near to Chagan-Uzun massif. Observation of the main rock complexes of island arc and imbricated structure of Kurai ridge. The package of plates to be a synform fold of north-west strike is clearly found (fig.41). Upwards, the following tectonic units are distinguished:

1. Lower plate of 1.5 km thickness consisting of Lower-Middle Cambrian turbidites of fore-arc trough of normal island arc;
2. The package of plates of primitive island arc including gabbro-diorite massifs, complex of parallel dikes and sills of tuffs and volcanic rocks up to 1 km thickness;
3. The package of sheets of gabbro-pyroxenites up to 1 km thickness;
4. The package of thick (1.5-2 km) plates of carbonate-terrigenous black

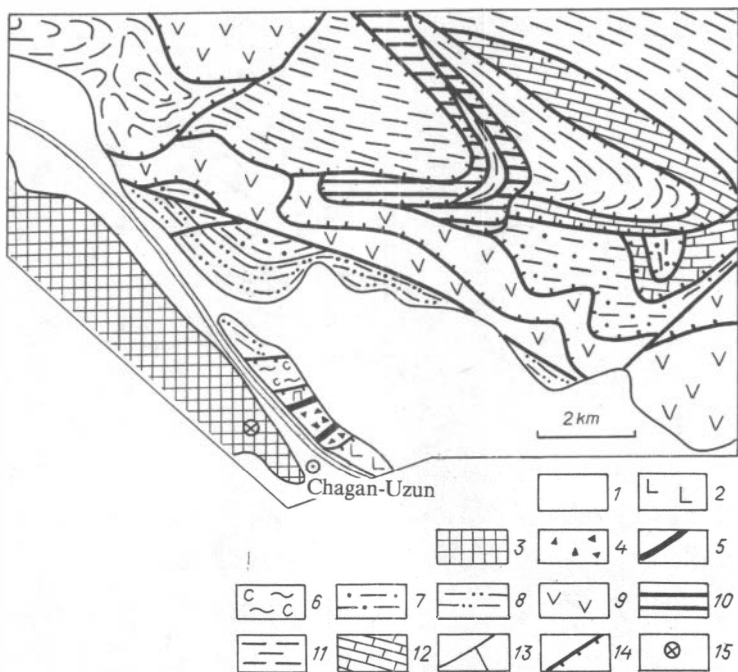


Fig.41. Geological structure of Kurai ridge (compiled by M.M.Buslov):

1 - Neogene-Quaternary deposits; 2 - Vendian-Early Cambrian metabasalts; 3-6 - Chagan-Uzun ophiolite massif: 3 - undivided main body, 4 - serpentinite melange, 5 - blocks of garnet amphibolites, 6 - massive and schistose serpentinites; 7-8 - Lower-Middle Cambrian rocks of fore-arc trough of normal island arc: 7 - Middle Cambrian tuff-terrigenous turbidites, 8 - Early Cambrian calc-greywacke turbidites and andesites; 9-12 - primitive island arc: 9 - undivided Vendian-Lower Cambrian rocks: lavas, tuffs, dikes, and sills, 10 - Meshtuyaryk layered gabbro-pyroxenite complex, 11 - Lower Cambrian blackshale turbidites of marginal sea or inner slope of island arc, 12 - Lower-Middle Cambrian carbonate rocks; 13 - Late Paleozoic faults; 14 - Early Paleozoic deformed thrusts; 15 - location of Stops for observation.

shales and turbidites of the outer slope of island arc or marginal sea. It overlies the different structural elements of 2-3 packages;

5. The upper plate of 0.5-1 km thickness is similar in composition to 2 package.

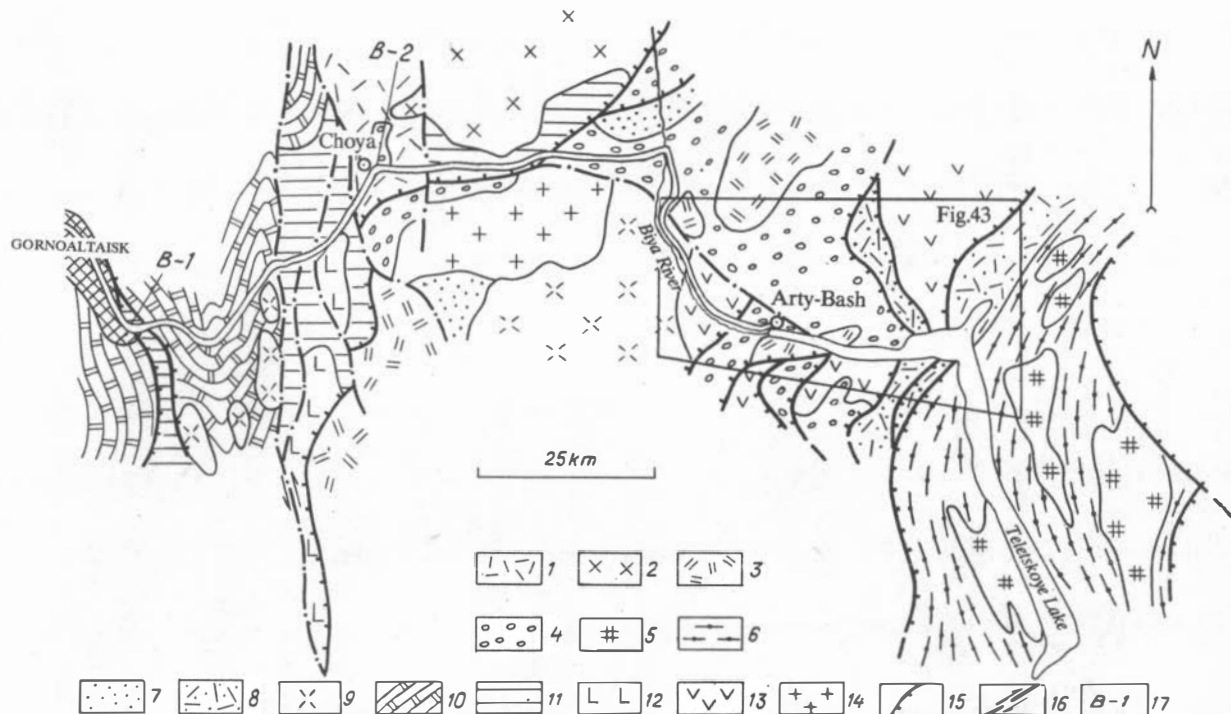


Fig.42. The scheme of Route B by Teletsk motorroad (compiled by M.M.Buslov and N.A.Berzin):

1-3 - Devonian active margin complexes: 1, 2 - volcano-plutonic belt: 1 - dacite-rhyolite and andesite lavas, tuff sandstones, and tuff mudstones, 2 - granitoids (D_{1-2}), 3 - basalt-rhyolite lavas, tuffs, and sediments (D_1^2 - D_2) of back rift zone; 4-6 - Ordovician-Early

Silurian complexes of collisional stage: 4 - red coarse clastic rocks ($O_{1,3}$), 5, 6 - Teletsk zonal metamorphic complex: 5 - two-mica collisional granites, 6 - metamorphic rocks; 7-9 - complexes of normal island arc stage (C_1^2 - C_3) olistostromes of inter-arc trough (C_2 - C_3), 8 - dikes, lavas of andesites and shoshonites, tufts, sediments, limestones (C_1^2), 9 - gabbro-diorite-plagiogranite (C_2); 10-12 - paleoguyot rocks ($V-C_1^1$); 10 - siliceous carbonate, 11 - siliceous-carbonate-terrigenous, 12 - predominantly basalts, tufts, sediments; 13 - dikes, lavas of tholeiite basalts and boninites, sediments ($V-C_1$); 14 - post-collisional intrusions of coarse-crystalline granites and alaskites (C_2-P_1); 15 - thrusts; 16 - strike-slip faults and their direction; 17 - location of observation points.

The total thickness of the tectonic package of plates of Kurai Ridge exceeds 5-6 km.

ROUTE B

Gornoaltaisk - Biya River - Teletskoye Lake

General review

The route goes from the Chuya motorroad through the north-eastern part of Gorny Altai (150 km route's length). Here, the Vendian rocks of Katun seamount, Vendian-Early Cambrian rocks of primitive island arc, Early-Middle Cambrian complexes of normal island arc, Ordovician collisional stage deposits and Devonian active continental margin rocks are widespread (fig.42).

Near to Gornoaltaisk city and further to the east about 90 km the way passes the Vendian siliceous-carbonate and sedimentary-volcanic rocks of Katun seamount. They are intruded by the massifs and dikes of Middle Cambrian and Devonian granitoids which belong to active marginal geodynamic environments. Near to Choya Village a tectonic block (6-8 km width), which consists of Early Ordovician molasse (Choya suite) and Middle Devonian andesite-dacite lavas, tufts and terrigenous rocks, is situated among the rocks of seamount.

90 km from Gornoaltaisk city the way crosses Late Paleozoic thrust: the Vendian siliceous-carbonate-terrigenous rocks are thrust over Ordovician sandstones and mudstones. Along strike the thrust is traced on many hundreds kilometers and divided by across strike-slip faults of Mesozoic age.

Then, 20 km way passes poorly exposed places with separate outcrops of Early Ordovician rocks.

After it, the road crosses Biya River and goes along the Quaternary deposits of its right bank. There are outcrops of Early-Middle Ordovician sandstones and mudstones,

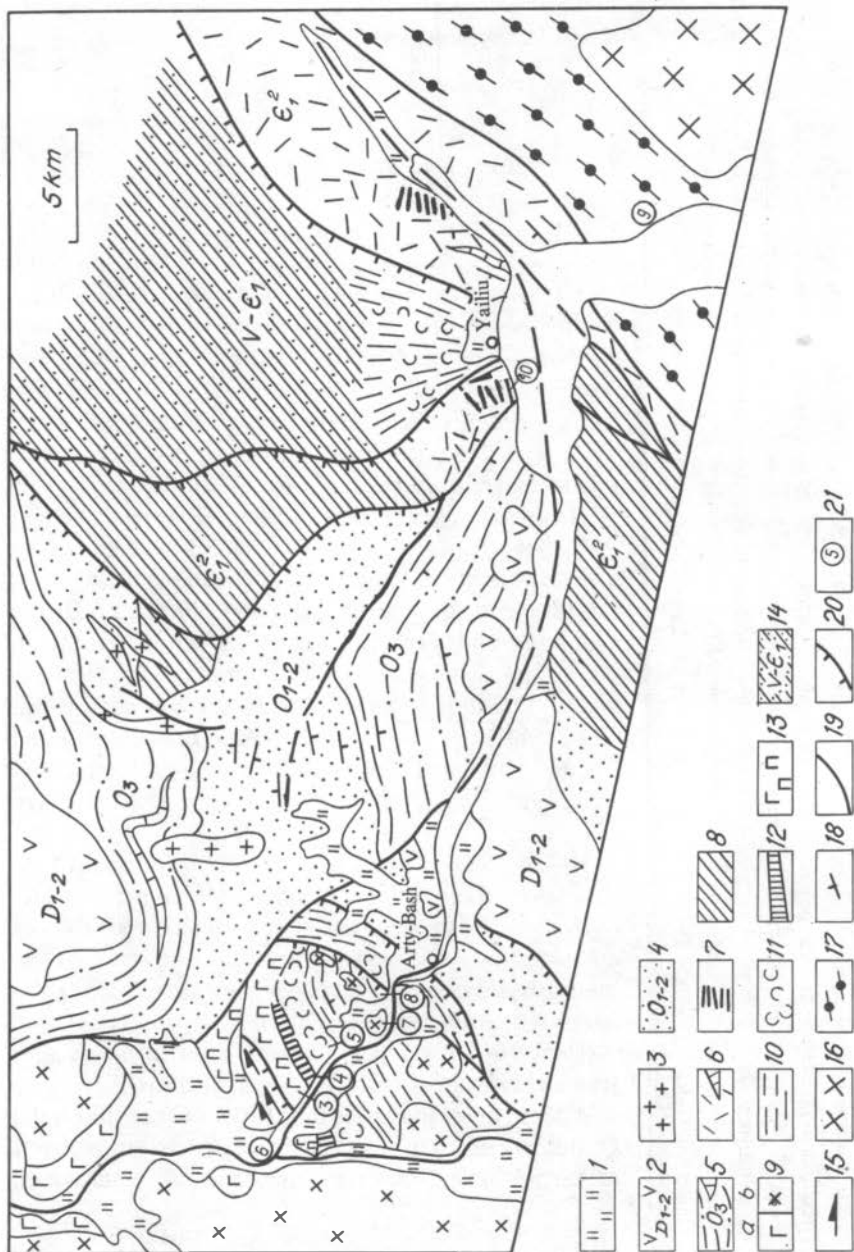


Fig.43. Geological structure of Biya River sources and Teletskoye Lake district (compiled by N.L.Dobretsov, M.M.Buslov and V.A.Simonov):

1 - Quaternary sediments; 2-3 - the rocks of back rifts of Devonian active margin; 2 - basalt-rhyolite lavas, tuffs and sediments (D_{1-2}); 3 - subvolcanic bodies of granosyenite-porphyrates and quartz porphyries; 4-5 - Ordovician molasse of collisional stage: 4 - terrigenous (O_{1-2}); 5 - carbonate-terrigenous (O_3); 6-9 - rocks of normal island arc stage (ϵ_1^{-2}): 6 - shoshonite and andesite lavas, limestones and terrigenous rocks, 7 - shoshonite and andesite dikes, 8 - undivided rocks, 9 - granitoids (ϵ_2); 9a - gabbro, 9b - diorites and plagiogranites; 10-15 - primitive island arc rocks ($V-\epsilon_1$): 10 - siliceous-terrigenous sediments and tuffs, 11 - pillow-lavas, lavabreccias and tuffs, 12 - sheeted dikes and dike-sill series, 13 - layered gabbro-pyroxenite complex, 14 - undivided rocks; 15 - winchite-barroisite-chlorite schists; 16-17 - Teletsk metamorphic complex; 16 - two-mica granites, 17 - zonal metamorphic rocks; 18 - direction of bedding plunging; 19 - strike-slip faults; 20 - thrusts; 21 - location of Stops.

somewhere. Near to Kebezen' Village among Middle Cambrian granitoids there are small outcrops of the Vendian primitive island arc rocks.

After this point, the observation of the major objects of field trip begins. North from Teletskoye Lake, in the right bank of Biya River sources (fig.43) in tectonic sheets the Vendian-Cambrian island arc rocks including ophiolites occur.

The island arc rocks are divided by the sheets composed of Ordovician and Devonian rocks. All of them are thrust in west-east direction. The most thick sheet (5-6 km) is composed of Early Cambrian rock assemblage considered as ophiolite by N.L.Dobretsov, M.M.Buslov and V.A.Simonov. Ophiolites present: 1) layered gabbro-pyroxenite complex, 2) sheeted-dike complex, 3) pillow-lavas and pillow-breccias, 4) clayish-siliceous rocks and sills. Ophiolites are intruded by the plutons, dikes and sills of Middle Cambrian island arc granitoids.

To the west, the ophiolites are overthrust by volcanic-sedimentary island arc complex metamorphosed to winchite-barroisite and green schists. This complex likely lies in the base of the other thick sheets which most part is located out of the region considered (fig.43). In the east, the ophiolite plate is separated from adjacent units by the faults accompanied by dynamic schists of greenschist facies and mylonitic dislocations.

The next group of sheets composed of island arc complexes is located north from Teletskoye Lake. Three large units can be distinguished here. The western unit consists

of the Early Cambrian sheeted dike complex, pillow-lavas, tuffs, tuffites, sandstones, shales and limestones formed during the normal island arc development stage. Limestones contain the fauna remnants of the second half of Early Cambrian. In the base of this sheets there are actinolite and barosite schists.

The central unit is composed of the Vendian-Cambrian basalts, tuffs and terrigenous-siliceous rocks.

In the eastern unit the Early-Middle Cambrian rocks are exposed: sheeted dike complex, sills, andesitic and andesite-basaltic lavas, tuffs and marble-like limestones. Limestones include fauna of Archaeocyata of the Early Cambrian.

From the east the low-metamorphosed island arc rocks are overthrust by the zonally metamorphosed rocks of Teletsk complex which consists of green schists, amphibolites, marbles, gneisses, granite-gneisses and two-mica granites. The metamorphic complex represents garnet-sillimanite, biotite-cordierite, biotite-chlorite and chlorite subzones. There are relics of volcanic and sedimentary rocks among greenschists.

The age of Teletsk metamorphic rocks is variously accepted: from Riphean to Early Paleozoic. The existing isotopic dates within this part of Gorny Altai are limited: 610 Ma for granite-gneisses and 410 Ma for garnet-biotite gneisses (K-Ar biotite dates).

Being located among low-metamorphosed island arc rocks the Teletsk complex can be considered as their metamorphic analogue. Metamorphic rocks relate to the boundary of Gorno-Altai and West Sayan blocks, and their formations can be referred to the collision of these two structural units.

To characterize the geochemical peculiarities of Vendian-Cambrian lavas and dikes we studied bulk rock composition (table 24), REE contents (table 25), composition of minerals and homogenized melt inclusions (table 26).

In the diagram TiO_2-K_2O (fig. 44) there are two rock series different in age and structural position. The high Ti variations under low K-content are typical of Vendian-Early Cambrian ophiolites. The magmatic rocks of ophiolites form a trend: boninites - island arc tholeiites - back-arc basalts.

Middle Cambrian sills intruding ophiolites and dikes from Early Cambrian rocks (to the north from Teletskoye Lake) with low Ti and variable K form another trend: island arc tholeiites - calc-alkaline rocks - alkaline rocks (shoshonites).

In the diagram TiO_2-Zr (fig.45) and $Y-Zr$ (fig.46) the magmatic rocks are

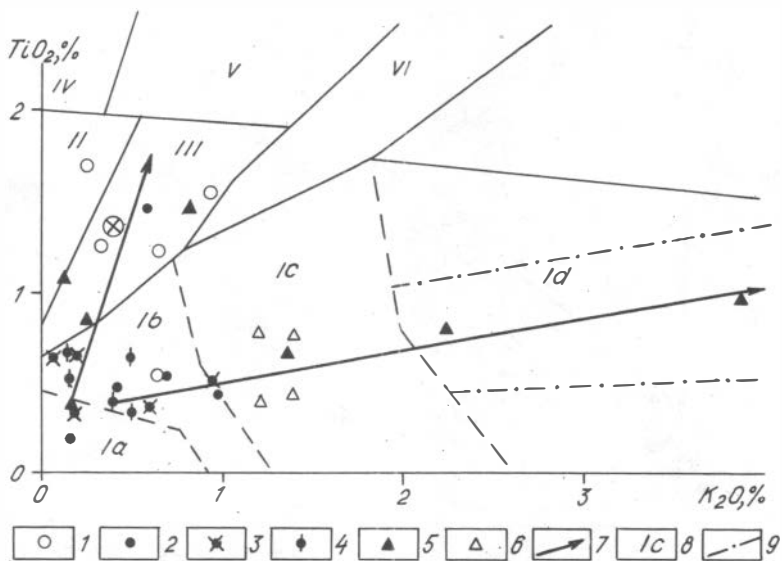


Fig.44. TiO_2 and K_2O relationship in rocks and clinopyroxenes of Vendian-Cambrian volcano-plutonic assemblages of Biya River sources and Teletskoye Lake district (compiled by V.A.Simonov using the diagram of Yu.V.Mironov, 1991):

1-4 - assemblage of Vendian-Early Cambrian primitive island arc stage: 1 - metalavas, 2 - dikes, 3 - sheeted dike complex, 4 - sills; 5-6 - assemblage of Early Cambrian normal island arc stage: 5 - bulk composition of dikes, 6 - composition of homogenized melt inclusions in clinopyroxene phenocrysts; 7 - compositional trends; 8 - fields of volcanic rocks: from island arc (Ia - boninites, Ib - tholeiites, Ic - calc-alkaline rocks, Id - alkaline rocks), from mid-oceanic ridges, back-arc spreading centers and intercontinental rifts (II); from back-arc spreading centers and transform faults (III); from oceanic islands (IV); from oceanic islands and platform activation areas (V); from platform activation areas (VI); 9 - ranges of TiO_2 values for shoshonite series rocks (Bogatikov (Ed.), 1985; Bogatikov et al., 1987).

divided into oceanic and island arc groups. The primitive island arc ophiolites have an oceanic trend and correspond to the field of Troodos ophiolites in Cyprus. The Early Cambrian dikes are referred to island arc series.

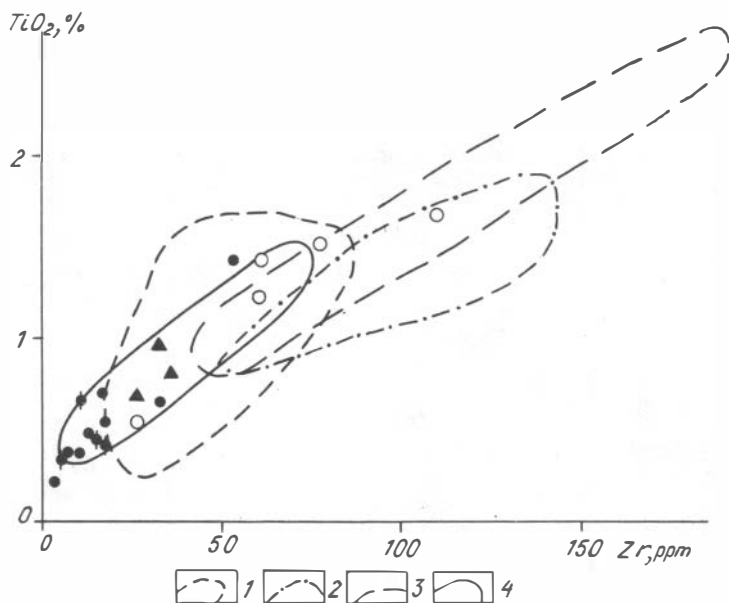


Fig.45. Diagram TiO_2/Zr in Vendian-Cambrian volcano-plutonic assemblages of Biya River sources and Teletskoye Lake district (compiled by V.A.Simonov): 1-4 - boundaries of fields: 1 - volcanic rocks of island arcs (Sharaskin & Zakariadze, 1982; Tarney & March, 1991); 2 - basalts of back-arc basins (Sharaskin & Zakariadze, 1982; Tarney & March, 1991); 3 - MORB (Saunders et al., 1980; Tarney & March, 1991); 4 - pillow-lavas and dikes of ophiolites of Troodos, Cyprus (Tarney & March, 1991).

The data on composition of clinopyroxenes and melt inclusions in these minerals (table 26, fig.44) confirm the conclusions made using petrochemistry and geochemistry. Pyroxenes from the porphyrites of Vendian-Early Cambrian ophiolite section relate to boninite field. Pyroxenes from Early Cambrian porphyrites fall in the field of island arc tholeiite series. Melt inclusions in pyroxenes of Early Cambrian porphyrites correspond to the fields of tholeiite and sub-alkaline island arcs and add the island arc trend made according to other data.

Thus, the rock fragments of the early primitive and normal stages of island arc formation occur north from Teletskoye Lake near Biya sources. Successive development of island arc magmatic systems from boninite to

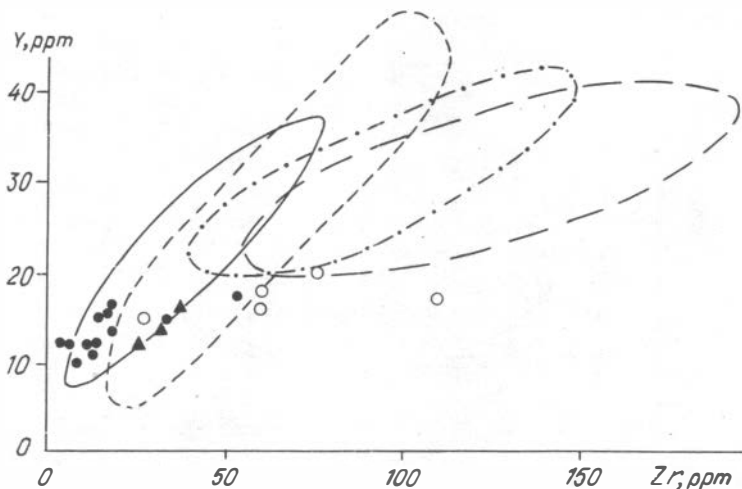


Fig.46. Diagram Y-Zr for Vendian-Cambrian volcano-plutonic assemblages of Biya River sources and Teletskoye Lake district (compiled by V.A.Simonov) (see legend to fig.45).

shoshonite series resulted from subduction zone "jumping" and increase of the Benyoff zone depth. Such process is traced by the change of melt composition: Ti and K increase and SiO_2 decreases from boninites to shoshonites.

Day 3. Study of the Vendian rocks of Katun seamount, Vendian rocks of primitive island arc, Early-Middle Cambrian complexes of normal island arc and Ordovician deposits of the collisional stage.

Stop B-1. Located to the east from Gornoaltaisk city. Rock outcrops expose three tectonic sheets easterly dipping at $60-70^\circ$. The sheets are composed of various Vendian rocks of Katun seamount (fig.42).

The lower sheet represents cherts, siliceous mudstones and carbonate rocks cut by diabase and granite dikes. Among the schistose mudstone-carbonate rocks with thin interbeds of cherts there are blocks of cherts, diabases and granites (fig.47).

The central sheet of 100 m thickness consists of carbonate rocks crossed by gabbro, gabbro-diabase and diabase dikes. Carbonate schists occur in the base of sheet.

The upper sheet is composed of interbedding carbonate and siliceous

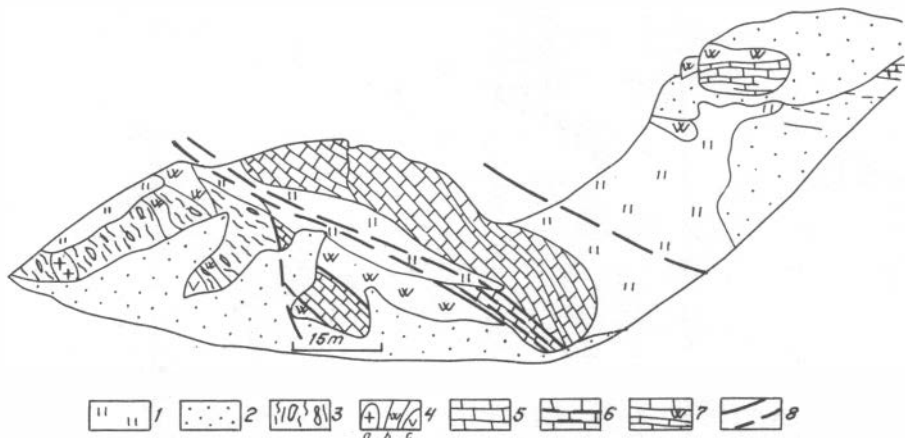


Fig.47. Schematic section showing the pile of imbricated structure of Katun seamount in Gornoaltaisk district, Stop B-1 (compiled By M.M.Buslov):

1 - vegetation; 2 - deluvium; 3-4 - lower sheet: 3 - schistose carbonate-terrigenous-siliceous rocks with blocks of non-altered rocks, 4 - large blocks of granites (a), cherts (b) and diabases (c); 5, 6 - middle carbonate sheet: 5 - layered limestones and dolomites of Baratal suite, 6 - schists after carbonate rocks; 7 - upper siliceous-carbonate sheet (Baratal suite); 8 - faults: visible (a) and supposed (b).

rocks. Siliceous rocks form thick interbeds of 8-10 m thickness well seen in rock outcrops on the light background of carbonate rocks. The sheet is crossed by gabbro dikes, as well.

Stop B-2. Located in Choya Village (fig.42). There are outcrops of the Early Ordovician molasse of Choya suite. The suite consists of conglomerates, arkose and polymict sandstones, siliceous-clayish schists and shales, rarely limestones. The pebbles of conglomerates include the pebbles of magmatic rocks: plagiogranites, pyroxene-plagioclase and plagioclase porphyrites. Siliceous rocks and limestones are found, as well. Debris corresponds to the Vendian-Cambrian island arc rocks of the Gorno-Altai block likely formed during its collision with the West Sayan block.

Stop B-3. Located in the right bank of Biya River (fig. 43). There are deluvium and outcrops of the layered gabbro-pyroxenite complex cut by the dikes of pyroxene porphyrites, diabases and gabbro-diabases. Bulk rock compositions are cited in table 24. In the diagram TiO_2 - K_2O (fig. 44) dikes fall

in the field of island arc tholeiites. Study of pyroxene from sample C-1g-92 showed that it corresponds to boninite series pyroxenes. Gabbro and pyroxenites make up the upper tectonic sheet of the overturned Vendian-Early Cambrian ophiolite section. Along the route they are changed by sheeted dike complex (fig. 43).

Stop B-4. Sheeted dike complex. Thickness of dikes is 10-30 cm. There is metagabbro steppe among them. Dikes have variable bulk composition. In the diagram TiO_2-K_2O they fall in the field Ia of boninites (sample C-8g-92), island arc tholeiites (sample C-8a-92, C-9b-92) and basalts of back-arc spreading centers (sample C-8c-92) (field II in fig. 44). According to bulk composition the sheeted dike complex corresponds to pillow lava composition.

Stop B-5. Located 1 km to the east from previous Stop. There are outcrops of pillow lavas of pyroxene porphyrites. The rocks have undergone greenschist metamorphism - pyroxene is replaced by chlorite everywhere. Lava bulk composition relates to back-arc spreading centers and island arc tholeiites (fig. 43).

Stop B-6. Located to the south from Kebezen' Village (fig. 43) in the sole of metamorphic slab thrust over low-altered island arc ophiolites (Stop B-3, B-4, B-5). The metamorphic sequence is exposed 200 m from the contact. It is composed of winchite-barroisite-actinolite schists (fig. 48, table 27), chlorite schists, siliceous interbeds and acid metatuffs including metadacite fragments. Somewhere, the tuffs are transformed into albite-quartz-mica micro gneisses.

In the diagram TiO_2-K_2O (fig. 44) barroisite-actinolite schist fall in the field III of basalts of back-arc spreading centers and is analogous to basalts and low-metamorphosed ophiolites of underlying slab. Commonly, metamorphic rocks are comparable with the volcanic-sedimentary part of island arc ophiolites formed due to dynamometamorphism under island arc imbricating.

Composition of amphiboles from amphibole schists corresponds to barroisites, winchites and actinolites (fig. 48). Since the ferriferous amphiboles contain no more 30% of sodium component and rock do not carry other indicative minerals of high pressure it is difficult to evaluate the P-T parameters of metamorphism.

N.A. Berzin believes that the whole association observed in Stops B-3,4,5,6 is not ophiolite. Together with barroisite-bearing rocks (Stop B-6) it forms a single island arc complex which along with basalts includes coarse tuffs of rhyolite, dacite, andesite and mixed composition. Gabbro pyroxenites and their crossing dikes are intrusive bodies inside this island arc association, but may occur close to the basement of this island arc.

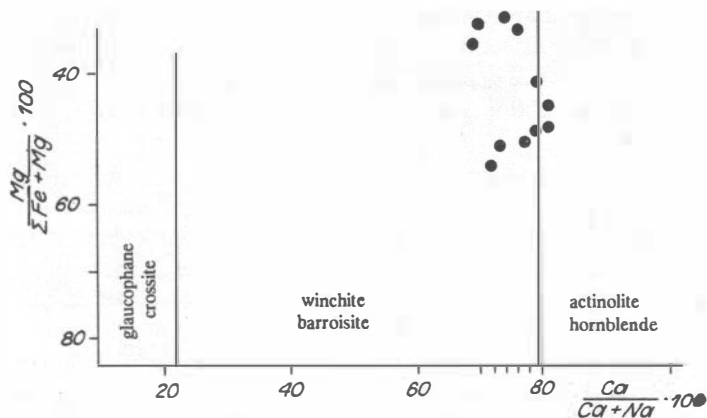


Fig.48. Diagram of Ca-Na amphiboles: position of amphiboles from metamorphic rocks of Stop B-6 (compiled by M.M.Buslov).

Stop B-7. Located 2 km east from Stop B-5. The road crosses the island arc Middle Cambrian granitoid massif relating to Sarakokshin pluton. It is composed of gabbro-diorites cut by diabase dikes. There are numerous xenoliths of hornfels-like metabasites among granitoids.

Stop B-8. Located 1 km from the previous Stop. Among the sedimentary rocks of the upper part of ophiolite section there are widespread dikes and sills from 10 cm to n*m thickness. They represent pyroxene porphyrites, gabbro-diabases, diabases and diorites. Bulk composition of dikes is cited in table 24. All of them correspond to the field of island arc tholeiites (fig. 44) and characterize the stage of normal island arc development.

Day 4. Ship journey on Teletskoyè Lake. Lake's length more than - 80 km, width - 5 km, depth - 400 m. The lake is aligned in NNW-SSE direction along the Altai-Harus dextral wrench fault. Its northern prolongation coincides with the North Sayan left-lateral fault zone and with more discrete left-lateral strike-slip faults of smaller dimensions. From its tectonic situation, general orientation and great depth Teletskoye Lake is thought to be developed as a pull-apart basin in transective situation similar to well-known Baikal Lake. To examine this model it is necessary to carry out additional detail investigations including heat flow measurement, deep seismic sounding and structural estimations of active tectonics. But the numerous morphological features can be seen during excursion.

The structure of lake bottom consists of three Quaternary deep grabens of sub-lateral, north-eastern and submeridional strike carrying the features of regional Late Paleozoic-Mesozoic faults. Some of them were reactivated in Cenozoic.

Stop B-9. Located in the right bank of Teletskoye Lake. Near water-fall Korby there are outcrops of metamorphic rocks of Teletsk complex represented by grey, grey-green schists and metasandstones.

The blocks carried by Korbu River include the rocks of other subzones of metamorphic complex: cordierite gneisses, quartz-biotite and quartz-muscovite-biotite schists.

Stop B-10. Located in the northern bank of Teletskoye Lake nearby to Yailiu Village. Island-arc rocks form three large sheets (fig.43) which are well observed from the ship board. The sheets are dipping westwards beneath the Ordovician terrigenous rocks. Among Early Cambrian rocks the dykes and sills of clinopyroxene porphyrites and diabases are of most interest. They are exposed along bank cliffs of Teletskoye Lake, somewhere forming sheeted-dike complex. Thickness of dikes from $n \cdot 10$ cm to 1 m. Bulk composition of clinopyroxene porphyrites corresponds to shoshonites. In the diagram TiO_2 - K_2O their clinopyroxene composition falls on the field of island arc tholeiite series, the composition of clinopyroxene melt inclusions relates to the fields of tholeiite and sub-alkaline island arc series (table 25,26, fig.44).

According to structural position, the shoshonite rocks form a marginal eastern part of Gorno-Altai island arc system and characterize its back part.

REFERENCES

- Afonin, A.I.**, 1976, Supposed skeleton fauna *Protospongia* and *Chanclloria* in Precambrian deposits of Gorny Altai. *Geology and Geophysics*, No.11, pp. 16-21 (in Russian).
- Batchelor R.A. and Bowden P.**, 1985, Petrogenetic interpretation of granitoid rock series using multicationic parameters. *Chemical Geology*, No. 48, pp.43-55.
- Beccaluva, L., Piccardo, G.B. and Serri, G.**, 1980, Petrology of northern Apennine ophiolites and comparison with other Tethyan ophiolites. *Ophiolites. Proc. Intern. Ophiol. Symp.- Cyprus: Panaiotou. Geol. Surv. Dept.*, pp.314-331.
- Beccaluva, L., Girolamo, P.D., Macciotta, G. and Morra, V.**, 1983, Magma affinities and fractionation trends in ophiolites. *Ophioliti*, No. 8, pp.307-324.
- Berzin, N.A., Coleman, R.G., Dobretsov, N.L. et al., and Zhao Min**, 1993, Geodynamic Map of the Paleasian Ocean (Western part). *Abstr. 4th Int. Symp. IGCP Proj. 283, Novosibirsk* (in press).
- Bogatikov, O.A.** (Ed.), 1985. *Magmatic rocks. V.3*, Nauka, Moscow, 485 p. (in Russian).
- Bogatikov, O.A.**, 1987, Petrology and geochemistry of island arcs and marginal seas, Nauka, Moscow, 336 p. (in Russian).
- Bogolepov, K.V. and Yanshin, A.L.**, 1973, To the modern hypotheses of ultrabasic formation and structure of Chagan-Uzun massif in Gorny Altai. *Geology and Geophysics*. No.8, pp.12-25 (in Russian).

Dobretsov, N.L. (Ed.), 1991. Geology and Tectonics of Gorny Altai. Guide-book for excursion, IGG Publ., Novosibirsk, 71 p. (in Russian).

Dobretsov, N.L. and Kirdyashkin, A.G., 1993, Blueschists belts of North Asia and models of subduction-accretion wedge. In: R.G. Coleman (Ed.) Reconstruction of Paleasian Ocean, VSP Int. Sci. Publ., the Netherlands, pp. 91-106

Dobretsov, N.L., Konnikov, E.G., Medvedev, V.N. and Sklyarov, E.N., 1985. Ophiolites and olistostromes of the East Sayan. In: Riphean-Lower Paleozoic ophiolites of North Eurasia. Nauka, Novosibirsk, pp.34-58 (in Russian).

Dobretsov, N.L., Simonov, V.A., Buslov, M.M. and Kurenkov, S.A., 1992. Oceanic and island arc ophiolites of the south-eastern part of Gorny Altai. Geology and Geophysics, No.12, pp.3-14 (in Russian).

Gusev, N.I., 1991, Reconstruction of geodynamic regimes of Precambrian and Cambrian volcanism in the south-eastern part of Gorny Altai. In: Paleodynamics and origin of South Siberian perspective zones. UIGG&M SB RAS, Novosibirsk, pp.32-55 (in Russian).

Izokh, E.P., Kononov, A.N. and Kononov, O.A., 1987, Systematics and formation analysis of Gorny Altai granitoids. In: Systematics of magmatic formations (Eds Polyakov, G.V. & Kutolin, V.A.). Nauka, Novosibirsk, pp.97-147 (in Russian).

Kepezinskas, V.V., Kepezinskas, K.B., Bobrov, V.A. and Parkhomenko, V.S., 1985. Geochemistry of volcanic rocks of Mongolia metaophiolite formations and environment of Paleooceanic lithosphere formation. In: Geochemistry of rare-earth elements in mafics and ultramafics, Novosibirsk, pp.4-26 (in Russian).

Kepezinskas, K.B., Kepezinskas, V.V. and Zaitsev, N.S., 1987, Evolution of Mongolia earth's crust in the Precambrian-Cambrian, Nauka, Moscow, 168 p. (in Russian).

Kononov, A.N. 1965. Late Paleozoic Yaloman granitoid complex of Central Altai. Geology and Geophysics, No.4, pp.78-91 (in Russian).

- Kononov, A.N.**, 1969, Yaloman granodiorite-adamellite complex of the central part of Gorny Altai, Krasnoyarsk Publ., Krasnoyarsk, 163 p. (in Russian).
- Krasov, N.F.**, 1993, On the geodynamic position of granitoids of Yaloman complex (Gorny Altai) according to their petrochemistry. Abstr. 4th Int. Symp. IGCP Proj.283, Novosibirsk (in press).
- Kuznetsov, P.P.**, 1980. Structural peculiarities of ultramafic belts of Altai-Sayan area. Nauka, Novosibirsk, 95 p. (in Russian).
- Kuznetsov, Yu.A.**, 1936, Some data on geology of Gorny Altai, Vestnik ZSGT, No.1-2 (in Russian).
- Kuznetsov, Yu.A.**, 1939, Geological structure of the central part of Gorny Altai. Material on geology of West Siberia, No.41, pp.78-93. (in Russian).
- Kuznetsov, Yu.A.**, 1964, Major types of magmatic formations, Nedra, Moscow, 387 p. (in Russian).
- Lepezin, G.G.**, 1978, Metamorphic complexes of Altai-Sayan folded area. Nauka, Novosibirsk, 288 p. (in Russian).
- Maniar, P.D. & Piccoli, Ph.M.**, 1989, Tectonic discrimination of granitoids. Geol. Soc. Am. Bull., No. 101, pp.635-643.
- Meen, J.K.**, 1987, Formation of shoshonites from calc-alkaline basalt magmas: geochemical and experimental constraints from the type locality. Contrib. Miner. Petrol., No. 97, pp.333-351.
- Mikhaleva, L.A. and Skuridin, V.A.**, 1971, Early Caledonian formation of batholith granites of Gorny Altai and its metallogeny. Nauka, Novosibirsk. 197 p. (in Russian).
- Mironov, Yu.V. and Kotlyar, A.L.**, 1991, Plate Tectonic cycle and peculiarities of basalt composition, 3rd Int. Conf. "Processes on plate boundaries..", Moscow, p.23 (in Russian).

- Nicolas, A.**, 1989, Structures of ophiolites and dynamics of oceanic lithosphere. Netherlands: Kluwer Acad. Publ., 368 p.
- Peive, A.V.** (Ed.), 1980, Geology of Phillipines Sea bottom, Nauka, Moscow, 621 p. (in Russian).
- Pitcher, W.S.** 1979. Comments on the geological environments of granites. In: M.P.Atherton and J.Tarney (Eds). Origin of granite batholiths - geochemical evidence. Shiva, Orpington, pp.1-8
- Pitcher, W.S.** 1982. Granite type and tectonic environment. K.J.Hsu (Ed.), Mountain Building Processes. Academic Press, London, pp.19-40
- Polyakov, G.V.** (Ed.), 1986, Magmatic complexes of Gorny Altai. Guide-book for excursion, Novosibirsk, 57 p. (in Russian).
- La Roche (de)**, 1977, A diagram for a chemical classification of igneous rocks referred to their mineral content, Science de la Terra, No.21, pp.63-87.
- Repina, L.N., Khomentovsky, V.V. and Zhuravleva, I.T.**, 1964, Biostratigraphy of Lower Cambrian of Altai-Sayan folded areas, Nauka, Moscow, 363 p. (in Russian).
- Repina, L.N. & Romanenko, E.V.**, 1978, Trilobites and stratigraphy of the Lower Cambrian of Altai area. Nauka, Moscow, 303 p. (in Russian).
- Rodygin, A.I.**, 1968, The Precambrian of Gorny Altai. Tomsk, 329 p. (in Russian).
- Saunders, A.D., Tarney, J., March, N.G.**, 1980. Ophiolites as ocean crust or marginal basin crust: A geochemical approach. Ophiolites. Proceedings Intern. Ophiol. Symp. Panaiotou. Geol. Surv. Dept., Cyprus, pp.193-204.
- Sharaskin, A.Ya.**, 1982, Petrography and geochemistry of basement rocks from five Leg 60 sites. Init. Repts Deep Sea Drilling Proj., Washington, D.C., Vol.60, pp.647-656.

Sharaskin, A.Ya. and Zakariadze, G.S., 1982, Peculiarities of magmatism under formation of trenches and island arcs of Philippine Sea. In: Magmatism and metamorphism as indicators of geodynamic island arc regimes, Nauka, Moscow, pp.210-221 (in Russian).

Simonov V.A., Kuznetsov P.P., 1991 Boninites in Vendian-Cambrian ophiolites of Gorny Altai. Doklady Akademii Nauk SSSR, Vol. 316, pp.448-451 (in Russian).

Sklyarov E.V., 1990. Ophiolites and blueschists of Southeast Sayan. Guidebook for excursion. Ulan-Ude, 58 p.

Tarney, J., March, N.G., 1991. Major and trace element geochemistry of Holes CY-1 and CY-4: Implications for petrogenetic models. Cyprus crustal study project: initial report, Holes CY-1 and 1a. Geological Survey of Canada, Ottawa, pp.133-175

Tsamerian, O.P., Sobolev, A.V., Zakariadze, G.S., 1991. Implication of phenocryst mineralogy data to characterize the ophiolite volcanic series of Maly Caucasus, Geochemistry, No.11, pp.1561-1572 (in Russian).

Volkov, V.V., 1966, The Main peculiarities of Gorny Altai geological development (Late Precambrian - Early Paleozoic). Nauka, Novosibirsk, 162p. (in Russian).

Vysotsky, S.V., 1989. Ophiolite association of Pacific island arc systems. Vladivostok, 196 p. (in Russian).

Yolkin, E.A., Yazikov, A.Yu., Buslov, M.M. et al. 1993. Devonian paleogeographic reconstructions of the western part of Altai-Sayan folded area and their geodynamic interpretation. Abstr. 4th Int. Symp. IGCP Proj.283, Novosibirsk (in press).

APPENDIX

Table 1. Bulk composition of magmatic rocks of the northern part of Gorny Altai and Stops 1 and 2

N	Number of analyses	SiO ₂	TiO ₂	Al ₂ O ₃	Fe ₂ O ₃	FeO	MnO	MgO	CaO	Na ₂ O	K ₂ O	P ₂ O ₅	LOI	Total
1	17	<u>46.88</u>	<u>2.05</u>	<u>14.02</u>	<u>7.95</u>	-	<u>0.20</u>	<u>7.40</u>	<u>8.68</u>	<u>2.91</u>	<u>0.77</u>	<u>0.19</u>	-	-
		2.59	0.52	2.80	2.45		0.07	2.37	2.39	1.22	0.36	0.15		
2	17	<u>46.65</u>	<u>2.46</u>	<u>16.09</u>	<u>2.25</u>	<u>9.67</u>	<u>0.20</u>	<u>6.80</u>	<u>8.50</u>	<u>2.93</u>	<u>0.68</u>	<u>0.24</u>	-	-
		2.17	0.33	1.28	1.16	1.40	0.04	1.48	2.14	0.77	0.19	0.22		
3	8	<u>45.50</u>	<u>1.96</u>	<u>15.10</u>	<u>4.19</u>	<u>8.15</u>	<u>0.20</u>	<u>7.75</u>	<u>9.94</u>	<u>2.38</u>	<u>0.48</u>	<u>0.25</u>	-	-
		1.71	0.37	1.31	2.06	2.30	0.03	2.10	1.13	1.14	0.34	0.12		
Stop 1														
4	1	52.32	2.261	12.44	-	10.06	0.094	6.19	7.60	5.04	0.68	0.289	2.76	99.74
5	1	48.50	2.205	12.74	-	10.68	0.152	6.48	9.02	4.20	0.56	0.237	4.43	99.22
6	1	47.62	2.399	13.04	-	12.59	0.146	7.42	8.81	3.69	0.41	0.313	3.42	99.88
7	1	47.13	2.212	12.01	-	12.24	0.160	7.65	10.27	3.23	0.48	0.241	4.03	99.67
Stop 2														
8	1	47.27	2.39	14.38	-	11.80	0.17	8.95	7.29	3.46	0.72	0.22	3.18	99.86
9	1	45.87	2.23	15.05	-	12.80	0.21	8.00	8.63	2.99	0.61	0.20	3.10	99.72
10	1	47.36	1.70	10.12	-	12.70	0.18	12.68	7.57	1.91	0.46	0.16	4.64	99.49

Note: 1 - basalts from the right bank of Katun River between Maima and Surtaika Villages; 2 - basalts from the left bank of Katun River to the south-west from Aya Lake (Kaimaskaya suite); 3 - subvolcanic gabbro-dabase bodies in basalts of Kaimaskaya suite; 4-7 - amygdaloidal pillow-lavas of Stop 1; 8-9 - pyroxene porphyrites; 10 - diabase; over the line - average oxide values, under the line - standart deviation.

Analyses 1-3 were obtained with volume-silicate method in the central laboratory of PGO "Zapsibgeologiya" of Novokuznetsk city; analyses 4-10 were obtained with X-ray fluorescence spectroscopy in UIGG&M, SB RAS, Novosibirsk.

Table 2. Trace elements in basalts of Stops 1, 6 and 7, ppm

Sample numbers	Rb	Sr	Y	Zr	Nb
Stop 1					
1	6.5	120.4	23.9	140.8	20.5
2	4.33	179.4	20.5	140.0	19.2
3	2.56	267.8	18.7	124.4	17.7
4	2.7	336.4	18.4	129.5	16.7
Stop 6					
1	10.7	23.6	1.6	180.7	6.3
2	0.80	348.3	15.7	91.7	7.6
3	0.89	615.8	22.3	151.4	2.3
Stop 7					
1B	6.2	47.9	16.6	20.8	12.9

Note: Analyses were defined with atomic-emission method in UIGG&M, SB RAS, Novosibirsk city. Bulk composition of basalts is cited in tables 1 and 5.

Table 3. Bulk composition of magmatic rocks of Manzherok and Ust-Syoma suites (section Cheposh - Ust-Syoma) for Stop 2

Oxide	Basalts of Manzherok suite					Basalts of Ust-Syoma suite							
	1	2	3	4	5	6	7	8	9	10	11	12	
SiO ₂	50.57	47.38	46.59	44.30	<u>46.32</u> 2.49	47.42	49.71	48.51	47.53	50.43	<u>48.65</u> 2.52	<u>48.94</u> 2.19	
TiO ₂	1.88	1.55	2.24	3.52	<u>2.49</u> 0.73	0.81	0.64	1.01	0.66	0.67	<u>0.78</u> 0.19	<u>0.70</u> 0.17	
Al ₂ O ₃	14.39	15.51	14.19	14.30	<u>14.30</u> 1.77	16.10	17.27	16.16	14.89	13.33	<u>15.90</u> 2.16	<u>13.78</u> 3.50	
Fe ₂ O ₃	1.87	1.97	2.33	2.73	<u>2.08</u> 0.9	5.69	1.00	1.04	4.13		<u>2.93</u> 1.75	<u>2.94</u> 2.72	
FeO	11.05	8.96	9.58	11.68	<u>10.35</u> 1.71	6.25	9.33	8.46	7.10	11.27	<u>7.88</u> 1.85	<u>6.84</u> 1.84	
MnO	0.17	0.18	0.19	0.25	<u>0.19</u> 0.04	0.16	0.18	0.15	0.19	0.23	<u>0.21</u> 0.06	<u>0.17</u> 0.04	
MgO	6.25	7.16	6.38	4.65	<u>6.17</u> 1.90	5.41	4.96	6.08	7.30	8.00	<u>6.46</u> 2.03	<u>9.98</u> 2.22	
CaO	4.07	5.89	7.28	6.84	<u>7.71</u> 2.49	10.52	7.46	11.00	9.21	9.93	<u>8.48</u> 1.91	<u>8.50</u> 1.89	
Na ₂ O	2.60	3.82	3.32	3.34	<u>3.58</u> 0.66	3.37	3.23	2.64	3.10	1.59	<u>2.52</u> 1.02	<u>2.24</u> 0.84	
K ₂ O	0.23	0.77	0.85	1.45	<u>0.79</u> 0.62	0.48	1.54	1.40	0.38	1.03	<u>1.39</u> 0.85	<u>1.30</u> 0.84	
P ₂ O ₅	0.19	0.16	0.31	0.82	<u>0.32</u> 0.2	0.29	0.13	0.12	0.25	0.24	<u>0.21</u> 0.13	<u>0.20</u> 0.83	
LOI	6.81	6.78	6.80	5.71	-	3.41	3.65	2.69	6.06	2.72	-	-	
Total	100.03	100.13	100.06	99.59	-	100.20	99.26	92.26	100.79	99.48	-	-	

Note: 1-5 - basalts of Manzherok suite: 1 - aphyric basalt, 2-3 spilites, 4 - diabase porphyrite, 5 - average value (n=30); 6-11 - basalts of Ust-Syoma suite: 6-8 - pyroxene-plagioclase basalts, 9-10 - pyroxene porphyrite of Stop 5, 11- average value (n=28), 12 - average value for (n=10) dikes of gabbro-diabases and diabases, comagmatic to Ust-Syoma suite, have higher MgO-content and lower Al₂O₃ content and like analyses 9-10 have boninite trend.

Analyses were made with volume-silicate method in the central laboratory of PGO "Zapsibgeologiya", Novokuznetsk, n- number of analyses; over line - average value of oxides, under line - standard deviations.

T a b l e 4. Composition of clinopyroxenes from porphyrites of Ust-Syoma Village district, Gorny Altai
(sample N° U/S-92 , Stop 5)

Grain of pyroxene	Plot Grain	SiO ₂	TiO ₂	Al ₂ O ₃	Cr ₂ O ₃	FeO	MnO	MgO	CaO	Na ₂ O	K ₂ O	Total
1	centre	54.27	0.09	0.57	0.53	2.28	0.07	18.12	22.77	0.17	0.01	99.48
2	centre	54.81	0.08	0.46	0.56	2.17	0.05	18.71	22.85	0.16	0.01	99.87
3	edge-A grain	53.77	0.12	1.01	0.61	3.88	0.08	17.91	21.91	0.19	0.02	99.50
3	centre1	54.12	0.12	0.73	0.54	2.57	0.05	18.51	22.94	0.15	0.01	99.75
3	centre2	54.07	0.09	0.69	0.56	2.76	0.05	18.22	22.89	0.15	0.01	99.49
3	centre3	54.32	0.10	0.66	0.52	2.63	0.05	18.37	22.91	0.14	0.02	99.72
3	edge B grain	53.8	0.13	1.01	0.80	3.56	0.07	17.70	22.31	0.14	0.01	99.53

N o t e: For grain 3 the plots from A edge to B edge were analysed. Mineral composition was defined using X-ray microanalyzer "Camebax-micro", UIGG&M SB RAS, Novosibirsk.

Table 5. Composition of homogenized melt inclusions in clinopyroxenes from porphyrites of Ust-Syoma suite (Stop 5)

N	N sample	SiO ₂	TiO ₂	Al ₂ O ₃	Cr ₂ O ₃	FeO	MnO	MgO	CaO	Na ₂ O	K ₂ O	Total
1	Y/C-92-1	55.77	0.39	9.95	0.13	5.13	0.11	9.16	13.54	1.91	1.10	97.20
2	Y/C-92-1	56.95	0.16	11.30	0.12	4.15	0.11	8.41	11.78	2.40	1.98	97.37
3	Y/C-92-1	55.88	0.48	11.24	0.20	5.41	0.09	7.76	11.47	2.29	1.79	96.61
4	Y/C-92-5	51.30	0.19	9.93	0.18	5.97	0.15	11.84	14.69	1.01	1.20	96.47
5	Y/C-92-5	55.25	0.15	8.74	0.20	4.98	0.13	10.87	15.32	0.72	2.12	98.49
6	Y/C-92-6	51.76	0.60	11.83	0.04	11.96	0.17	7.79	11.30	1.68	1.00	98.13
7	Y/C-92-6	52.99	0.33	6.99	0.08	9.66	0.19	10.74	13.60	1.19	0.54	96.31
8	Y/C-92-6	54.24	0.45	8.82	0.06	11.76	0.19	9.49	12.21	0.81	1.15	99.19
9	Y/C-92-6	45.75	0.63	8.09	0.04	12.90	0.25	14.08	14.89	1.18	0.63	98.45

Note: Composition of inclusions was defined using X-ray microanalyzer "Camebax-micro", IUGG&M SB RAS, Novosibirsk.

Table 6. Bulk composition of basalts from Bulukhta and Cherga Rivers district (Stops 6-7)

N sample	n	SiO ₂	TiO ₂	Al ₂ O ₃	FeO ₃	FeO	MnO	MgO	CaO	Na ₂ O	K ₂ O	P ₂ O ₅	LOI	Total
I	14	<u>48.08</u> 2.68	<u>1.84</u> 0.19	<u>14.78</u> 0.89	<u>5.98</u> 1.38	<u>5.0</u> 1.94	<u>0.16</u> 0.02	<u>4.43</u> 1.96	<u>11.07</u> 2.18	<u>3.92</u> 0.85	<u>0.38</u> 0.32	<u>0.25</u> 0.09	<u>5.92</u> 0.98	-
Basalts of Stop 6														
6-1	1	42.48	1.51	14.86	10.67	-	0.18	9.94	9.93	2.88	0.12	0.13	6.98	99.68
6-2	1	46.61	1.33	15.61	9.35	-	0.14	5.29	13.19	0.41	1.38	0.14	6.06	99.55
6-3	1	41.95	1.65	13.73	11.97	-	0.18	9.69	12.13	2.12	0.16	0.16	7.28	100.02
6-4	1	47.43	2.17	14.85	13.22	-	0.15	6.00	8.57	3.66	0.19	0.24	2.96	99.47
II	9	<u>49.33</u> 3.49	<u>0.82</u> 0.23	<u>14.98</u> 3.4	<u>3.44</u> 1.28	<u>7.14</u> 1.10	<u>0.18</u> 0.06	<u>6.59</u> 2.42	<u>8.48</u> 4.06	<u>2.51</u> 1.42	<u>0.91</u> 0.84	<u>0.14</u> 0.08	<u>4.02</u> 0.95	-
Basalts of Stop 7														
7-1a	1	50.06	0.98	13.55	9.34	-	0.16	6.98	6.95	2.97	0.24	0.08	8.36	99.68
7-1b	1	42.44	0.51	13.81	10.28	-	0.20	8.57	9.48	2.64	0.30	0.04	11.76	100.06
7-2	1	41.35	0.39	12.26	8.97	-	0.19	12.05	12.84	1.47	0.22	0.03	10.2	99.98
7-3	1	46.08	0.42	15.38	8.66	-	0.16	8.02	13.26	2.74	0.20	0.04	5.00	99.97

Note: I - average composition of basalts (n=14) from the lower part of Bulukhta-Cherga section; 6 - 1,2,3,4 - basalts of Stop 6 from the lower part of Bulukhta-Cherga section: 6-1 amygdaloidal basalt of eastern lava flow, 6-2 lavabreccia, 6-3 - amygdaloidal basalt from the western lava flow, 6-4 - clastalline dolerite of the central part of western lava flow.

II - average composition of basalts (n=9) of the upper part of from the lower part of Bulukhta-Cherga section: 7 - 1a,1b, 2, 3 - basalts of Stop 7 from the upper part of from the lower part of Bulukhta-Cherga section: 7-1a - fragment of crystalline rock (metadolerite) in lava flow, 7-1b - plagioclase porphyrite from lava flow, 7-2 - pyroxene-plagioclase porphyrite, 7-3 - fine clastic lavabreccia of basalt porphyrite.

Table 7. Bulk composition of Middle-Devonian volcanic rocks from Ursul River (Stop 9)

N	Rocks	SiO ₂	TiO ₂	Al ₂ O ₃	Fe ₂ O ₃	FeO	MnO	MgO	CaO	Na ₂ O	K ₂ O	P ₂ O ₅	LOI	Total
Kuratin suite														
1	Orthoclase rhyolite porphyry (K-1)	75.36	0.20	12.02	2.94	-	0.08	0.40	0.12	3.89	4.02	0.03	0.78	99.93
2	Rhyolite porphyry	73.18	0.22	12.96	1.27	1.93	0.06	0.53	0.28	4.77	3.59	0.06	1.46	100.30
3	Quartz rhyolite porphyry	74.50	0.25	12.04	0.64	2.87	0.06	0.48	0.11	5.32	2.60	0.03	1.32	100.20
4	Rhyolite felsite-porphyry	72.43	0.17	14.93	1.42	2.88	-	0.26	1.33	4.67	1.36	-	1.21	100.63
5	Plagioclase rhyolite-porphyry	73.36	0.20	13.07	0.76	3.59	0.04	0.32	0.17	3.34	5.58	0.03	0.50	99.36
6	Dacite porphyry	68.32	0.34	16.16	1.50	1.82	-	1.05	3.94	2.30	2.90	-	1.16	99.49
7	Quartz dacite porphyry	73.22	0.12	13.48	1.17	1.21	-	2.10	3.01	3.85	1.45	-	0.56	100.17
8	Plagioclase dacite porphyry	66.71	0.53	15.17	1.54	2.24	-	1.50	5.70	2.36	2.41	-	1.72	99.87
9	Dacite porphyry	64.66	0.83	15.67	2.01	3.64	-	1.93	4.60	2.58	1.92	-	1.66	99.50
10	Andesite porphyrite	57.82	0.57	18.11	4.78	1.67	-	4.70	8.30	1.13	0.62	-	2.09	99.80
Ongudais suite														
11	Andesite porphyrite	66.18	0.66	16.74	1.70	4.39	0.10	1.62	3.21	2.48	1.64	0.11	3.85	99.60
12	--- " ---	59.65	0.50	17.08	1.83	4.67	0.07	2.43	5.06	4.26	0.09	-	4.09	100.53
13	--- " ---	58.87	0.78	16.09	2.45	4.19	0.14	2.69	3.99	2.16	1.59	0.14	4.28	99.40
14	Pyroxene andesite porphyrite	57.35	0.80	16.75	3.37	4.53	0.18	2.52	5.50	2.97	1.70	0.16	3.04	99.02
15	Andesite-basalt porphyrite	57.10	0.82	14.32	2.96	8.87	0.30	3.90	5.08	2.34	1.02	0.16	2.78	99.62
16	Andesite-basalt porphyrite	52.35	0.77	16.25	2.26	6.58	0.15	5.53	8.01	1.68	0.33	0.16	5.31	99.40
17	Andesite-basalt porphyrite	53.53	0.80	15.56	2.37	7.29	0.10	5.76	7.46	1.60	0.29	-	5.78	100.54

Note: Analyse 1 was made in the United Institute of Geology, Geophysics and Mineralogy SB RAS, Novosibirsk, analyses 2-17 are taken from the paper of Polyakov (Ed.) (1986).

Table 8. Average composition of Yaloman complex rocks (Chiketaman and Yaloman plutons),
Stops 11 and 13

N	Rocks	SiO ₂	TiO ₂	Al ₂ O ₃	Fe ₂ O ₃	FeO	MnO	MgO	CaO	Na ₂ O	K ₂ O	P ₂ O ₅	n
Granitoids of Chiketaman pluton													
1	Diorite	55.89	0.82	15.98	3.09	5.85	0.15	4.36	7.56	2.99	1.36	0.14	6
2	Quartz diorite	60.72	0.73	15.38	2.27	5.03	0.11	2.97	5.47	3.07	1.91	0.13	9
3	Tonalite	63.73	0.59	15.68	1.87	3.96	0.09	2.91	4.87	2.76	2.29	0.12	4
4	Granodiorite	64.79	0.52	14.14	2.11	4.01	0.11	2.51	4.09	3.44	2.51	0.11	5
Granitoids of Yaloman pluton													
1	Diorite	54.47	0.77	17.01	2.66	5.74	0.14	4.64	7.72	2.87	1.01	0.16	9
2	Quartz diorite	60.74	0.71	15.61	2.34	4.87	0.12	3.03	5.19	3.13	1.91	0.14	21
3	Tonalite	65.15	0.54	15.58	2.64	3.33	0.12	1.92	4.09	3.21	2.01	0.12	11
4	Granodiorite	66.08	0.52	14.99	1.81	3.41	0.08	1.67	3.94	3.31	2.76	0.13	25
5	Granodiorite	70.15	0.34	13.89	1.56	2.07	0.09	0.63	2.09	4.44	2.95	0.07	6
6	Adamellite	70.94	0.34	13.89	1.55	2.09	0.06	0.78	2.16	3.51	3.21	0.11	32
7	Granite	70.97	0.21	13.44	0.44	2.29	0.08	0.68	2.95	3.78	4.46	0.11	6
8	Alaskite	75.23	0.19	12.57	0.79	1.43	0.06	0.21	0.78	3.41	4.48	0.08	17

Note: Analyses taken from Kononov (1969); n - number of analyses.

Table 9. Average bulk-rock composition of Chiketaman pluton rocks (compiled by N.F.Krasov, 1993)

N	n	SiO ₂	TiO ₂	Al ₂ O ₃	FeO	MnO	MgO	CaO	Na ₂ O	K ₂ O	P ₂ O ₅	H ₂ O	Total
1	6	59.34	0.71	14.92	7.75	0.13	4.42	6.03	2.63	1.92	0.12	2.11	100.06
2	7	60.65	0.67	14.97	8.17	0.13	3.51	5.10	2.97	2.04	0.11	1.63	99.95
3	6	61.59	0.66	15.05	7.06	0.12	3.06	5.54	3.30	1.85	0.12	0.92	99.26
4	4	61.61	0.69	15.5	6.75	0.2	3.74	5.01	2.22	2.16	0.13	2.34	100.35
5	7	61.77	0.72	15.78	6.79	0.10	2.90	5.12	2.73	2.07	0.13	1.70	99.82
6	8	65.59	0.53	14.68	5.37	0.08	2.89	4.19	2.72	2.50	0.11	1.31	99.95
7	7	66.11	0.48	14.68	5.08	0.10	2.34	3.70	2.73	2.96	0.11	1.57	99.88
8	3	70.48	0.24	15.23	2.57	0.05	1.69	3.83	2.58	2.88	0.06	0.8	100.41
9	6	74.76	0.13	12.90	2.02	0.06	0.34	1.24	2.95	4.86	0.04	0.44	99.73
10	4	60.64	0.72	15.41	7.27	0.09	5.07	5.71	2.69	2.03	0.15	1.58	101.34
11	4	51.59	0.88	15.57	10.33	0.10	6.81	8.11	3.12	1.30	0.15	2.09	100.05
12	12	58.48	0.74	16.31	7.97	0.16	4.08	4.53	2.71	1.70	0.17	3.25	100.10

Note: 1, 4, 5 - tonalite; 2-Q-diorite-porphyrity; 3-Q-diorite; 6-granodiorite; 7- granodiorite-porphyrity; 8-adamellite; 9-aplite-granite; 10- metapelite xenoliths; 11-metabasite xenoliths; 12-wall-rock.

Analyses made with X-ray fluorescence method in the United Institute of Geology, Geophysics and Mineralogy, SB RAS, Novosibirsk.

T a b l e 10. Isotopic ages of Yaloman pluton granitoids

N	Rocks	Location of sample selection	Absolute age, Ma	
			by bulk comp.	by biotite
1	Quartz diorite	Chiketaman massif	303	230
2	Tonalite	Chiketaman massif	262,303	280
3	Granodiorite	Chiketaman massif	262	
4	Granodiorite	Kadrin massif	317	
5	Adamellite	Kadrin massif	219	
6	Adamellite	Yaloman massif	236,299	252
7	Granite	Kuvash massif	280	
8	Granite	Shebalin massif	279	
9	Alaskite	Kuvash massif	225	

N o t e: Analyses 1,3 -8 were obtained in the Laboratory of absolute age ZSGU, Novokuznetsk city; analyses 2 were obtained in the Laboratory of absolute age of Siberian Institute of Geology, Geophysics and Mineral Resources, Novosibirsk city.

D a t e g r o u p s: 299-317 (by bulk composition) - Late-Middle Carboniferous.
230-280 (by bulk composition and biotite) - Permian.
219-225 (by bulk comp.) - Early Triassic.

Table 11. Radiology age of metamorphic rocks of Kurai complex and garnet amphibolites of Chagan-Uzun massif (K-Ar method)

N	Rocks	Mineral	Age, Ma
1	Metamorphic schist	Hornblende	440
2	"	"	370
3	"	"	360
4	Gneiss	"	350
5	"	"	346
6	"	"	340
7	"	"	320
8	"	"	320
9	Amphibolite	"	365
10	"	Biotite	394
11	Biotite schist	"	500
12	"	"	490
13	"	"	480
14	"	"	460
15	"	"	450
16	"	"	440
17	"	"	300
18	Garnet amphibolite	Amphibole	473
19	"	"	435
20	"	"	419

Note: analyses 1-4, 6-8 - are taken from Lepezin (1988), 11,12 and 15-17 from Rodygin (1968), 13,14 from Mikhaleva & Skurigin (1971), 19,20 from Bogolepov & Yanshin (1973), 5,9,10 и 18 were obtained by M.Buslov in Laboratory Okayama of University of Japan with help of students O.Toshikori and D.Masako lead by Prof. T.Itaya.
Date groups: 300-370 - Late Devonian-Carboniferous, 419-500 - Ordovician-Silurian.

Table 12. Bulk rock composition for Vendian-Early Cambrian ophiolites of Kurai terrane of the primitive island arc (Kurai ridge to the north from Chagan-Uzun Village)

N	N sample	SiO ₂	TiO ₂	Al ₂ O ₃	Fe ₂ O ₃	MnO	MgO	CaO	Na ₂ O	K ₂ O	P ₂ O ₅	LOI	Total
1	2	3	4	5	6	7	8	9	10	11	12	13	14
1	C-12zh-91	43.54	0.03	0.71	7.11	0.16	34.43	3.14	0.30	0.01	0.03	10.58	99.68
2	CA-3/2-91	49.99	0.04	0.74	7.32	0.14	23.02	14.52	0.30	0.00	0.03	3.96	99.73
3	CA-2/7-91	49.81	0.06	0.85	8.22	0.17	22.53	14.37	0.30	0.00	0.03	3.73	99.74
4	CA-2/10-91	51.50	0.03	0.72	6.21	0.13	23.66	13.22	0.30	0.00	0.03	4.40	99.87
5	CA-2/3-91	52.51	0.03	0.90	6.21	0.14	20.19	18.09	0.30	0.00	0.03	1.84	99.91
6	CA-2/5-91	50.61	0.10	2.67	9.14	0.16	18.73	15.83	0.30	0.01	0.03	2.36	99.61
7	CA-4/1-91	50.45	0.11	3.02	8.19	0.18	18.37	16.87	0.30	0.00	0.03	2.72	99.91
8	C-14a-91	48.72	0.10	3.87	9.99	0.18	18.87	14.96	0.30	0.00	0.03	3.04	99.72
9	C-14b-91	50.38	0.06	1.10	8.42	0.17	20.35	16.76	0.30	0.00	0.03	2.54	99.78
10	CA-6-91	49.47	0.50	17.60	12.53	0.23	5.50	8.89	2.23	0.14	0.03	3.10	100.19
11	CA-7-91	51.99	0.35	17.85	10.45	0.20	4.92	9.51	1.95	0.26	0.04	2.54	100.07
12	CA-8-91	49.87	0.47	18.27	12.33	0.24	4.46	9.74	1.83	0.34	0.04	2.82	100.41
13	CA-9a-91	52.38	0.64	16.48	12.40	0.27	3.87	9.18	1.52	0.29	0.03	2.58	99.61
14	CA-10-91	52.42	0.16	7.64	10.00	0.21	14.35	11.09	0.99	0.07	0.03	2.80	99.74
15	C-106a-89	54.70	0.23	11.28	10.57	0.21	10.22	7.89	1.13	0.54	0.03	3.04	99.84
16	C-106b-89	54.55	0.24	11.19	11.02	0.22	10.21	7.37	1.90	0.24	0.03	3.30	100.27
17	C-107b-89	54.66	0.34	9.41	10.85	0.25	10.23	9.78	2.15	0.32	0.04	1.92	99.95
18	C-3b-90	52.98	0.44	12.54	11.74	0.23	8.44	9.55	1.80	0.39	0.04	1.96	100.11
19	C-5a-90	54.98	0.24	11.37	11.57	0.31	8.96	7.62	2.15	0.62	0.03	2.28	100.12
20	C-13/1-90	50.20	0.29	10.25	9.95	0.20	11.77	3.99	0.95	0.06	0.03	2.30	99.96
21	C-13/3-90	50.55	0.30	10.75	9.76	0.20	11.78	2.10	1.41	0.10	0.03	2.86	99.82
22	C-107a-89	47.82	1.26	15.81	17.22	0.15	6.78	3.43	3.62	0.13	0.10	3.58	99.91
23	C-110b-89	53.96	1.22	13.29	16.14	0.22	3.86	4.34	5.68	0.07	0.12	1.60	100.53
24	C-110c-89	49.57	1.25	15.35	14.84	0.23	3.28	12.19	0.53	0.03	0.23	2.74	100.25

Table 12 (end)

1	2	3	4	5	6	7	8	9	10	11	12	13	14
25	C-111c-89	53.36	1.37	15.49	12.32	0.26	4.73	4.10	5.10	0.06	0.42	3.08	100.29
26	C-111d-89	55.42	1.30	16.00	12.12	0.21	4.09	2.62	5.12	0.11	0.42	3.00	100.43
27	C-113b-89	50.27	2.95	14.12	14.23	0.23	5.18	6.33	3.76	0.06	0.74	2.34	100.24
28	C-113c-89	50.14	2.95	14.14	13.47	0.25	5.25	6.36	4.19	0.08	0.75	2.16	99.79
29	C-113d-89	47.50	2.63	15.06	14.54	0.28	6.10	6.42	4.72	0.24	0.60	2.52	100.66
30	C-113e-89	47.13	2.39	15.24	14.30	0.30	6.58	7.70	3.34	0.39	0.54	2.74	100.66
31	C-18-90	51.58	0.49	15.16	11.43	0.13	4.82	6.34	5.35	0.16	0.06	5.07	100.60
32	C-19-90	60.17	0.46	13.12	10.10	0.11	4.20	3.39	4.63	0.13	0.05	3.74	100.10
33	C-21-90	56.81	0.54	15.50	9.84	0.09	3.87	7.27	3.47	0.09	0.05	2.74	100.27
34	C-23-90	60.24	0.40	12.35	7.43	0.08	3.08	7.70	4.40	0.09	0.06	4.53	100.35
35	C-43-90	47.00	0.76	15.46	13.88	0.26	3.28	6.72	1.69	1.02	0.05	9.70	99.86
36	C-33-90	52.21	0.81	16.35	12.35	0.27	3.61	3.25	5.06	0.04	0.09	5.65	99.71
37	C-41-90	63.80	0.58	15.62	7.68	0.15	0.95	2.36	3.92	0.73	0.12	4.06	99.98
38	C-4A-90	47.46	0.45	18.34	10.00	0.18	6.89	10.12	2.01	1.00	0.03	3.36	99.84
39	B-T5-91	50.98	0.61	18.46	10.75	0.15	4.67	4.99	5.96	0.41	0.06	2.87	99.92

Note: Meshtuyaryk complex rocks: 1-4 - olivine pyroxenites and wherlites, 5-9 - pyroxenites, 10-14 - gabbro and gabbro-diabases; 15- Balkhash suite rocks: 15-21 - low-Ti dikes and lavas of boninites, 22-26 - high-Ti lavas with oceanic characteristics, 27-30 - sheeted-dike complex with island-arc characteristics associated with boninites, 35-39 - dike-sill complex with island-arc characteristics. Bulk rock composition was defined with X-ray fluorescence analysis in the OIGG&M SB RAS, Novosibirsk city.

Table 13. REE and trace elements content in the ophiolite rocks of Kurai terrane of primitive island arc, ppm

N	N sample	La	Yb	Sc	Zr	Y	Nb
1	C-106a-89	6.3	1.3	16.0	41.0	7.7	1.4
2	C-106b-89	3.3	1.3	17.0	18.0	7.3	4.6
3	C-107b-89	3.2	1.2	17.0	22.0	8.0	3.8
4	C-3b-90	2.3	1.3	15.0	18.0	5.5	4.6
5	C-5a-90	1.0	1.0	14.0	13.0	5.0	2.0
6	C-13/1-90	1.9	0.7	8.3	13.0	4.2	3.2
7	C-13/3-90	1.7	0.8	11.0	11.0	3.6	4.3
8	C-107a-89	1.6	1.8	10.0	36.0	7.3	1.4
9	C-107g-89	1.4	1.8	13.0	48.0	8.5	1.2
10	C-110c-89	3.0	3.8	5.3	120.0	24.0	4.0
11	C-111c-89	3.5	4.6	3.4	150.0	31.0	3.4
12	C-111g-89	2.3	4.4	2.7	120.0	30.0	2.1
13	C-113b-89	10.0	3.6	9.0	140.0	29.0	3.5
14	C-113c-89	12.0	4.6	8.3	150.0	35.0	4.0
15	C-113e-89	12.5	3.2	8.1	130.0	25.0	8.7
16	C-113a-89	7.7	2.9	7.0	110.0	23.0	4.0
17	C-113g-89	7.0	2.5	5.3	110.0	21.0	4.8
18	C-14-90	2.4	1.7	35.0	37.0	10.0	6.8
19	C-16-90	4.5	1.8	19.0	27.0	9.0	5.7
20	C-18-90	4.8	2.6	23.0	39.0	13.0	5.5
21	C-19-90	4.2	2.1	18.0	36.0	12.0	7.1
22	C-21-90	5.3	2.2	19.0	40.0	13.0	6.2

Note: 1-7 - boninites (dikes and lavas); 8-12 - pillow-lavas and massive lavas; 13-17 - sheeted dikes; 18-22-sheeted dikes associated with boninites. Analyses were obtained with atomic-emission method in Siberian Institute of Geology, Geophysics Mineral Resources, Novosibirsk city.

T a b l e 14. Composition of minerals and homogenized melt inclusions from boninites of Kurai terrane of primitive island arc

N	N sample	SiO ₂	TiO ₂	Al ₂ O ₃	Cr ₂ O ₃	FeO	MnO	MgO	CaO	Na ₂ O	K ₂ O	Total
1	C-107b-89	40.83	0.01	0.0	0.03	Olivine 8.34		51.00	0.0	0.0	-	100.64
2	C-106b-89	54.13	0.09	0.41	0.41	Clinopyroxenes 4.49	0.16	19.77	20.00	0.08	-	99.47
3	C-107b-89	54.30	0.02	0.40	0.60	2.80	-	19.51	21.29	0.13	-	99.05
4	C-3b-90	54.21	0.01	0.37	0.53	2.57	0.10	19.56	22.02	0.10	-	99.47
5	C-3b-90	54.14	0.01	0.53	0.49	3.49	0.15	18.57	21.73	0.11	-	99.22
6	C-13/3-90	53.56	0.03	0.76	0.56	2.81	0.10	18.65	22.48	0.12	-	99.07
7	C-13a-91	53.65	0.05	0.84	0.37	3.35	0.09	17.95	22.92	0.09	-	99.32
8	C-13a-91	0.0	0.67	5.43	53.25	Chromites 28.17	0.23	11.02	-	-	-	98.78
9	C-54c-90	0.04	0.06	3.50	67.26	15.07	0.11	13.42	-	-	-	99.46
10	C-54c-90	0.04	0.07	3.53	66.53	16.18	0.13	12.68	-	-	-	99.16
11	C-106b-89	0.04	0.08	4.77	65.54	14.40	0.08	14.09	-	-	-	99.00
12	C-106b-89	0.05	0.10	5.66	59.58	28.46	0.76	5.16	-	-	-	99.78
13	C-13/3-90	51.00	0.34	11.15	0.0	Melt inclusions in clinopyroxenes 12.78	0.23	8.55	12.88	1.00	0.09	98.03
14	C-13/3-90	52.89	0.29	14.23	0.01	10.35	0.18	8.06	11.08	1.35	0.18	98.61
15	C-13/3-90	53.67	0.22	11.17	0.09	8.12	0.17	8.72	13.29	1.20	0.20	96.84
16	C-13/1-90	52.30	0.18	10.17	0.05	6.21	0.14	11.28	15.90	1.02	0.11	97.36
17	C-13/1-90	54.70	0.27	14.10	0.04	7.83	0.15	7.29	10.62	1.23	0.12	96.34
18	C-13/1-90	52.12	0.19	13.23	0.05	8.05	0.15	9.10	14.16	1.19	0.07	98.29

N o t e: Composition of minerals and homogenized melt inclusions were determined by microprobe analyzer "Camebax-micro", UIGG&M, SB, RAS, Novosibirsk city.

Table 15. Bulk composition of Boninite series rocks (Simonov & Kuznetsov, 1991)

Components	1	2	3	4	5	6	7	8	9	10	11
SiO ₂	54.70	54.55	54.66	54.64	56.17	56.36	55.76	55.80	57.94±0.90	53.85	55.93
TiO ₂	0.23	0.24	0.34	0.27	0.28	0.29	0.20	0.20	0.17±0.05	0.34	0.32
Al ₂ O ₃ *	11.28	11.19	9.41	10.63	10.93	13.63	11.51	11.15	11.51±1.11	10.94	15.79
Fe ₂ O ₃ *	10.57	11.02	10.85	10.81	11.11	9.05	9.37	9.13	9.34±0.46	9.26	7.91
MnO	0.21	0.22	0.25	0.23	0.24	0.15	0.14	0.15	0.18±0.06	0.18	0.12
MgO	10.22	10.21	10.23	10.22	10.51	10.98	10.82	15.68	12.02±1.35	14.72	10.56
CaO	7.89	7.37	9.78	8.35	8.58	6.41	6.79	7.19	7.76±1.10	8.31	5.36
Na ₂ O	1.13	1.90	2.15	1.73	1.78	3.47	1.96	0.86	1.46±0.43	1.14	2.21
K ₂ O	0.54	0.24	0.32	0.37	0.38	0.42	0.82	0.69	0.50±0.17	0.27	0.80
P ₂ O ₅	0.03	0.03	0.03	0.03	0.03	0.05	0.04	0.05	0.04±0.02	0.12	0.07
LOI	3.04	3.30	1.92	2.72				3.81		1.49	1.51
n	1	1	1	3	3	13	5	5	14	2	4
Rb	8.8	3.4	4.7	5.6				11	9.7±2.6		34.1
Ba	127	102	140	123				18	27±5.2		46
Sr	104	88	110	101		110		72	71±13		140
Ni	82	93	91	89		150	314	356	192±77	460	53
Co	40	41	46	42		34			40±3.7	115	37
Cr	800	830	1050	893		500	958	915	786±180	1800	234
V	210	210	290	237		100				400	219
Be	0.6	0.4	0.4	0.5							
Cu	58	10	90	53		60				130	
Zn	117	124	92	111		54				140	
n	1	1	1	3		13	5	5	5-14	1-2	4

Note: 1-5 -boninites of Gorny Altai (1-C-106a-89; 2-C-106b-89; 3-C-108b-89; 4- average dry compositions of boninites from East Sayan ophiolites (Dobretsov et al., 1985); 7 - average boninite composition after N.L.Dobretsov et al., (Peive (Ed.), 1980, Petrology and Geochemistry, 1987); 8,9 - average dry compositions of Maryan arc boninites (8) and Bonin islands (9) (Petrology and Geochemistry ..., 1987); 10 - boninites of Tonga arc (Vysotsky et al., 1983; Petrology and Geochemistry..., 1987); 11 - boninites of 458 DSDP well, Maryan trench (Sharaskin, 1982). Oxides are cited in weight %, trace elements in ppm, LOI or H₂O. N - amount of analyses, Fe₂O₃ - total iron.

Table 16. Gas composition in boninites ($\text{cm}^3/\text{kg sample.}; \text{H}_2\text{O} - \text{mas}\%$).
 volume%
 (Simonov, Kuznetsov, 1991)

N Sample	H ₂ O	CO ₂	CO	CH ₄	H ₂	Total	Total r.g.	$\frac{\text{CO}_2}{\text{CO}_2 + \text{Tot.r.g.}}$	$\frac{\text{H}_2\text{O}_{\text{mas.}}}{\text{CO}_2}$
1 Average from samples C-106a, C-107b	1.87	<u>926.3</u> 50.3	<u>193.4</u> 10.5	<u>17.7</u> 1.0	<u>705.0</u> 38.3	1841.5	915.1	0.50	10.3
2 16-26/2 glass	1.58	<u>202.6</u> 40.3	<u>41.7</u> 8.3	<u>8.1</u> 1.6	<u>249.8</u> 49.8	502.1	299.5	0.40	39.8
3 C-106a pyroxene	0.24	<u>1049.9</u> 38.0	<u>254.6</u> 9.2	<u>20.4</u> 0.7	<u>1440.3</u> 52.1	2765.3	1715.3	0.38	1.2
4 16-26/2 pyroxene	0.13	<u>92.8</u> 14.8	<u>69.0</u> 11.0	<u>11.3</u> 1.8	<u>452.5</u> 72.1	627.4	532.8	0.15	7.3

Note: The tables involves composition of gases emanated out of samples under 400-1000°C. Total - all the gases besides H₂O, Tot.r.g.-CO+CH₄+H₂; CO₂/CO₂+Tot.r.g. - degree of volatile oxidation. H₂O/CO₂- ratios in mass.% ; 1,3 - Gorny Altai boninites (1- bulk sample, 3- pyroxenite phenocrysts); 2,4 - boninites of Tongue trench, samples given by A.V. Sobolev (2-glass, 4- orthopyroxenes). r.g. - reduced gases.

Table 17. Bulk composition of magmatic and metamorphic rocks of Baratal terrane and Stop 24

N Sample	SiO ₂	TiO ₂	Al ₂ O ₃	Fe ₂ O ₃	FeO	MnO	MgO	CaO	Na ₂ O	K ₂ O	P ₂ O ₅	LOI	Total
----------	------------------	------------------	--------------------------------	--------------------------------	-----	-----	-----	-----	-------------------	------------------	-------------------------------	-----	-------

Basalts of the third layer of oceanic crust (Arydzhan suite)

Average contents and standard deviation (denominator) for selected metabasalts and basaltic porphyrites (20 samples).

1	<u>48.43</u> 2.06	<u>1.68</u> 0.21	<u>13.80</u> 1.09	<u>3.87</u> 1.14	<u>8.07</u> 1.22	<u>0.21</u> 0.02	<u>5.67</u> 0.97	<u>9.83</u> 1.96	<u>2.90</u> 0.84	<u>0.26</u> 0.14	<u>0.16</u> 0.06	<u>4.98</u> 2.38	99.86
---	----------------------	---------------------	----------------------	---------------------	---------------------	---------------------	---------------------	---------------------	---------------------	---------------------	---------------------	---------------------	-------

The same for sills and dikes of diabases comagmatic to Arydzhan suite (23 samples)

2	<u>49.53</u> 3.08	<u>1.54</u> 0.16	<u>14.94</u> 1.32	<u>3.25</u> 0.95	<u>8.97</u> 1.34	<u>0.20</u> 0.03	<u>5.17</u> 1.64	<u>7.16</u> 1.60	<u>4.03</u> 1.10	<u>0.68</u> 0.32	<u>0.27</u> 0.18	<u>3.82</u> 1.28	99.56
---	----------------------	---------------------	----------------------	---------------------	---------------------	---------------------	---------------------	---------------------	---------------------	---------------------	---------------------	---------------------	-------

Pyroxene porphyrites of Arydzhan suite of Stop 24

3	92-T-1	48.99	1.008	14.90	11.97	n.d.	0.150	5.71	9.99	2.87	0.18	0.113	4.02	99.43
4	92-T-2	49.16	1.096	15.07	12.12	n.d.	0.142	5.78	9.97	2.74	0.10	0.118	4.15	100.44
5	92-T-3	47.07	1.034	15.23	12.70	n.d.	0.171	6.73	9.58	2.98	0.09	0.112	3.92	99.64
6	92-T-4	48.69	1.140	15.50	12.12	n.d.	0.149	6.09	9.44	3.06	0.10	0.110	3.92	100.20
7	92-T-5	48.87	1.129	15.48	13.01	n.d.	0.159	6.46	6.88	3.75	0.14	0.116	4.08	100.09

Seamount basalts (Sagalak suite)

8	730	49.67	1.51	13.73	2.12	9.48	0.20	6.75	9.36	2.90	0.32	0.15	3.12	99.26
9	12048-4	48.90	3.25	13.91	9.26	5.47	0.20	3.63	5.38	4.10	1.00	0.60	4.71	100.41
10	586	59.20	1.18	14.75	4.98	5.90	0.19	7.23	7.13	3.80	0.44	0.14	3.89	98.83
11	157	49.67	2.13	13.66	2.73	8.76	0.26	7.81	8.36	2.80	1.40	0.17	2.99	100.19

Barroisite-actinolite schists after magmatic rocks of Baratal terrane

12	621	47.60	2.23	13.30	3.15	11.47	0.24	6.53	10.42	2.20	0.22	0.23	2.08	99.85
13	621a	44.10	2.40	12.90	3.45	12.55	0.29	7.67	10.18	2.40	0.17	0.19	3.46	100.04
14	2863	46.89	2.15	13.62	3.29	11.49	0.23	6.95	10.14	1.75	0.33	0.17	2.97	99.98
15	2865-1	50.13	1.64	13.44	4.67	8.39	0.20	6.85	9.84	2.0	0.30	0.11	1.94	99.91
16	2864-1	48.25	2.17	13.26	4.75	10.46	0.23	6.65	8.72	2.09	0.23	0.14	2.14	99.09
17	529-4	46.75	1.54	10.93	3.11	10.39	0.21	11.14	7.86	2.86	0.14	0.15	3.63	98.71
18	8523-1	48.05	2.08	13.61	4.00	10.31	0.17	6.84	9.25	3.30	0.17	0.15	2.01	99.93
19	905	48.46	1.99	12.50	2.76	12.18	0.14	8.70	8.75	2.14	0.34	0.16	2.69	100.86
20	904	47.39	1.96	13.88	4.34	9.41	0.24	6.95	12.00	1.64	0.24	0.20	2.42	100.77
21	907	51.14	1.73	12.56	3.06	9.70	0.24	6.58	10.29	1.81	0.80	0.14	2.41	100.54

Note: analyses 1-2, 8-21 were defined with volume-silicate method in the Central Laboratory PGO "Zapsibgeologiya", Novokuznetsk city. Analyses 3-7 were obtained with X-ray fluorescence method in UIGG&M, SB RAS, Novosibirsk city.

Table 18. Mineral composition of amphibole schists of Baratal terrane (sample B904)

Components	Amph1	Amph2	Sphe	Epidote
SiO ₂	42.57	43.56	30.44	38.48
TiO ₂	0.70	0.70	38.64	3.87
Al ₂ O ₃	12.54	12.88	1.09	24.00
Cr ₂ O ₃	0.04	0.06	0.10	0.061
FeO	16.44	16.34	0.48	7.61
MnO	0.31	0.31	0.50	0.104
MgO	10.29	10.11	0.04	0.733
CaO	10.89	11.11	28.73	24.00
Na ₂ O	2.11	2.11	0.63	0.187
K ₂ O	0.17	0.18	0.02	0.078
H ₂ O	2.00	2.00	2.00	2.00
Total	98.06	99.38	100.67	100.46
Ti	0.08	0.078	4.767	0.258
Al	2.242	2.266	0.211	0.097
Cr	0.005	0.007	0.014	0.004
Fe	2.087	2.040	0.061	0.563
Mn	0.040	0.039	0.008	0.008
Mg	2.328	2.249	0.01	0.097
Ca	1.770	1.777	5.051	2.214
Na	0.620	0.612	0.02	0.032
K	0.033	0.034	0.004	0.009
Si	6.459	6.503	4.994	3.408
Total	15.66	15.61	15.14	9.10

T a b l e 20. Bulk composition and trace elements content in various parts of boninite lava flow, Stop 26

Components	950	951	952
SiO ₂	50.80	52.30	53.88
TiO ₂	0.18	0.30	0.37
Al ₂ O ₃	8.83	14.81	11.53
P ₂ O ₅	0.02	0.03	0.04
FeO	7.83	8.26	8.98
Fe ₂ O ₃	1.21	2.00	1.62
CaO	12.45	7.75	8.78
MgO	13.94	7.52	9.45
Na ₂ O	1.25	2.66	2.12
K ₂ O	0.46	0.32	0.35
MnO	0.22	0.20	0.22
H ₂ O	0.04	0.12	-
LOI	3.61	3.59	3.20
Total	100.84	99.86	100.54

Elements	ppm	ppm	ppm
Cu	77	137	28
Zn	59	82	88
Co	51	32	40
Ni	102	32	58
Cr	937	154	514
V	204	240	210
Ba	170	177	84
Sr	70	121	90
Rb	5	2	3

N o t e: 950 and 951 - massive central part of lava flow; 952 - marginal part of lava flow. Analyses were defined with atomic-emission method in UIGG&M, SB RAS, Novosibirsk.

T a b l e 19. Bulk composition and trace elements content (ppm) of pebbles from magmatic rocks of the Early-Middle Cambrian molasse of inter-arc trough, Stop 23

N Sample	SiO ₂	TiO ₂	Al ₂ O ₃	Fe ₂ O ₃	FeO	MnO	MgO	CaO	Na ₂ O	K ₂ O	P ₂ O ₅	CO ₂	LOI	Total	Rb ppm	Sr ppm
Granitoids																
1 7666-4	73.95	0.40	11.65	1.82	1.83	0.01	0.16	2.01	4.81	1.19	0.04	0.2	1.24	99.11	5	254
2 81-5	71.11	0.32	12.64	1.41	2.87	0.06	1.01	2.96	4.50	0.55	0.06	1.1	2.06	99.55	10	170
3 597-2	70.89	0.33	12.71	1.02	2.34	0.07	1.14	3.16	4.10	0.80	0.07	0.8	2.34	98.97	9	338
4 81-8	68.67	0.29	13.44	2.54	2.58	0.08	2.12	3.80	4.20	0.80	0.10	0.9	2.12	100.74	15	250
5 3010	67.73	0.34	11.83	2.78	3.16	0.08	2.63	4.51	3.72	0.80	0.06	1.2	2.57	100.21	18	423
6 81-7	63.91	0.42	15.68	2.14	2.72	0.07	0.90	3.78	4.00	3.16	0.15	1.5	2.92	99.85	85	310
Alkaline gabbro and gabbro-diabases																
7 7666-6	50.54	0.50	15.24	3.94	6.12	0.18	7.28	8.49	1.91	2.13	0.04	0.8	3.68	100.05	40	270
8 7666-7	50.11	0.63	15.60	3.78	5.84	0.18	7.60	7.48	1.75	2.84	0.05	0.3	3.64	99.50	46	338
9 81-9	52.60	0.65	16.14	3.38	6.61	0.07	6.49	5.64	1.92	3.10	0.13	0.4	3.59	100.32	61	187
10 7009	55.43	0.80	15.95	5.07	5.02	0.14	6.18	4.09	2.10	2.40	0.18	0.7	3.59	100.95	64	338
11 3011	56.11	0.52	13.80	3.44	4.31	0.13	6.38	7.61	2.48	1.60	0.09	2.0	4.25	100.72	34	261
12 B-92-M5	49.40	0.53	17.01	11.52	-	0.17	6.80	6.87	2.47	1.23	0.04	-	4.12	100.26	-	-
13 B-92-M6	54.96	0.99	15.30	11.64	-	0.11	3.43	3.20	4.11	0.67	0.10	-	5.55	100.07	-	-
14 5-92-M8	47.70	0.48	17.03	11.08	-	0.16	6.63	5.57	2.05	1.92	0.03	-	5.04	99.82	-	-
15 B-92-M11	52.40	0.42	16.61	10.41	-	0.16	6.75	4.69	2.26	1.42	0.03	-	4.66	99.93	-	-
Pyroxenites																
16 B-92-M15	43.65	2.04	14.50	19.83	-	0.19	5.84	7.59	1.16	0.82	0.05	-	3.98	99.71	-	-
17 B-92-M16	43.03	0.34	9.95	9.70	-	0.18	15.54	12.02	0.47	0.11	0.03	-	8.47	99.85	-	-
Volcanic rocks																
8 81-1	54.37	1.00	14.70	3.48	7.90	0.22	5.47	5.07	4.50	0.19	0.17	0.8	3.65	100.72	5	156
19 81-2	52.28	0.80	14.16	7.63	4.02	0.15	4.46	9.59	3.72	0.25	0.12	2.00	3.74	100.87	4	423
20 3010-1	62.51	0.55	13.26	1.67	4.74	0.11	4.46	5.07	3.62	0.38	0.13	1.80	4.20	100.70	7	422
21 3010-3	63.47	0.57	13.26	2.95	3.87	0.11	3.24	4.51	3.80	0.44	0.12	1.40	3.52	99.86	9	423
22 81-4	66.95	0.32	12.19	1.14	4.02	0.07	1.62	4.79	4.40	0.17	0.06	2.80	4.40	100.13	6	129
23 B-92-M4	44.76	0.40	17.98	9.01	-	0.16	8.62	6.33	1.53	2.10	0.03	-	8.74	99.72	-	-

24 B-92-M7	50.29	0.72	15.54	11.79	-	0.18	8.54	5.66	1.67	1.27	0.08	-	4.28	100.10
25 B-92-M1047.41	0.78	16.15	8.77	-	0.15	3.91	10.33	2.54	0.41	0.08	-	9.10	99.64	
26 B-92-M1441.88	2.10	14.15	19.94	-	0.17	6.18	5.88	0.82	0.41	0.04	-	7.44	99.05	
27 B-92-M1	61.91	0.66	16.29	6.65	-	0.09	1.81	3.52	4.55	0.89	0.22	-	3.14	99.79
28 B-92-M2	42.74	0.46	11.65	10.21	-	0.21	14.47	7.84	0.3	0.55	0.08	-	11.44	99.68
29 B-92-M3	46.92	0.70	15.67	11.72	-	0.17	8.48	7.67	1.77	0.80	0.09	-	6.18	100.19

Note: Oxide contents for samples 1-12, 9-23 were obtained with volume-silicate method in the Central laboratory PGO "Zapsibgeologiya", Novokuznetsk city, content of Rb and Sr was defined using X-ray spectroscopy in the Central laboratory of PGO "Beryozovgeologiya", Novosibirsk city; oxide contents for 13-18 samples were defined using X-ray fluorescence method, trace elements using atomic-emission method in UIGG&M, SB, RAS, Novosibirsk city.

T a b l e 21. Bulk composition of Chagan-Uzun massif rocks, Stop 25

N	N sample	SiO ₂	TiO ₂	Al ₂ O ₃	Fe ₂ O ₃	MnO	MgO	CaO	Na ₂ O	K ₂ O	P ₂ O ₅	LOI	Total
1	C-101b-89	51.60	1.46	14.03	14.96	0.24	4.20	7.11	6.01	0.54	0.13	0.48	100.78
2	C-102b-89	51.27	1.38	13.95	14.59	0.23	4.19	7.88	4.21	0.32	0.13	0.78	99.08
3	C-102c-89	47.17	1.65	14.60	16.42	0.24	4.88	8.71	4.18	0.37	0.16	1.34	99.78
4	C-103c-89	50.69	1.44	13.88	14.80	0.22	4.34	7.95	4.69	0.32	0.13	1.04	99.52
5	C-104c-89	51.40	1.42	14.02	14.68	0.23	4.21	7.85	5.02	0.40	0.13	0.48	99.86
6	C-100-89	40.24	0.03	1.16	9.30	0.15	41.20	1.33	0.30	0.02	0.03	6.60	100.19
7	C101a-89	41.51	0.03	1.27	8.45	0.13	39.25	1.91	0.30	0.02	0.03	7.12	99.84
8	C-104a-89	39.67	0.03	0.98	8.39	0.13	39.97	1.50	0.30	0.01	0.03	9.12	99.96
9	C-104d-89	40.09	0.03	1.12	8.46	0.13	40.22	1.17	0.30	0.01	0.03	8.65	100.05
10	C-105b-89	40.23	0.03	1.06	7.37	0.12	40.66	1.75	0.30	0.02	0.03	8.57	99.96
11	Chu-3	46.69	1.80	14.03	14.24	0.25	7.60	8.56	4.06	0.23	0.15	2.08	99.70
12	Chu-4	47.37	1.61	12.72	13.28	0.24	7.78	11.08	3.54	0.08	0.11	2.34	100.15
13	Chu-6	48.66	1.84	12.87	15.22	0.23	6.88	7.27	4.09	0.18	0.18	1.94	99.39
14	Chu-7	48.31	1.54	11.84	14.47	0.24	8.75	10.09	3.00	0.08	0.08	1.48	99.89
15	C-16a-91	47.89	1.61	13.67	13.00	0.22	7.18	10.69	2.89	0.13	0.16	2.46	99.90
16	Ch-9	48.33	1.77	12.76	14.35	0.21	7.03	7.48	3.26	0.18	0.13	4.58	100.09
17	Ch-11	45.29	2.28	13.14	17.66	0.35	8.00	6.96	3.15	0.34	0.18	2.54	99.90
18	Ch-915	47.10	2.17	13.13	15.12	0.23	6.93	9.22	3.95	0.26	0.17	1.38	99.69
19	Ch-916	47.88	2.22	12.39	15.04	0.25	6.71	9.24	3.29	0.28	0.21	1.87	99.42
20	B-965a	45.02	2.42	13.81	16.60	0.15	7.09	10.87	2.51	0.33	0.21	3.18	100.87
21	965a	45.93	2.99	13.65	15.75	0.28	6.43	10.10	2.07	0.25	0.19	3.47	100.86
22	Ch-13	44.48	2.12	14.17	16.04	0.29	7.79	10.52	2.52	0.36	0.13	1.70	100.17
23	Ch-14	46.86	1.85	13.52	14.68	0.22	7.74	9.39	3.51	0.18	0.16	1.20	99.32

N o t e: 1-5 island arc dikes in Chagan-Uzun ophiolite massif; 6-11 - ultramafics; 11-15 - amphibolites of the metamorphic sole; 16-19 - garnet amphibolites; 20-23 - eclogites.

Analyses were defined with X-ray fluorescence method in UIGG&M, SB RAS, Novosibirsk city.

T a b l e 22. Bulk composition of metamorphic rocks of Chagan-Uzun massif.

Sample	SiO ₂	TiO ₂	Al ₂ O ₃	Fe ₂ O ₃	MnO	MgO	CaO	Na ₂ O	K ₂ O	P ₂ O ₅	LOI	Total	Rb	Sr	Y	Zr	Nb
Ch-911-A	46.89	1.380	12.83	9.82	0.173	6.14	10.44	4.28	0.13	0.110	7.56	99.75	1.18	184.1	21.6	71.2	2.48
Ch-912	45.50	1.615	13.62	12.11	0.271	7.39	10.99	1.44	0.18	0.140	6.61	99.88	0.83	207.0	31.3	79.7	3.55
Ch-913	43.76	1.805	15.01	14.74	0.240	8.02	7.15	2.40	0.37	0.159	5.88	99.55	5.26	250.1	41.3	110.5	2.4
Ch-914	46.44	1.944	13.48	14.81	0.241	8.60	7.94	2.42	0.32	0.185	2.80	99.19	3.2	168.1	36.9	104.5	4.2
Ch-915	47.10	2.171	13.13	15.12	0.234	6.93	9.22	3.95	0.26	0.174	1.38	99.69	1.01	186	38.3	100	3.3
Ch-916	47.88	2.218	12.39	15.04	0.249	6.71	9.24	3.29	0.28	0.205	1.87	99.42	1.37	189.1	34.2	94.6	3.6
Ch-917	47.36	2.170	13.58	15.29	0.286	7.45	8.29	3.49	0.22	0.162	0.94	99.25	1.66	94.7	39.0	107.1	3.0
Ch-918	50.63	1.766	12.97	11.73	0.223	6.71	8.05	2.20	0.94	0.219	4.38	99.87	12.2	308.8	19.1	134.6	10.1
Ch-919	46.55	1.586	14.06	13.23	0.220	7.52	10.36	3.40	0.15	0.190	2.48	99.76	0.34	177.5	29.6	76.5	2.7

N o t e: Bulk rock compositions were obtained with X-ray fluorescence method, trace elements concentrations were obtained with atomic-emission method in UIGG&M, SB RAS, Novosibirsk city.

T a b l e 23. Mineral composition of eclogites from Chagan-Uzun massif. (Stop 25)

Components	Cpx2	Cpx3	Cpx1 in garnet	Ga1 centre	Ga1 edge	Ga1 edge	Ga2 centre	Ga2 edge	Amph1 centre	Amph1 edge	Amph1 edge	Amph2 centre	Amph2 edge	Amph2 edge	Chlorite	Epidote
SiO ₂	56.0	55.9	58.7	38.4	38.1	38.5	38.5	38.4	47.5	49.6	49.6	46.1	48.4	50.1	25.8	38.45
TiO ₂	0.04	0.04	0.03	0.07	0.03	0.05	0.04	0.04	0.43	0.21	0.14	0.74	0.29	0.06	0.01	0.24
Al ₂ O ₃	9.82	9.45	13.0	21.15	21.0	21.1	21.2	21.3	11.3	8.46	6.10	13.1	10.6	4.60	19.6	26.3
Cr ₂ O ₃	0.01	0.013	0.0	0.02	0.02	0.01	0.02	0.04	0.00	0.02	0.00	0.01	0.04	0.02	0.15	0.11
F ₂ O ₃	1.10	1.12	-	-	-	-	-	-	-	-	-	-	-	-	-	8.96
FeO	5.18	5.20	5.69	24.6	25.3	24.4	24.7	26.4	13.2	16.5	19.1	14.4	14.8	17.3	30.3	-
MnO	0.01	0.013	0.08	0.80	1.55	0.38	0.66	0.19	0.03	0.12	0.19	0.04	0.07	0.23	0.38	0.00
MgO	7.28	7.64	4.24	3.34	3.24	3.70	3.41	4.10	11.7	10.7	11.0	10.3	10.3	11.4	12.4	0.12
CaO	13.7	14.1	10.35	12.3	11.0	12.0	12.3	10.1	8.86	10.0	10.6	8.97	8.94	11.4	0.05	23.5
Na ₂ O	6.88	6.76	7.33	0.04	0.03	0.02	0.03	0.02	4.10	2.61	1.41	4.16	3.67	1.41	0.02	0.01
K ₂ O	0.01	0.00	0.04	0.00	0.00	0.00	0.00	0.00	0.40	0.29	0.19	0.48	0.36	0.11	0.00	0.00
H ₂ O	-	-	-	-	-	-	-	-	2.00	2.00	2.00	2.00	2.00	2.00	11.0	2.00
Total	100.03	100.27	100.46	100.72	100.27	100.16	100.86	100.59	99.52	100.51	100.33	100.26	99.47	99.63	99.75	99.69
Si	2.012	2.011	2.017	2.944	3.003	3.009	2.996	2.997	6.921	7.230	7.333	6.713	7.079	7.499	2.764	6.155
Ti	0.001	0.001	0.001	0.005	0.002	0.003	0.003	0.002	0.047	0.023	0.015	0.081	0.032	0.007	0.001	0.029
Al	0.416	0.400	0.533	1.949	1.948	1.946	1.946	1.959	1.947	1.454	1.063	2.253	1.826	0.810	2.476	4.973
Cr	0.000	0.000	0.000	0.002	0.002	0.001	0.002	0.002	0.000	0.002	0.000	0.001	0.004	0.002	0.012	0.011
Fe+3	0.060	0.060	-	-	-	-	-	-	-	-	-	-	-	-	-	1.080
Fe+2	0.126	0.126	0.165	1.604	1.665	1.954	1.610	1.726	1.606	2.010	1.364	1.760	1.811	2.160	2.712	-
Mn	0.001	0.000	0.002	0.053	0.103	0.025	0.044	0.012	0.003	0.015	0.024	0.005	0.009	0.029	0.035	0.000
Mg	0.390	0.410	0.219	0.387	0.380	0.431	0.394	0.478	2.536	2.331	2.422	2.235	2.257	2.545	1.982	0.028
Ca	0.524	0.524	0.480	1.030	0.924	1.003	1.030	0.842	1.383	1.557	1.680	1.401	1.403	1.825	0.006	4.023
Na	0.480	0.468	0.526	0.005	0.005	0.004	0.004	0.003	1.115	0.737	0.405	1.175	1.041	0.408	0.004	0.004
K	0.000	0.000	0.002	-	-	-	-	-	0.075	0.054	0.035	0.090	0.066	0.021	0.000	-
Total	4.010	4.028	3.945	8.029	8.032	8.016	8.029	8.022	15.676	15.416	15.343	15.712	15.529	15.305	9.992	16.303

T a b l e 24. Bulk rock composition of Biya sources and Teletskoye Lake district, Stops B-3-9.

N	Groups	N sample	SiO ₂	TiO ₂	Al ₂ O ₃	Fe ₂ O ₃	MnO	MgO	CaO	Na ₂ O	K ₂ O	P ₂ O ₅	LOI	Total
1	Pillow	C-6A-92	52.76	0.567	14.71	8.89	0.217	5.28	9.00	2.84	0.64	0.298	4.45	99.67
2		C-6B-92	45.21	1.438	14.30	11.39	0.175	5.78	11.41	2.92	0.65	0.171	6.24	99.71
3	Lavas	C-6B-92	46.63	1.703	14.04	12.53	0.172	5.36	11.10	1.32	0.26	0.179	6.70	100.00
4		C-6G-92	39.35	1.244	12.59	8.98	0.179	5.60	16.32	2.84	0.34	0.162	11.81	99.42
5		C-6D-92	50.01	1.566	13.46	9.99	0.094	3.59	9.39	4.00	0.94	0.241	5.90	99.21
6	Basalt sills	C-1A-92	48.81	0.665	17.19	10.11	0.249	8.56	5.68	3.99	0.17	0.064	4.13	99.63
7		C-1B-92	49.13	0.418	10.12	9.68	0.172	14.45	12.92	0.46	0.40	0.057	1.81	99.62
8		C-1G-92	47.61	0.337	9.51	9.76	0.174	17.17	12.29	0.30	0.49	0.034	2.42	100.10
9		C-1D-92	49.06	0.431	10.84	9.77	0.166	14.24	12.36	0.30	1.00	0.061	1.84	100.08
10		C-3A-92	47.56	0.540	14.83	10.34	0.174	9.81	10.67	1.28	0.16	0.042	4.48	99.89
11		C-3B-92	54.76	0.642	16.64	7.24	0.126	5.25	8.21	3.22	0.50	0.139	2.75	99.49
12		C-8A-92	45.72	0.479	13.94	8.42	0.238	5.23	14.51	2.24	0.43	0.178	8.45	99.84
13	Dikes	C-8B-92	49.52	0.548	15.52	10.99	0.203	7.95	8.46	2.20	0.70	0.153	3.54	99.80
14		C-8C-92	47.83	1.468	13.67	14.67	0.119	7.31	6.79	3.86	0.60	0.248	3.98	100.57
15		C-8D-92	46.61	0.216	10.86	8.58	0.157	14.68	15.16	0.30	0.15	0.030	3.31	100.06
16	Dikes	C-7C-92	47.27	0.373	10.58	9.93	0.210	12.61	9.96	5.97	0.61	0.180	2.81	100.52
17	in	C-7G-92	47.48	0.364	8.72	9.93	0.171	15.91	10.44	3.65	0.18	0.110	3.27	100.23
18	gabbro	C-7D-92	44.97	0.650	16.04	8.70	0.123	5.54	10.56	3.87	0.16	0.186	9.75	100.55
19		C-7E-92	54.33	0.728	17.46	4.60	0.099	6.71	7.14	5.18	0.95	0.086	2.44	99.75
20		C-7Zh-92	49.20	0.655	16.48	9.61	0.122	6.77	12.24	1.82	0.06	0.165	2.78	99.91
21		CA-11/1-92	47.28	0.193	20.41	5.09	0.089	7.02	14.80	1.82	0.65	0.030	2.58	99.96
22		CA-11/2-92	47.47	0.213	13.87	8.00	0.148	12.25	15.13	0.30	0.19	0.030	2.52	100.12
23		CA-11/3-92	47.72	0.214	14.91	7.28	0.136	11.22	15.68	0.56	0.32	0.030	1.80	99.87
24	Gabbro	CA-11/4-92	46.31	0.191	12.61	8.93	0.181	13.04	14.85	0.30	0.20	0.030	3.34	99.99
25		CA-11/5-92	45.20	0.160	9.97	7.76	0.165	14.00	17.27	0.30	0.12	0.030	5.05	100.03
26		CA-11/6-92	50.67	0.664	16.17	10.96	0.247	5.78	8.91	1.64	0.84	0.222	3.59	99.71
27	Pyro-	CA-12/1-92	46.70	0.392	10.34	10.81	0.208	13.92	13.98	0.30	0.23	0.196	2.57	99.65
28	xenites	CA-12/2-92	45.70	0.203	6.94	10.18	0.193	17.65	14.33	0.30	0.07	0.030	4.71	100.31
29		CA-12/3-92	48.47	0.226	6.13	9.98	0.184	17.75	13.09	0.30	0.08	0.030	4.49	99.73
30		CA-12/4-92	47.58	0.364	10.02	10.35	0.193	14.37	14.72	0.30	0.19	0.049	2.07	100.27
31		CA-12/5-92	48.53	0.186	7.43	7.89	0.148	16.69	16.40	0.30	0.07	0.030	2.49	100.17
32	Shoshonitic	912-A	46.73	0.685	14.69	9.90	0.166	10.69	10.57	1.62	1.37	0.208	3.12	99.79
33	Dykes	9112-B	45.61	0.800	16.90	10.35	0.227	4.73	10.47	2.21	2.25	0.332	6.78	100.71
34	schist	9113	42.63	0.962	19.84	10.95	0.177	8.68	5.88	1.10	3.87	0.279	5.59	100.02
35		B-970	47.14	1.28	14.19	8.89	0.37	7.79	8.80	2.90	0.39	0.19	3.36	100.45

N o t e: 1-31 - Vendian-Early Cambrian ophiolites of primitive island arc, 32-34 - dikes of shoshonite series of Early Cambrian normal island arc, 35 - winchite-barroisite-actinolite schist.

Analyses made using X-ray fluorescence method in UIG&M, SB RAS, Novosibirsk.

Table 25. Trace elements concentrations in rocks of Biya sources and Teletskoye Lake district, ppm

N	Rocks	N Sample	La	Yb	Sc	Zr	Y	Nb
1	Lavas	C-6A-92	6	1.5	36	27	15	4
2		C-6B-92	3	2.3	26	60	16	4.8
3		C-6G-92	3	1.8	24	60	18	7.2
4		C-6D-92	3	2.2	32	76	20	5.2
5		C-1A-92	4.5	1.6	35	11	12	3.6
6	Sills	C-1B-92	7.3	1.6	120	17	16	3.4
7		C-1G-92	7	1.4	80	6	12	3.2
8		C-1D-92	7.5	1.6	100	15	15	4
9	Dikes in	C-7B-92	5.5	1.1	22	12	11	2.5
10		C-7G-92	3	1.0	20	8	10	1.8
11	gabbro Dikes	C-7E-92	4	1.2	22	17	16	3.2
12		C-8A-92	6.2	1.9	22	14	12	5.2
13		C-8G-92	3	1.7	110	4	12	4.8
14		9112-A	6	1.7	32	26	12	4.5
15		9112-B	6.5	2.0	26	36	16	4.5
16		9113	5.5	1.6	36	33	14	3.6

Note: 1-13 - Vendian-Early Cambrian island arc ophiolites of primitive island arc, 14-16 - dikes of shoshonite porphyrites of Early Cambrian normal island arc. Atomic-emission analysis, Siberian Institute of Geology, Geophysics and Mineral Resources, Novosibirsk.

T a b l e 26. Composition of minerals and homogenized melt inclusions from porphyrites of Biya sources and Teletskoye Lake district

N	N sample	SiO ₂	TiO ₂	Al ₂ O ₃	Cr ₂ O ₃	FeO	MnO	MgO	CaO	Na ₂ O	K ₂ O	Total
Clinopyroxenes												
1	C-1g-92	53.87	0.10	2.70	0.92	3.73	0.09	15.99	21.97	0.13	0.0	99.52
2	C-1g-92	50.02	0.15	2.48	0.34	4.12	0.11	18.03	22.28	0.14	0.0	97.67
3	C-1g-92	49.51	0.16	2.71	0.42	5.22	0.14	16.34	22.83	0.16	0.0	97.49
4	C-1g-92	52.65	0.17	2.91	0.28	5.16	0.13	15.73	22.06	0.12	0.0	99.22
5	C-1g-92	53.01	0.09	2.42	0.91	3.91	0.11	16.22	22.22	0.13	0.0	99.02
6	9113/25	51.27	0.50	3.25	0.02	8.32	0.17	13.87	21.24	0.33	0.0	98.98
7	9113/25	49.19	0.74	6.71	0.07	8.28	0.19	12.99	21.20	0.40	0.0	99.03
8	9113/26	50.92	0.39	3.49	0.09	7.42	0.15	14.74	21.57	0.26	0.0	99.03
9	9113/26	49.23	0.76	5.88	0.02	9.27	0.18	13.26	20.83	0.40	0.07	99.89
10	9113/26	50.78	0.45	4.30	0.08	7.29	0.13	14.88	21.42	0.34	0.0	99.65
Amphiboles												
11	C-1g-92	50.37	0.26	9.28	0.20	8.70	0.15	15.13	12.27	0.90	0.17	97.42
12	C-1g-92	51.36	0.14	8.07	0.34	8.23	0.16	15.77	12.25	0.71	0.14	97.16
13	C-1g-92	63.77	0.15	5.22	0.31	7.48	0.16	17.06	12.53	0.61	0.07	97.37
14	C-1g-92	52.61	0.20	2.89	0.59	7.70	0.16	19.21	12.37	0.45	0.03	96.22
15	C-1g-92	53.30	0.14	4.94	0.54	8.54	0.18	16.98	12.35	0.39	0.05	97.40
Melt inclusions in clinopyroxenes												
16	9113/25	50.26	0.39	12.72	0.0	6.55	0.11	9.12	18.20	1.51	0.17	99.23
17	9113/26	49.53	0.77	11.82	0.02	9.96	0.19	7.43	13.31	1.94	1.40	96.37
18	9113/26	49.82	0.78	11.55	0.02	9.93	0.19	7.47	13.17	1.91	1.20	96.06
19	9112A/27	49.34	0.40	14.07	0.05	7.52	0.15	8.57	13.17	1.88	1.21	96.36
20	9112A/27	49.49	0.43	14.13	0.05	7.34	0.14	8.24	12.98	2.11	1.39	96.29

Table 27. Microprobe analysis of amphiboles of Stop B-6 rocks

Oxide	Sample 9128					Sample 970		Sample 9130		
SiO ₂	40.75	40.69	49.90	40.31	51.44	43.47	46.19	44.75	44.75	44.35
TiO ₂	0.13	0.15	0.14	0.18	0.06	0.10	0.08	0.17	0.16	0.15
Al ₂ O ₃	13.17	12.77	11.91	13.62	6.50	11.86	10.60	10.46	10.47	11.02
Cr ₂ O ₃	0.00	0.00	0.00	0.00	0.00	0.13	0.10	0.01	0.00	0.03
MnO	0.384	0.51	0.66	0.29	0.36	0.45	0.41	0.27	0.29	0.25
FeO	22.32	23.50	23.21	23.09	19.74	18.77	18.30	17.72	17.56	16.80
MgO	5.86	5.68	6.51	5.69	9.00	9.31	10.29	10.28	10.09	10.33
CaO	10.45	11.32	8.79	11.45	10.61	11.63	11.18	11.79	11.79	11.40
Na ₂ O	2.12	1.74	1.75	1.85	1.33	1.76	1.62	2.01	1.73	1.54
K ₂ O	0.19	0.38	0.22	0.29	0.22	0.20	0.24	0.82	0.76	0.32
H ₂ O	2.00	2.00	2.00	2.00	2.00	2.00	2.00	2.00	2.00	2.00
Total	97.39	98.74	98.09	98.76	101.26	99.69	101.01	100.27	99.29	98.18
Si	6.42	6.38	6.67	6.30	4.57	6.56	6.81	4.08	6.71	6.71
Ti	0.02	0.02	0.02	0.02	0.00	0.01	0.01	0.01	0.02	0.02
Al	2.44	2.36	2.18	2.51	0.68	2.11	1.84	1.12	1.86	1.96
Cr	0.00	0.00	0.00	0.00	0.00	0.02	0.01	0.00	0.00	0.00
Mn	0.05	0.07	0.09	0.04	0.03	0.06	0.05	0.02	0.04	0.033
Fe	2.94	3.08	3.02	3.02	1.47	2.37	2.26	1.35	2.22	2.13
Mg	1.38	1.33	1.51	1.33	1.19	2.10	2.26	1.40	2.27	2.33
Ca	1.76	1.90	1.46	1.92	1.01	1.88	1.77	1.15	1.91	1.85
Na	0.65	0.53	0.53	0.56	0.23	0.51	0.46	0.35	0.51	0.45
K	0.04	0.08	0.04	0.06	0.03	0.04	0.04	0.10	0.15	0.06
Total ¹	15.69	15.73	15.51	15.74	9.21	15.65	15.51	9.58	15.67	15.54

Note: Analyses made in UIGG&M, SB RAS, Novosibirsk.

CONTENTS

INTRODUCTION	3
Active continental margin stage	5
Collisional stage	7
Island arc stage	7
DESCRIPTION OF FIELD TRIP	13
Day 1. General review	13
Stops 1-3	15
Day 2. Section Cheposh - Ust-Syoma	20
Stop 4	20
Stop 5	28
Section Cherga-Bulukhta	29
Stops 6-8	29
Stop 6	31
Stop 7	32
Stop 8	33
ROUTE A. Syoma Pass - Chiketaman Pass - Aktash Village - Chagan-Uzun Village	33
Day 3. General review	33
Stops 9-15	33
Volcanic complex of Hercynian active margin	35
Stops 9-10	36
Granitoid bodies of Hercynian active margin	37
Stop 11-15	37
Stop 11	44
Stop 12-14	46
Stops 15	47

Days 4 and 5. General review	47
Kurai terrane of Vendian-Early Cambrian primitive island arc	50
Early Cambrian accretionary prism	56
Fore-arc and inter-arc troughs	62
Day 4.	
Stop 16	63
Stop 17	64
Stop 18	65
Stop 19, 20	66
Day 5.	
Stops 21-23	67
Stops 24,25A	69
Stop 25B	72
 ROUTE B. Gornoaltaisk - Biya River - Teletskoye Lake	
General review	75
Day 3. Stop B-1	81
Stops B-2, B-3	82
Stops B-4 - B-6	83
Stops B-7, B- 8	84
Day 4. Stops B-9,B-10	85
 REFERENCES	86
APPENDIX	91

Утверждено к печати
Институтом геологии СО РАН

Технический редактор О.М.Вараксина

Подписано к печати 07.06.93
Бумага 60x84/16. Печ.л.7,75+I вкл. Уч.-изд.л.7,80.
Тираж 600. Заказ 117.

Объединенный институт геологии, геофизики
и минералогии СО РАН
Новосибирск, 90. Ротапринт.